Identification of genes involved in progression of retinoblastoma

Inaugural Dissertation

to obtain the degree of
Dr. rer. nat.
Fachbereich Bio- und Geowissenschaften
at the
University Duisburg-Essen

by
Sandrine Gratias
From Figeac (France)

April 2005

A part of the present work will be published or has been submitted in the following journals:

Sandrine Gratias, Andreas Schüler, Ludger Klein Hitpass, Harald Stephan, Harald Rieder, Stephanie Schneider, Bernhard Horsthemke, Dietmar R. Lohmann. (2005) Genomic gains on chromosome 1q in retinoblastoma: consequences on gene expression and association with clinical manifestation (in press at the International Journal of Cancer).

Boris Zielinski, **Sandrine Gratias**, Grischa Toedt, Frank Mendrzyk, Daniel E. Stange, Bernhard Radlwimmer, Dietmar R. Lohmann, and Peter Lichter. Detection of chromosomal imbalances in retinoblastoma by matrix-based comparative genomic hybridization (under revision in Genes Chromosome and Cancer).

Corinna Grasemann, **Sandrine Gratias**, Harald Stephan, Andreas Schüler, Alexander Schramm, Ludger Klein Hitpass, Harald Rieder, Stephanie Schneider, Ferdinand Kappes, Angelika Eggert, Dietmar R. Lohmann. Gains and overexpression identify *DEK* and *E2F3* as targets of chromosome 6p gains in retinoblastoma (submitted to Oncogene).

Die der vorliegenden Arbeit zugrundeliegenden Experimente wurden am Institut für Humangenetik der Universität-Duisburg-Essen durchgeführt.

1. Gutachter: Prof. Dr. Bernhard Horsthemke
2. Gutachter: PD Dr. Ludger Klein-Hitpass
3. Gutachter: /

Vorsitzender des Prüfungsausschusses: Prof. Dr. Peter Bayer

Tag der mündlichen Prüfung: 29.06.2005

ABBREVIATIONS

µg	microgram
µl	microlitre
A	Adenine
BAC	Bacterial Artificial Chromosome
bp	base pair
BSA	Bovine Serum Albumin
C	Cytosine
cDNA	complementary DNA
DNA	deoxyribonucleic acid
Dnase	Desoxyribonuclease
dNTP	Deoxyribonucleoside triphosphate
EDTA	ethylendiaminetetraacetic acid
FAM	6-carboxyfluorescein
G	Guanine
h	hour
kbp	kilobase pair
M	molar (mol/l)
Mb	Mega base pair
mg	milligram
min	minute
ml	millilitre
mM	millimolar
mRNA	messenger RNA
NCBI	National Center for Biotechnology Information, USA
nm	nanometre
PCR	Polymerase Chain Reaction
pmol	picomol
pRB	retinoblastoma protein
Rb	disease retinoblastoma
RB1	retinoblastoma gene
RNA	ribonucleic acid
ROX	5-carboxy-X-rhodamin
rpm	rounds per minute
RT	room temperature
s	second
SAM	significance analysis of microarray
SDS	sodium dodecyl sulfate
SNP	Single Nucleotide Polymorphism
STR	Short Tandem Repeat
T	Thymine
TAMRA	Carboxy tetramethyl rhodamine
U	unit
U	Uracile

1 INTRODUCTION

1.1 Tumorigenesis

To stay healthy, a multicellular organism has to maintain homeostasis. Different regulatory processes are required to keep the whole organism in a state of balance. It is essential that the cells forming the different tissues communicate and this involves several regulatory pathways, through which the cells send and receive signals that control cell division, differentiation or apoptotic cell death. A neoplastic cell is a cell that proliferates without control and colonizes territories normally reserved for other cells. The tumour that is formed in consequence of proliferation of neoplastic cells is a growing mass without any function for the organism as a whole. As long as the neoplastic cells remain clustered together in a single mass, the tumour is benign. If the neoplastic cells acquire the capacity to invade other tissues or form distant colonies (metastases), the tumour is malignant and defined as a cancer.

The transition of a normal to a neoplastic cell is mainly due changes of the genetic program, which can have different origins:

- DNA damage caused by environmental agents such as chemical carcinogens, radiation
- deregulation by oncogenic viruses (including alteration of regulatory pathways by viral oncoproteins)
- spontaneous mutations that occur mainly during replication or mitosis
- inherited mutations that confer predisposition to neoplastic cell proliferation

It is generally accepted that the formation of a neoplasm cannot be generated by a single mutation [1]. The number of genetic alterations needed to change a normal into a cancer cell varies according to the type of cancer and the type of alteration. Tumours can be classified as liquid or solid. Liquid tumours are composed of neoplastic cells whose precursors are normally mobile (i.e. leukaemia, lymphoma [1]). Solid tumours are composed of epithelial or mesenchymal cells that normally are immobile. It is generally assumed that liquid tumours require only 1 or 2 mutations to develop [2] whereas for solid tumours in adults at least 3 mutations are required [3].

Hanahan and Weinberg [4] have summarized the capabilities a cell must acquire to become a cancer cell:

1) growth signal autonomy
2) evasion of apoptosis
3) insensitivity to antigrowth signals
4) sustained angiogenesis
5) limitless replicative potential and
6) capacity to invade tissue and grow at metastatic sites

The number of mutations required to gain these abilities varies. For example, in some cells mutation of the *TP53* gene facilitates both cell proliferation and evasion of apoptosis whereas in other cancers, several mutations additional to tumour related genes may be required to attain these capabilities. While the number of mutations necessary to form a cancer cell is variable, the end stage, a cancer cell, is invariant and mutations in different sets of genes may lead to the same phenotype. As is to be expected from the functional changes that define the malignant phenotype, the proteins encoded by these cancer genes are often involved in pathways that regulate growth, apoptosis, angiogenesis and replication. For example, the p53 protein is a transcription factor that inhibits cell growth and stimulates cell death. The p53 pathway (Fig 1-1-b) can be disrupted by point mutation in the p53 gene, or by any other alteration on the genes involved in the pathway. The pathway itself rather than its single components is the functional target of the oncogenic alterations that promote cancer development. Nevertheless, it is important to identify the specific genes that are subject to oncogenic alterations as this knowledge can help to determine which pathways have been hit in a certain type of cancer.

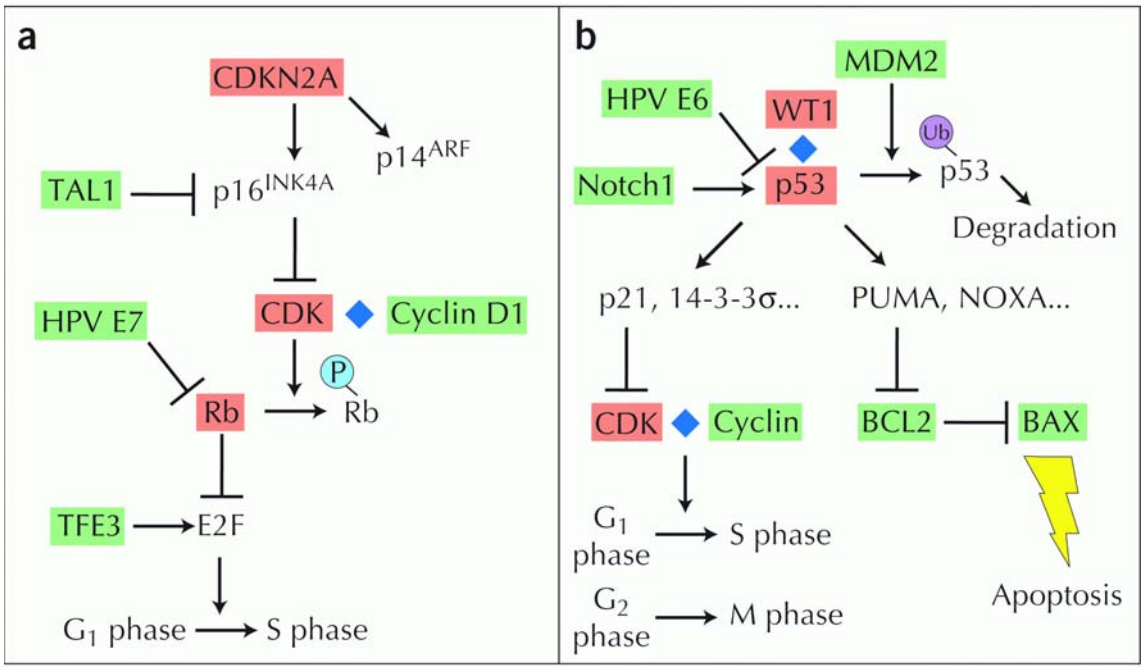

Fig 1-1. Rb (a) and p53 (b) pathways. Diamonds indicate protein-protein interactions, arrows and T-bars indicate transcriptional induction and repression, respectively. Small circled "P", "OH" and "Ub" represent covalently attached phosphate, hydroxyl and ubiquitin groups, respectively (adapted from Nature Reviews Genetics, November 2003, Volume 4).

1.2 Cancer genes

In general three types of genes can be distinguished that can be the target of oncogenic alterations: oncogenes, tumour suppressor and stability genes [1].

1.2.1 Oncogenes

An oncogene may be defined as a derivate of a normal gene (proto-oncogene) that can induce a normal cell to become a cancer cell under certain circumstances. Most proto-oncogenes encode proteins that participate in the regulation of growth and/or differentiation of normal cells. There are different ways by which a proto-oncogene can become an oncogene:

- the gene may be altered by a small change in sequence such as point mutation which results in activation of the gene product irrespective of regulatory input (e.g. K-*ras* activated by point mutations in codons 12 and 61 in adenomas and adenocarcinomas of the colon [5])
- the gene may be altered by a chromosomal translocation that involves breakage and rejoining of the DNA . Such alterations can result in a hyperactive fusion

protein, or – if the translocation has brought into proximity a regulatory DNA sequence – that causes increased amounts of normal transcripts with concomitant overproduction of the encoded protein (for example in chronic myelogenous leukaemia with the Philadelphia chromosome)

- errors in DNA replication can cause gene amplification. This can result in production of increased amounts of a protein that is structurally normal (*erb*B-2, [6])

Gene amplification is a frequent finding in cancer cells. The amplification can be related to endo-replication leading to an increase of all or parts of chromosomes (for example trisomy 13 or isochromosome 6p, respectively). The other form of amplification corresponds more to a multiplication of the amplified segment. The amplified segment can appear as a homogeneously staining region (HSR), which is an intra-chromosomal structure that is interpolated in the normal banding pattern of a regular chromosome. The cell can also house extra-chromosomal structures, such as double minute chromosomes (size ranging from 250 kb to several Mb) or episomes (size ranging from 100 to 200 kb).

1.2.2 Tumour suppressor genes

In a simplistic way, a tumour suppressor gene is a gene that "prevents" formation of a cancer. The prototype tumour suppressor is the retinoblastoma gene, *RB1*, which is inactivated in the childhood tumour retinoblastoma. From a statistical analysis of the clinical manifestation of this tumour, Alfred Knudson inferred the two-step mutation hypothesis [10]. The hypothesis has laid the fundament of the tumour suppressor gene concept. In general this concept assumes that a cell that is defective in only one of its two alleles behaves as a normal cell, i.e. there is no loss of control until both gene copies are put out of action. However, loss-of-function of one allele may enhance the susceptibility to cancer. The first as well as the second allele may be lost by a chromosomal deletion, inactivated by a point mutation or via epigenetic silencing. The second copy is usually lost by a less specific mechanism: the chromosome carrying the remaining normal allele may be lost from the cell by a variety of chromosomal mechanisms such as mitotic recombination or may be replaced by the mutant allele through gene conversion (Fig 1-2).

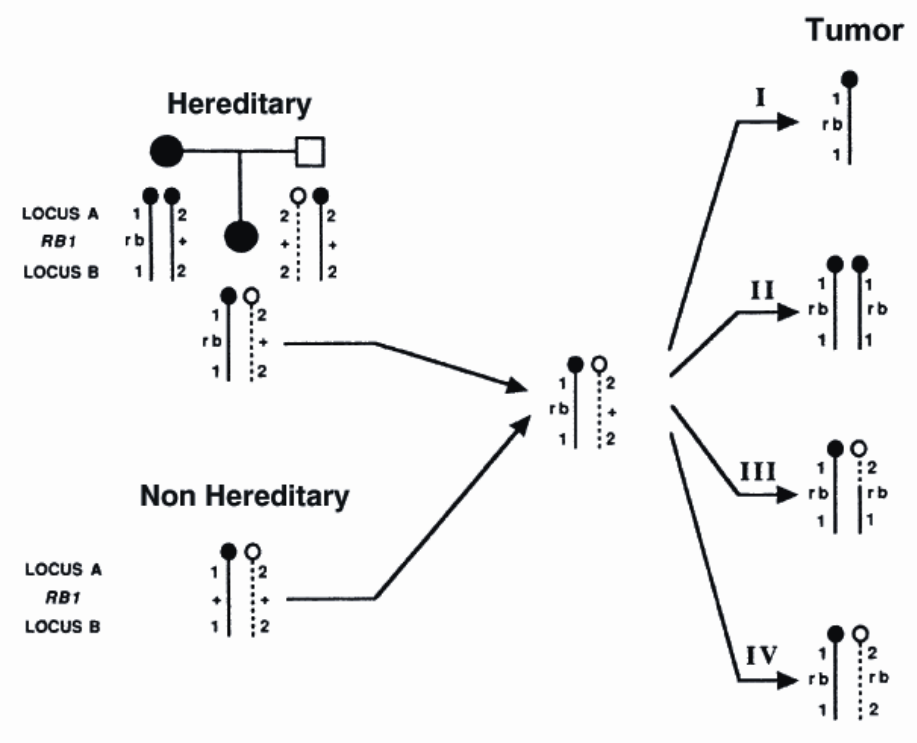

Fig. 1-2. Chromosomal mechanisms leading to loss of heterozygosity of chromosome 13 in retinoblastoma. In hereditary retinoblastoma, one germline mutation and one somatic mutation occurs. In non hereditary retinoblastoma, two somatic mutations occur. I: non disjunction, II: non disjunction with duplication of the chromosome, III: mitotic recombination, IV: local mutation. rb, mutant *RB1* allele; + wild-type *RB1* allele; (A and B) (alleles 1 and 2) are polymorphic loci proximal and distal of the *RB1* allele (adapted from Cavenee et al. 1983).

1.2.3 Stability genes

As in the case of tumour suppressor genes, both alleles of stability genes (or caretakers) must undergo mutation in order to contribute to tumour initiation and progression. However, this contribution is indirect because inactivation of stability genes does not directly promote growth of tumours. Rather, the resulting genetic instability causes an increased mutation rate that in turn promotes clonal evolution. Stability genes are involved in mismatch repair (MMR), nucleotide-excision repair (NER) and base-excision repair (BER).

1.3 Retinoblastoma

Retinoblastoma is the most common intraocular malignancy in children with an incidence of 1 in 15.000 – 20.000 newborns [7-9].

The observation of a leukokoria (a white reflection in the pupil) is often the first sign of retinoblastoma, some patients can also show strabismus. Glaucoma, uveitis or blood in the vitreous are rarely the first symptoms but can appear in later stages of the disease. The diagnosis is made by examination of the retina. In addition, ultrasound scan examinations, computer tomography and bone marrow puncture can also be necessary. The treatment chosen depends on the size, the location and the age of the patient. The tumour may be destroyed within the eye using cryo-coagulation, photo-coagulation or radiotherapy. If the tumour is big or has invaded extraocular tissues, the eye is usually removed (enucleation). Treatment of retinoblastoma is very effective, and the survival rate at 5 years is greater than 90%. However, in children with hereditary retinoblastoma, who have a tumour susceptibility because they are heterozygous for an oncogenic *RB1* gene mutation, second primary neoplasms like osteosarcoma, glioma or lipoma can appear in adolescence and adulthood. These are a major cause of long term death of disease.

1.3.1 Genetics of retinoblastoma

Retinoblastoma initiates during retinal development as a result of *RB1* inactivation in the developing retina. According to the Knudson's two-hits hypothesis [10] (Fig. 1-2), two mutations that result in loss of function of both alleles of the tumour suppressor gene *RB1* [11, 12] are a prerequisite for the development of both the hereditary and the nonhereditary form of this tumour

- *Nonhereditary retinoblastoma*
  About 60% of affected children develop retinoblastoma in one eye only (unilateral retinoblastoma). In some of these patients, multiple tumour foci can be discerned (unilateral multifocal retinoblastoma). In most of these children (88-98%), the two mutations that are needed to inactivate both *RB1* alleles have occurred successively in somatic cells.
- *Hereditary retinoblastoma*
  The remaining 40% of children with retinoblastoma have tumours in both eyes (bilateral retinoblastoma) and they often show more than one focus per eye (bilateral multifocal). The majority of these patients are heterozygous for an

oncogenic *RB1* gene mutation that has occurred *de novo* in the germ line of one of the parents or has been transmitted from mutation carrying parent.

Unilateral retinoblastoma is mostly detected later than bilateral retinoblastoma. This is reflected in the median age of the patients at diagnosis which is 11 months for bilateral and 22 months for unilateral retinoblastoma. About 10% of patients with bilateral retinoblastoma have familial disease. Children of patients with retinoblastoma are regularly examined and, therefore the tumour is diagnosed at an earlier stage.

1.3.2 Histopathology of retinoblastoma

Retinoblastoma can present two types of growth in the eye: the endophytical type of growth is characterized by tumour in the vitreous (in front of the retina) and often presents multiple free colonies. In the exophytic type of growth the tumour fills the retro-retinal compartment and thrusts the retina. These two forms of growth can co-occur in the same eye.

The histology is characterized by the presence of rosettes and fleurettes. A rosette (Flexner-Wintersteiner rosette) is a group of cubic cells organized in a tube shape and presenting a lumen containing a vessel. The cells composing the rosettes are primitive photoreceptors. Fleurette is a formation in which the cells are more differentiated than in rosettes, they have the specific shape of photoreceptors and are arranged like the rosette cells around a lumen.

The tumour appears often highly necrotic and calcified foci can be found in areas of necrosis.

1.3.3 The origin of retinoblastoma

The retina is composed of 2 parts: the retinal pigmented epithelium at the outer layer, and the neural retina in the inner layer [13] (Fig 1-3). The neural retina consists of amacrine, bipolar, Müller glia, ganglion, horizontal cells and light sensitive photoreceptors neurons (rods and cones); it begins to differentiate at 4-5 weeks of gestation. The retinal progenitor cells are multipotent and can give rise to all the cell types in the retina, they undergo unidirectional changes in competence. The first rods and cones appear in human embryos at 10-15 weeks, and the horizontal, bipolar and

ganglion cell layers appear in the middle of embryonic development. The retina is fully developed several months after birth.

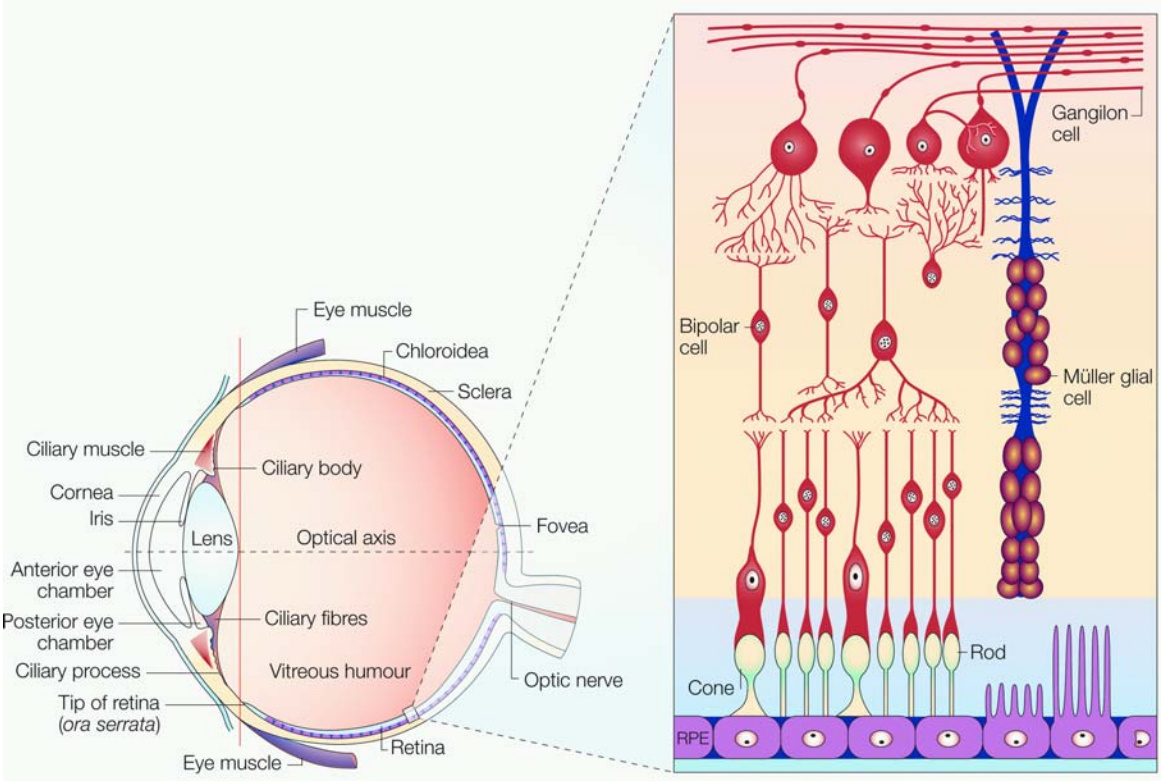

Fig 1-3. Schematic section through an adult human eye. The vertical line divides the anterior segment of the eye (the cornea, lens, iris and ciliary body) from the posterior segment (consisting mainly of the vitreous humour, retina and the choroidea). The panel on the right shows a close-up view of the components of the retina, which are (from the outside to the inside of the retina): the retinal pigmented epithelium (RPE), photoreceptor cells (rod and cone), Müller glial cells, bipolar cells and ganglions cells (modified from Nature Reviews Genetics, November 2003, Volume 4).

The cell of origin of retinoblastoma is not clearly characterised but different models have been envisaged: the progenitor-cell model and the transition-cell model.

The progenitor-cell model proposes that the earliest defect following *RB1* inactivation is a continued division (ectopic proliferation) by a subset of progenitor cells of the retina, thus facilitating the appearance of post-RB mutations (additional genetic defects) necessary to promote transformation. The transformed progenitor cell generated has infinite self-renewal capacity that drives tumour growth [14].

The second cell of origin model is the transition-cell model. The retinal transition cells are not multipotent and not yet fully differentiated, but they are committed to a particular cell type. In this model *RB1* has no action on the progenitor cells but only on the post-mitotic transition cells, and in the absence of *RB1* (inactivation of *RB1*) the

transition-cell differentiation progress uncoupled from cell cycle exit, the transition cells migrate to their final destination and continue to divide.

1.3.4 The RB1 gene

RB1 was the first tumour suppressor gene to be cloned [15]. This gene spans 180 kb on the long arm of chromosome 13 (13q14) and contains 27 exons. The protein is involved in several cellular processes with the most prominent being regulation of the cell cycle. For this aspect of *RB1* function, the transcription factor E2F1 is an important cellular target. Hypophosphorylated pRb represses E2F-mediated gene transcription by recruiting chromatin remodelling complexes to the promoter in the resting cells. At the G1-S phase transition, pRb is hyperphosphorylated by CDK2, CDK4 and CDK6. Hyperphosphorylated pRb releases E2F, allowing it to activate transcription of its target genes (Fig 1-1-a). Thus, an overexpression of pRb causes cells to undergo arrest in G1 phase of cell cycle, and cells deficient in pRb show an accelerated G1 transition. Oncogenic alteration of the pRb pathway can occur by mutational inactivation of the *RB1* or *CDK2* tumour suppressor genes or mutational activation of the genes encoding cdk4 and cyclin D1 oncogenes.

In addition to its role in cell cycle control as a cellular proliferation inhibitor, pRb has a role in DNA replication [16, 17], differentiation [18] and apoptosis [18, 19]. The functions of pRb depend on the cellular context. For example, loss of *RB1* can lead to increase apoptosis in some circumstances, a consequence that is paradoxical to the classification of the *RB1* as a tumour suppressor [20].

1.3.5 Progression of retinoblastoma

Much evidence indicates that the two mutational events, which result in loss of pRB from a developing retinal cell, are not enough for transformation into malignancy. In a murine model Chen et al. [21] showed that *rb1* loss confers infinite proliferative capacity to the cells of origin of retinoblastoma, but – at the same time – renders them more susceptible to apoptotic cell death. This suggests that additional mutations in genes that regulate apoptosis are necessary for tumorigenesis to occur [20].

Furthermore, chromosome-banding studies [22-24] and comparative genomic hybridization [25-28] revealed that other genetic alterations occur during the development of retinoblastoma. One specific chromosomal rearrangement, isochromosome 6p, i(6p), is observed in 60% of retinoblastomas in cytogenetics studies. The presence of an i(6p) results in a low-level genomic amplification of chromosome 6p. Usually the two normal chromosomes 6 are still present [29]. Analysis by fluorescent *in situ* hybridization with probes specific for chromosome 6 suggests that some retinoblastomas without cytogenetic evidence of i(6p) also may have amplification of regions of 6p. This suggests that i(6p) may be important for retinoblastoma formation [30]. Recently, CGH studies have narrowed the region of gains on 6p to the band 6p22 [31].

There are other recurrent genomic alterations in retinoblastoma. These include gains on chromosome on 1q and 2p, and losses of 16q [32-34]. Gains on chromosome 1q have been detected in 40 to 50% of retinoblastomas [24-28, 35]. In one CGH study, the minimal region of gain on the long arm of chromosome 1 was localized to 1q31-q32 [28], a region containing the *GAC1* gene. Losses on 16q have been observed in 18 to 46% of retinoblastomas [25-28]. Marchong et al. defined a minimal region of loss on chromosome 16 at 16q22. This region is known to contain a cluster of cadherin genes, and the results of these authors pointed to *CDH11* as target of loss on chromosome 16. Gains of material on 2p were first observed in retinoblastoma cell line Y79 and in two primary retinoblastomas [36]. The amplification included the *N-Myc* gene, and an overexpression of this gene was also seen. Recently, CGH studies have shown that gains on 2p are present in 10 to 38% of retinoblastomas.

1.4 Aims

The overall aim of the present study was to identify the genes that are the functional targets of genetic alterations in retinoblastoma. This knowledge will provide insight into the biologic alterations underlying the progression of this tumour.

1.4.1 Chromosome 1q gains

The gene(s) targeted by the alterations on chromosome 1 are currently unknown. The aim of the project is firstly to identify this gene(s). The region 1q31-q32 that was identified previously by Herzog et al. contains the *GAC1* (*LRRN5*) gene that has been found to be amplified and overexpressed in malignant gliomas [37]. Next to this region is the *MDM4* gene, which, by amplification and overexpression, contributes to the development of gliomas [38, 39]. However, these genes are only some of many genes located in the region 1q31-q32, which spans about 25 Mb. In the present study we used Quantitative Multiplex PCR and array CGH to identify DNA segments with genomic imbalances in retinoblastoma. We have determined DNA copy numbers of several loci in this region to identify the single gene or the set of genes that are the functional targets of genomic gains. We have used genome-wide RNA expression analysis to evaluate the expression pattern of genes located in these regions. In addition, we have obtained detailed data on the patient's clinical manifestation to find out if clinical behaviour of tumours with genomic gains on 1q is distinct from that of tumours without gains.

1.4.2 Chromosome 16q losses

A previous study based on mapping of the minimal region of losses on 16q indicated that loss of the *CDH11* gene might contribute to progression of retinoblastoma [40]. We have used microsatellite analysis and pyrosequencing to further localise the region of loss of heterozygosity. Moreover, as epigenetic inactivation of tumour suppressor genes is relatively frequent, we have set up a specific methylation assay for *CDH11*. The results we obtained were compared with expression of the corresponding genes.

1.4.3 Chromosome 1p gains

Within the course of the study, array CGH was used to determine gains and losses on a genomic level. The results revealed a novel region of amplification on the short arm of chromosome 1. We combined genomic results and expression data to analyse the possibility of a novel oncogene involved in progression of retinoblastoma.

2 MATERIAL AND METHODS

2.1 Material

Standard chemicals and solutions were obtained from Boehringer Mannheim (Mannheim), Merck (Darmstadt), Sigma-Aldrich (Heidelberg), Serva (Heidelberg), Invitrogen (Karlsruhe), and BD Biosciences (Heidelberg).

2.1.1 Buffers, reagents and solutions

Standard solutions for molecular genetics

10X loading buffer:	0.25% Bromphenol blue or Xylene blue, 15% Ficoll, 10 mM EDTA
Chloramphenicol solution:	34mg/ml chloramphenicol in Ethanol 100%
LB-Medium:	1% Tryptone, 0.5% Yeast extract, 1% NaCl, 30µg/ml Chloramphenicol
LB-Plates:	LB-Medium, 1.2% Bacto-Agar (Difco), 12.5µg/ml Chloramphenicol
TAE-Buffer:	40 mM Tris-Acetat, 1 mM EDTA
TE:	10 mM TRIS-HCL (pH 7.8), 1 mM EDTA
Bisulfite solution:	for a final volume of 20 ml, 8.5 g sodium bisulfite is diluted in 15 ml H_2O under N_2 gas. The solution is then put on a rolling machine to assist complete dissolving. To complete the solution 0.9 ml hydrochinon at 50 mM and 1 ml 10N NaOH pH 5.0-5.3 are then added. Note: the bisulfite solution is light sensitive and, therefore, must be kept in darkness during the preparation and use for treatment of DNA.

Solutions and reagents for Matrix-CGH

20X SSC:	3M NaCl, 0.3 NaCitrat
Wash A:	50% Formamid, 2X SSC, pH 7.0

PN Buffer: 0.1M Na_2HPO_4, 0.1% nonidet P40 (USB Corporation, Cleveland), pH 8.0

2.1.2 Enzymes

AmpliTaq® DNA polymerase (5 U/µl):	Applied Biosystem, Darmstadt
AmpliTaq® Gold DNA polymerase (5U/µl):	Applied Biosystem
PCR Multiplex kit:	QIAgen, Hilden
Desoxyribonuclease I (DNase I) (3 U/µl):	Qiagen, Hilden
DNA Polymerase I, Klenow-Fragment (0.5 U/µl):	Boehringer, Mannheim
Proteinase K (10 µg/ml):	Boehringer, Mannheim

2.1.3 Oligonucleotide arrays

HG-U133A GeneChip® Arrays from Affymetrix Inc. (Santa Barbara, CA) were used for microarray hybridization analysis of RNA expression.

2.1.4 Primary tumours

Samples of retinoblastomas were obtained at the time of operative treatment, snap frozen in liquid nitrogen, and stored at -80°C. Prior to use for research, mutation analysis of the *RB1* gene was performed as part of a routine genetic service. Material from patients with resolved mutational status of the *RB1* gene was used for the present study. In addition, two primary gliomas were also used in the present study (both samples provided by Prof. G. Reifenberger, University of Düsseldorf).

2.1.5 Cell lines

Material from 6 retinoblastoma cell lines was investigated: WERI-Rb1 [41], Y 79 [42], RBL 30, RB 247C3, RB 355 and RB 383 [43]. We also analyzed DNA from a uveal melanoma cell line (Mel202, provided by G. Anastassiou and M. Zeschnigk).

2.1.6 Clones

Recombinant DNA cloned in Bacterial Artificial Chromosomes (BAC) was obtained at the *RessourcenZentrum/Primär Datenbank* (RZPD), Berlin (Table 2-1).

Table 2-1. BAC clones used on Matrix-CGH slides specific for chromosome 1

	Name	***Accession #***	***Genes enclosed in the BAC clones***	***Contig***	***Location***	***Position (Mb)***
BAC 1	RP11-295K2	AL596220	TPR ; C1orf27 ; PDC ; OCLM	NT_004487	1q25-q31.1	
BAC 2	RP11-108M21	AC025702 ; AL391065		NT_004487	1q25.1-1q31.1	182.7 Mb
BAC 3	RP11-207I9	AC022959		NT_004487		
BAC 4	RP11-110P20	AL136371		NT_004487	1q31.1	185.2 Mb
BAC 5	RP11-184F4	AL138927		NT_004487	1q31.1-1q31.3	186.5 Mb
BAC 6	RP11-101E13	AL136370	SSA2 ; UCH37 ; GLRX2	NT_004671	1q31.2-1q31.3	188.5 Mb
BAC 7	RP11-6I13	AL160173		NT_004671	1q31.1-1q31.3	189.1 Mb
BAC 8	RP11-378F16	AL161634			1q31.2-1q32.1	189.5 Mb
BAC 9	RP11-166A4	AL139214		NT_004671	1q31.1-1q31.3	199.2 Mb
BAC 10	RP11-189O8	AL354929		NT_004487	1q31.1-1q31.3	186.8 Mb
BAC 11	RP11-156A19	AL391258		NT_004487	1q31.1-1q31.3	187.1 Mb
BAC 12	RP11-25C18	AL160057		NT_004671	1q31.1-1q31.3	190.3 Mb
BAC 13	RP11-173E24	AL138926		NT_004671	1q31.1-1q31.3	190.9 Mb
BAC 14	RP11-88D12				1q31.3	191.2 Mb
BAC 15	RP11-80J4				1q31.3-1q32.1	192.1 Mb
BAC 16	RP11-91G12				1q31.3	192.3 Mb
BAC 17	RP11-332L8	AL513325	CRB1	NT_004671	1q31-q32.1	
BAC 18	RP11-448G4	AL365258	MGC27044	NT_004671	1q31.3-1q32.1	193.1 Mb
BAC 19	RP11-401A10	AL391627 ; AC093561	NEK7	NT_004671	1q31.3-1q32.1	193.6 Mb
BAC 20	RP11-553K8	AL157402	PTPRC ; ATP6V1G3	NT_004671	1q31.2-1q31.3	194.0 Mb
BAC 21	RP11-31E23	AL136321		NT_004671	1q31.3-1q32.1	194.3 Mb
BAC 22	RP11-109H10	AL139129 ; AC099673		NT_004671	1q31.1-1q32.1	194.7 Mb
BAC 23	RP11-249C10				1q31.3-1q32.1	195.6 Mb
BAC 24	RP11-65I22				1q32.1-1q32.1	198.1 Mb
BAC 25	RP11-150L7				1q32.1-1q32.1	196.6 Mb
BAC 26	RP11-532L16	AC097065 ; AL358153		NT_004671		
BAC 27	RP11-465N4	AC099676 ; AL512787	RNPEP ; LMOD1 ; ELF3 ; TIMM17A	NT_034408	1q32	
BAC 28	RP11-494K3	AL391822	NFASC	NT_034410	1q32.1	
BAC 29	RP11-80N9	AC096675 ; AL136142		NT_034410	1q32.1-1q32.3	200.3 Mb
BAC 30	RP11-23I7	AL161793	GAC1	NT_034410	1q32.1-1q32.3	200.2 Mb
BAC 31	RP11-430C7	AL512306	MDM4 ; GAC1	NT_034410	1q32.1	
BAC 32	RP11-563I16	AL450424				
BAC 33	RP11-284G5	AC048369				
BAC 34	RP11-203F10	AC024685 ; AL592114	REN ; KISS1 ; PEPP3 ; LOC149267	NT_034410		
BAC 35	RP11-74C13	AL592146	SOX13 ; REN ; FLJ10761	NT_034410		
BAC 36	RP11-335O13	AL357133	MYBPH ; ADORA1 ; CHIT1 ; CHI3L1	NT_034409	1q32.1-1q32.3	198.5 Mb

BAC 37	RP11-90O23	AL513343	ATP2B4	NT_034410	1q32.1	210.7 Mb
BAC 38	RP11-69I9	AL359927			1q32.1-1q32.3	200.5 Mb
BAC 39	RP11-6B6	AC096533 ; AL365261	Prostein ; ELK4 ; DKFZp761N1114	NT_034410	1q32.1-1q32.3	201.1 Mb
BAC 40	RP11-164O23	AL445493	C4BPB ; C4BPA ; PFKFB2 ; PRO0907	NT_021877		
BAC 41	RP11-156F12	AC024509 ; AC092806	SDCCAG8	NT_004734	1q44	238.7 Mb
BAC 42	RP11-348A7	AL391730	SCMH1 ; FLJ23878 ; CTPS	NT_077386		
BAC 43	RP11-285F7	AC058782 ; AL591895	KIAA0792 ; EPHX1	NT_004525	1q42.1	
BAC 44	RP11-115P16	AC073252 ; AL365444	ITPKB	NT_004525	1q42	222.6 Mb
BAC 45	RP11-454L1	AL365178	MCP ; CR1L	NT_021877		
BAC 46	RP11-385M4	AC092810 ; AL357038		NT_021877		
BAC 47	RP11-75I2	AC096636 ; AL358977	KCNH1 ; FLJ10724	NT_034412	1q32-q41	
BAC 48	RP11-565J7	AC092814 ; AL357036	DKFZP434B168 ; RAMP	NT_021877	1q32 1p36-q42	

From the NCBI database, http://www.ncbi.nlm.nih.gov/. All clones have the vector pBACe3.6 and were provided from the *RessourcenZentrum/Primär Datenbank* (RZPD), Berlin.

Table 2-2. Primers used for the Methylation Specific PCR of *CDH11* between methylated/modified and unmethylated/modified

Primer Set	Sense primer (5'-Forward)	Antisense primer (3'-Reverse)	Size (bp)	Anneal temp.	Position
***CDH11*-Meth**	T**C**GGAG**C**G**T**G**C**G**TT**A**C**G	G**AAAA**CCGACCCCGTCCG	98	64°C	-757
***CDH11*-Unmeth**	GGAGT**T**GGAG**T**G**TT**G**T**GT**TT**A**T**GGGG**T**	CT**A**C**A**A**AAA**CC**A**ACCCC**A**TCC**A**C**A**	106	64°C	-761

Bold: sequences differences between modified primers and unmodified DNA= modified because of bisulfite treatment. Underlined: differences between methylated/modified and unmethylated/modified

2.1.7 Primers and Probes

Sequences of oligonucleotide primers for PCR and sequencing were chosen using the Primer3 software (http://frodo.wi.mit.edu/cgi-bin/primer3/primer3_www.cgi), data available through databases at the NCBI (**http://www.ncbi.nlm.nih.gov/**), Primer Express software (version 2.0; ABI) for the Real Time PCR, and the DNASTAR software package (DNASTAR, Madison, WI, USA). All forward primers used in Quantitative Multiplex PCR were labelled with a 6-FAM fluorescent dye.

DNA oligonucleotides were custom synthesized by different companies: Biomers, Ulm, Germany; Applied Biosystems, Darmstadt, Germany; and Eurogentec, Seraing, Belgium.

2.1.8 Equipment

PCR Machines: GeneAmp® PCR System 9700 (Applied Biosystems)
GeneAmp® PCR System 2700 (Applied Biosystems)
Peltier Thermal Cycler 200 (MJ Research)

Capillary electrophoresis for sequencing and microsatellite analysis:
ABI PRISM® 3100 Genetic Analyzer (Applied Biosystems, Foster City, CA, USA)

Real-Time quantitative PCR, TaqMan®: ABI PRISM 7000 Sequence Detection System (Applied Biosystems)

Pyrosequencing™ machine: PSQ™HS 96A System, Pyrosequencing™ Vacuum Prep Workstation (Uppsala, Sweden)

2.2 Methods

2.2.1 Cell culture

Culture of retinoblastoma cell lines was performed by Harald Stephan at the Children's Hospital (Div. of Haematology and Oncology), University of Duisburg-Essen. Cell lines were cultivated in DMEM with 15% foetal calf serum, 100 U Penicillin/ml, 100 µg streptomycin/ml, 4 mM L-glutamine, 50 µM ethandiol and 10 µg insulin/ml at 37°C, 10% CO_2 and 80% humidity.

2.2.2 DNA extraction from blood samples

Genomic DNA was extracted from peripheral blood using the Nucleon BACC2-Kit (Amersham LIFE SCIENCE) according to the protocol supplied. In brief, 2 to 5 ml blood is collected and mixed up with 40 ml reagent A for 4 min on a rotating device. Leucocytes pellets are formed by centrifugation for 4 min at 3,500 rpm at room temperature (RT), and the supernatant is discarded. Reagent B (2 ml) is added to resuspend the pellet. Sodium perchlorate solution (500 µl) is added and after 20 min in an agitating water bath at 65°C, protein is removed and DNA extracted by mixing with 2 ml cold chloroform. Phases are separated by centrifuging for 1 min at 3,000 rpm. Without remixing the phases, 300 µl Nucleon resin is added to the tubes and spun down for 3 min at 3,500 rpm. The phase above the Nucleon resin layer, which contains the DNA, is transferred to a clean tube and spun down for 3 min at 3,500 rpm. DNA is precipitated from the supernatant in a fresh tube with 4 ml of cold absolute ethanol. The precipitate appears after mixing by inversion. The DNA is removed with a melted tip of a Pasteur pipette, washed in 70% ethanol, dried in the air for 15 min and dissolved in TE buffer on a rolling device for about 2 days.

2.2.3 DNA extraction from tumour samples

The tumour sample is homogenized in a glass homogenisator or using a Pasteur pipette in 250 µl of 75 mM NaCl/24 mM EDTA/10mM Tris HCl pH 8 and transferred in a 1.5 ml tube. After addition of 250 µl of 75 mM NaCl/24 mM EDTA, 25 µl 10% SDS and 10 µl Proteinase K (10 mg/ml) the mix is vortexed and incubated for 4 hours at 37°C in a water bath or on a rotating thermomixer (850 rpm). Phenol (300 µl) is added, mixed, and the sample is spun down 3-5 min at 13,000 rpm. The aqueous (upper) phase is collected with a pipette and transferred in a new tube. After adding 300 µl of chloroform/isoamylalcohol (96% $CHCl_3$/ 4% IAA) the solution is well shaken and centrifuged 3-5 min at 13,000 rpm. The last two steps have to be repeated 2 times. Next, the upper phase is transferred to a new tube, and 50 µl NaOAc and 900 µl 100% ethanol are added. The DNA precipitates from the solution after inverting the tube. The DNA is removed, washed in 70% ethanol, 15 min dried in the air, and dissolved in TE buffer (on a rolling device for about 2 days).

2.2.4 DNA extraction from BAC clones

Bacteria are grown in LB medium (with 30 µg/ml Chloramphenicol) overnight in a shaking incubator (New Brunswick Scientific G26) at 37°C and 275 rpm. For DNA extraction we adapted the QIAgen Plasmid Purification protocol. The first steps of preparation from buffer P1 to P3 are identical to the original protocol from QIAgen.

For preparation of analytic DNA amounts ("mini-preparation") a bacterial colony is incubated overnight in 5 ml LB medium. 1.5 ml of the overnight culture is centrifuged 3 min at 5,000 rpm and the pellet is taken in 300 µl Buffer P1 (50 mM Tris HCl pH 8.0, 10 mM EDTA ph 8.0, 100 µg/ml RNase A). After the addition of 300 µl Buffer P2 (200 mM NaOH, 1% SDS) the mix is incubated for 3 min at RT. 300 µl Buffer P3 (3M KOAc pH 5.5) are added and spun down 15 min at 10,000 rpm and 4°C. The supernatant is taken out, 500 µl 100% ethanol is added and, after inversion, the tube is centrifuged for 25 min at 13,000 rpm and RT to precipitate the DNA. The pellet is washed with 70% ethanol, dried and dissolved in 20 µl RNase solution (50 µg/ml RNaseA, 20 Units RNase T1 in H_2O) and incubated 1 hour at 37°C.

To extract large scale amounts of BAC-DNA ("maxi-preparation"), 900 µl of the overnight culture is incubated in 150 ml LB medium, overnight at 37°C and 275 rpm. The cells are harvested by centrifugation for 20 min, 4,500 rpm and RT, and the pellet resuspended in 20 ml Buffer P1. 20 ml Buffer P2 is added and the mix is incubated for 3 min at RT. Chilled Buffer P3 (20 ml) is added, the suspension is incubated for 15 min on ice, and centrifuged for 30 min at 10,000 rpm and 4°C. The supernatant is removed and centrifuged again for 15 min at 10,000 rpm and 4°C. The supernatant is applied to the QIAGEN-tip 500 (equilibrated before with Buffer QBT: 750 mM NaCl, 50 mM MOPS pH 7.0, 15% ethanol, 0.15% TritonX-100). After all the supernatant has flowed through, the column is washed 2 times with 30 ml Buffer QC (1 M NaCl, 50mM MOPS pH 7.0, 15% ethanol). The DNA is finally eluted with 5 ml hot Buffer QF (1.25 M NaCl, 50 mM Tris-HCl pH 8.5, 15% ethanol). The DNA is precipitated by adding 3.5 ml isopropanol, mixed and centrifuged at 10,000 rpm for 30 min and at 4°C. The DNA is washed with 70% ethanol, air-dried, dissolved in 100µl RNase solution and incubated for 1 hour at 37°C.

2.2.5 Restriction cleavage of DNA

For enzymatic digestion, 2 µg of BAC DNA are used. The DNA is mixed with 10 to 20 Units restriction enzyme and restriction buffer concentrate in a total volume of 20 µl. The restriction enzyme is stabilized by adding 0.1 µg/µl BSA. A complete cleavage of BAC DNA is reached 2 to 3 hours after begin of the reaction. The results of digestion are then determined by electrophoresis in 1% agarose gels.

2.2.6 RNA extraction from tumour samples

The protocol of RNA extraction is an adaptation of the QIAgen RNeasy Mini Protocol for Isolation of Total RNA from animal tissues (QIAgen, Hilden, Germany). All the buffers and columns that are contained in this kit are used excepted when specified. A 30 µg tumour sample is placed in 800 µl Buffer RLT (ß-ME 10µl/ml, Sigma-Aldrich, Taufkirchen, Germany) in a Lysing Matrix D column (Q.BIOgene, Heidelberg, Germany) and grinded in the Lysing Matrix for 45 s at 6.5 (Fast Prep, FP 120, Bio 101 Systems, Q.BIOgene). Dry ice is used to cool down the sample after grinding. At room temperature, the samples are shaken, vortexed and spun down for 5 min at 13,000 rpm at 4°C. The supernatant is taken out and placed in a new 1.5 ml tube, and spun down again in the same conditions as before. Leaving the protein pellet intact, the supernatant is placed in a 1.5 ml tube to which 750 µl Ethanol 70% is added, and then vortexed. The 1.5 ml solution obtained in this step is then placed on an RNeasy mini spin column and centrifuged for 15 s at 10,000 rpm at 4°C (in 2 steps). The flow-through is discarded. Digestion with DNaseI (QIAgen) is used to avoid the presence of DNA in the final extract. For this, 350 µl Buffer RW1 is added to the spin column and centrifuged for 15 s at 10,000 rpm. The flow-through is discarded. A mix of 10 µl DNaseI stock solution and 70 µl buffer RDD is thoroughly pipetted on the membrane of the column and incubated for 15 min at room temperature. After adding 350 µl buffer RW1 the column is centrifuged for 15 s at 10,000 rpm. The column is then placed on a new collection tube, 500 µl buffer RPE (with Ethanol) is added and spun down for 2 min at 13,000 rpm. The column placed on a new collection tube and the RNA is eluted with 50 µl RNase free water by centrifugation for 1 min at 10,000 rpm. The elution step is repeated one time.

2.2.7 DNA bisulfite treatment

Sodium bisulfite treatment modifies DNA by converting unmethylated, but not methylated, cytosines to uracil (see example below):

Genomic DNA (2µg/50µl) is mixed up with 5.5 µl 3M NaOH, incubated 15 min at 37°C, denatured 2 min at 95°C and placed on ice. As a positive control we also treated methylated DNA (2µg/50µl Q-BIOgene, CpGenome™ Universal Methylated DNA). The denatured DNA (55 µl) is then mixed with 500 µl of bisulfite solution overnight at 50°C in darkness. The bisulfite is then removed with the Wizard® DNA Clean-Up kit (Promega Corporation, Madison, USA) using a vacuum manifold. The treated DNA is mixed with 1 ml Wizard® DNA Clean-Up Resin, and pipetted into the syringe barrel put on a minicolumn connected to the vacuum. The vacuum is applied to draw the solution in the minicolumn and is then broken. The column is washed with 2 ml 80% isopropanol and the help of the vacuum (the vacuum can be applied 30 s longer after the solution has been pulled through the minicolumn to dry the resin). The column is transferred to a 1.5 ml tube, centrifuged 2 min at 10,000 rpm, placed on a new 1.5 ml tube and eluted with 50 µl H_2O (65°C) incubated 1 min and centrifuged 20 min at 13,000 rpm. If necessary, the concentration of the DNA is increased by reconcentration (see below). Bisulfite treated DNA is used as a template for Methylation Specific PCR (MSP).

2.2.8 Reconcentration of the DNA/RNA eluates

DNA eluate is mixed with 5.5 µl 3M NaOH and incubated for 15 min at 37°C. After addition of 55 µl 6M NH_4OAc pH 7, 1 µl Glycogen (5 mg/ml, Roche, Mannheim, Germany) and 350 µl 100% ethanol is mixed and centrifuged for 20 min at 13,000 rpm.

The DNA pellet is washed with 300 µl 70% ethanol and again centrifuged for 5 min at 13,000 rpm. After the removal of the supernatant, the pellet is dried in a SpeedVac (SpeedVac Concentrator, Bachofer, Reutlingen) for 7 min with heating. The DNA is finally resuspended in 30 µl H_2O.

RNA eluates of individual sample preparations are pooled together. Glycogen (1 µl at 5 mg/ml, Roche), 3M NaOAc pH 5.2 (1/10 Vol., Sigma-Aldrich) and Ethanol 100% (2.5 Vol.) are added. The RNA is precipitated at -20°C for at least 1 hour and pelleted by centrifugating for 20 min at 4°C at 13,000 rpm. The supernatant is removed and the RNA pellet is washed with Ethanol 75% and again centrifuged 2-3 min at 4°C at 13,000 rpm. The washing step is repeated 2 times. The pellet is dried on a thermoblock at 30°C (Thermomixer comfort, Eppendorf, Hamburg, Germany) for 5 to 10 min. The pellets are finally dissolved in water for 20 min on ice. The RNA is stored at –80°C.

2.2.9 Measurement of DNA and RNA concentration

The DNA and RNA probes are diluted in water and light absorption at 260 and 280 nm is determined in a spectral photometer Ultrospec III (Pharmacia). An absorbance of 1 at 260 nm (OD_{260}) corresponds to 50 µg/ml double stranded DNA, 33 µg/ml simple stranded DNA, and 40 µg/ml RNA. Therefore, the OD_{260} is multiplied with the factor 50 or 40 and the dilution factor to obtain the nucleic acid concentration in µg/ml for DNA or RNA, respectively. The quotient OD_{260}/OD_{280} is determined to estimate the proportion of protein contamination in the solution. A DNA solution that is protein-free has a quotient of 1.8 and the corresponding value for RNA is between 1.8 and 2.1.

2.2.10 PCR analyses (with and without labelled primers)

The reactions are carried out and modified according to the work of Saiki et al. [44] and Mullis und Faloona [45]. As polymerase the thermostabile *AmpliTaqGold*® DNA Polymerase (Applied Biosystems) was used. Reactions were performed in 20 µl reaction volume tubes or in 96 wells “optical plates” (Applied Biosystems). The final reaction mix (20 µl) contained 1 Unit *AmpliTaqGold*®-Polymerase (5 U/µl), 1 mM $MgCl_2$ (0.8 µl at 25 mM), 0.5 µM of each 5’- and 3’ primer (1 µl of a primer mix at 10 µM), dNTPs (each at 1.25 mM), 1X reaction buffer (50 mM KCl, 10 mM Tris-HCl (pH 8.3), 0.001%

Gelatine; 2 µl) and 50 ng DNA. The thermal profile of the reaction was as follows: initial denaturation and polymerase activation for 10 min at 95°C was followed by 35 cycles of denaturation (25 s, 95°C), annealing (30 s, at the appropriate temperature for each primer pair) and elongation (30 s, 72°C). Subsequently an extended synthesis time of 7 min at 72°C was added to reduce the variation introduced by nontemplate nucleotide addition. Control reactions without DNA were performed in each set of PCRs.

2.2.11 Methylation Specific PCR (MS-PCR)

Two PCR reactions are performed for each DNA sample. One is specific for methylated *CDH11* alleles, and one specific for unmethylated alleles. This specificity is provided by the primer pair sequences that hybridize to the target sequences corresponding to bisulfite treated methylated and unmethylated alleles (Table 2-2). The PCR mixture contained 3.5 Unit *AmpliTaqGold*®-Polymerase (5 U/µl), 1X reaction buffer (50 mM KCl, 10 mM Tris-HCl (pH 8.3), 0.001% Gelatine; 2 µl), dNTPs (each at 1.25 mM), 1.25 mM $MgCl_2$ (1µl at 25 mM), 1 µM primer of each primer (1 µl of a primer mix at 20µM), and bisulfite-modified DNA (~150 ng) in a final volume of 20 µl. The PCR reactions were conducted as mentioned before, with an annealing temperature specific for each primer pair. Controls without DNA and with bisulfite treated artificially methylated DNA were performed in each set of PCRs.

2.2.12 Quantitative Multiplex PCR (QMPCR)

Our methodology for QMPCR is based on the protocol that was developed by the group of B. Gallie [31] for deletion analysis of the *RB1* gene. We established multiplex reaction sets to determine relative DNA copy numbers of 30 loci on chromosome 1q (Table2-3). Two control targets located on chromosome 6 and chromosome 10 were included in each set. Sequences of primer pairs were chosen using the Primer3 program (http://frodo.wi.mit.edu/cgi-bin/primer3/primer3_www.cgi) and data available through databases at the NCBI (http://www.ncbi.nlm.nih.gov/). All forward primers were labelled with a 6-FAM fluorescent dye (Biomers, Ulm, Germany). For multiplex PCR, the QIAgen Multiplex PCR kit was used (QIAgen, Hilden, Germany). Individual

reactions contained 12,5 µl QIAgen reaction mix, 2,5 µl primer mix (each primer at 1,75µM) and 150 ng DNA in a final volume of 25 µl. Cycling was performed in a GeneAmp PCR System 2700 (Applied Biosystems, Foster City, CA, USA) with a denaturation step of 15 min at 94°C; 19 cycles of denaturation (30 s at 94°C), annealing (90 s at 58°C or 60°C), extension (90 s at 72°C); and a final extension step at 72°C for 10 min. Only 19 cycles were used to stay in the exponential phase of amplification, which is a prerequisite for comparative quantification.

Calculation of relative copy number

For normalization of values, peak areas of each product within one QMPCR were divided by the peak area of the control locus on chromosome 10q obtained in the same reaction. To determine the relative DNA copy number for each locus, normalized peak integrals were compared to the mean of the values obtained in normal control DNA (constitutional DNA from 5 healthy individuals, Fig. 2-1). Numerical processing of QMPCR data was performed with Excel 2000 (Microsoft). According to this algorithm, a value of ‘1’ was obtained for loci with a DNA copy number of 2. As a control we investigated the uveal melanoma cell line, Mel 202, which has 3 copies of the entire chromosome 1 as determined by cytogenetics analysis (Nareyeck G., Zeschnigk M. et al. manuscript under revision). The corresponding DNA copy number value was 1.5. We validated our methodology by analysis of DNAs from gliomas with known amplification of a region in 1q that includes the *MDM4* gene [38, 39]. For subsequent evaluation by Significance Analysis of Microarrays (cf. “Expression analysis”) and comparisons with CGH data, samples were considered to have gains of material of the 1q32 region if more than one marker in this region showed a value equal or higher than 1.5.

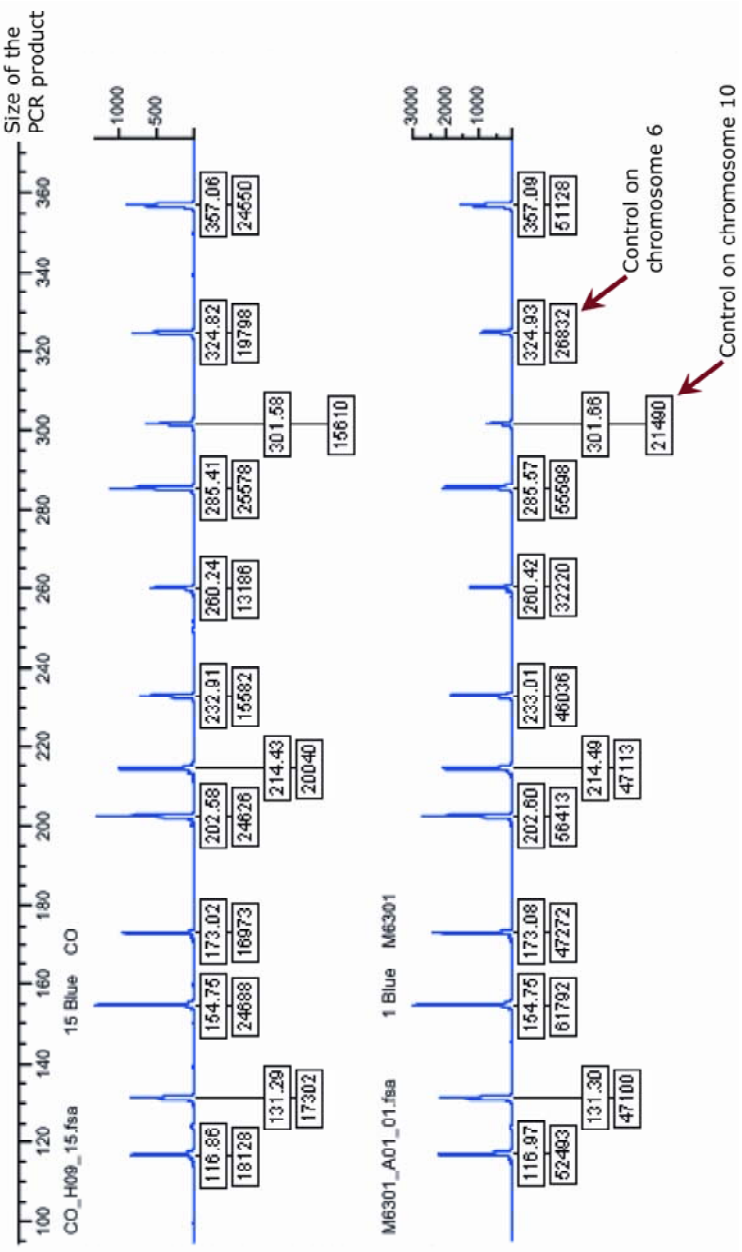

Fig. 2-1. QMPCR electropherograms with results from DNA from a normal person and a tumour (M6301). The upper square indicates the size of the PCR product, the lower square indicates the area under the curve.
Example of calculation from the copy number, with the first PCR product, the control on chromosome 10 and one normal person only: (52493/21490)/(18128/15610)=2.10

Table 2-3. Loci analysed by QMPCR (NCBI database)

Locus	Gene Symbol	Position (kb)	Name/ Location	Forward Primer	Reverse Primer	Size	PCR Set
1q21	*GJA5*	144,735	RH69491	CGAGAGAGGACAACAGCTTC	TGATGTTGCAACCTTTCCTT	247bp	3
	MCL1	147,763	SHGC-34987	GACCTTATGGCTCTGAGATGG	TCAGTCTCGGAACATGACCT	119bp	5
	ENSA	147,811	Intron 1	TCGTTCCACCAAAATCACTT	ACAGGCCCAGTTTCTATTCC	204bp	5
	LASS2	148,154	IB3045	GTCCCTCTGCTGAAATGCTA	CAAAAAGTGGGGGCTGTACT	260bp	5
	HTCD37	148,197	D1S2426	AGTCAAACTGTCCCCCTCAT	TTTTTAACGCAACCCTTTCC	134bp	5
	SNX27	148,801	Exon 12	CCAGGCCATGCACATTTA	CCACACAACCCAAAGGATT	284bp	5
	JTB	151,163	RH63845	GGCTCCAAAGAACCAAGAGT	TGGAACAACGCTTATTTTGG	233bp	5
	ADAR	151,771	SHGC-2343	TCAAGGAATGCACAGTAGCC	GAAACGAGCCGTGTCAGAT	215bp	5
	SYT11	153,046	Exon 4	GACAGTGGTGGTCCTCAAAG	GCAAGGATCTTGAAGTGTGG	156bp	5
1q32	*ZNF281*	197,663	RH71424	TACGTAACAGCGCAGACAGA	AAGGCTGTAATTCCATCAAGC	174bp	5
	ELF3	199,265	RP11-465N4	AGCTCCCACTCCTCAGACTC	CTTGCAGTCACGAAAACCAT	238bp	2
	MYOG	200,340	SHGC-11939	TAGGCCAGACTATCCCCTTC	CTCCCCCTTCTTCTCTCTCA	340bp	4
	FMOD	200,598	WI7331	TGGGTAGCTCTTTGAAGGTG	GGACAAACCAGGTGAAACAG	354bp	3
	LAX	200,916	SHGC-85748	CCTGGGTCTTCATTCATCAG	TTATGCAGACTTTCAGCCATTCA	175bp	4
	SNRPE	201,008	SHGC-76200	TGGATCAAGACATGGAAGGT	CGCCTCTCGTAAATTCTGG	206bp	3
	SOX13	201,219	Exons 3&4	TGCTTGGGTTCCTTAGAGTG	AGGTGGGAGGACTGTTTAGG	265bp	2
	REN	201,301	RP11-74C13	ACAAACCTGAGCCTCTGTCC	GCCCAACTTACGGTGATGAT	159bp	2
	PEPP3	201,365	G20493	AAAAGAATGCTGCTGAAAGG	GGCCTTAGAAGAAGGGTGAA	167bp	3
	PIK3C2B	201,569	WI-11932	CAATTCCCGAGAAAGGAGAT	TACTGGCTTTGTGCCTGTAGC	120bp	1
	MDM4	201,629	Exon 10	GATGTCCCTGATTGTCGAAG	GCAATCCTCCATGTTTTCTG	219bp	1&2
	LRRN5 (GAC1)	201,763	R43317	AAAGAGTGAATCGGGTTGGG	GAGGCCACTCCATCTCACCT	201bp	1
	CNTN2	202,189	WI-15551	GGAAAGGATGGCCCATTTAT	CTGGTATTGGGAGGTTTCTG	158bp	1
	RBBP5	202,233	SHGC-35381	TCAGAAAGGGAACAACGAAG	GATTCTTTGCTGGAGATGGA	186bp	1
	HUCEP11	202,393	G62057	CCCAAGTCAGGAAGACCATT	TCACTCTCCAGCCTTCATCC	128bp	3
	RAB7L1	202,915	SHGC-76255	TTGCAGGTGTTCAAACCAAT	ACTTCGGTGGTTTGTTGTGT	206bp	4
	IKBKE	203,727	RH70483	CAAAGGCCACATTTATTCCA	CCACCTCAGGCAACATAGAG	223bp	4
	RASSF5	203,764	D1S3553	GAGCAACACAACCAAAGAAGG	TACTAAAGCACAGTTAGACCCAAGG	130bp	4
1q41	*CENPF*	211,833	Intron 4	TGAGCTACTGGATTGAGCTTTT	CCTGCAAGGCTTTAACCTCT	357bp	5
1q42	*COG2*	227,813	SHGC-35435	GGGAAGCCATCCTCCACTC	GAGGTCTTTCCTACTGGCGC	100bp	2
1q44	*SMYD3*	242,859	RH122476	CTTAAACCTCCTCCCCAGAA	TTTAATGGATCCAAGGAGCA	276bp	3
6q	Control I		SHGC-84483	AGGAAATGGAAGGGATTCTGAAG	TGGTAAAGGTTTCATGGGAAAGA	325bp	1,2,3,4,5
10q	Control II		SHGC-78184	AGCTGCCACATAAGCCAGATAAG	CTGGGCTGATAATCCAACCATAG	301bp	1,2,3,4,5

2.2.13 Quantitative Microsatellite Analysis Real Time PCR: QuMA

We assessed the DNA copy number at 3 loci using the quantitative real-time PCR assay described by Ginzinger et al. [46], Fig 2-2. The QuMA technique allows analysis of allelic imbalance that result in loss or gain of a single copy of a gene; it determines DNA copy numbers by Real time PCR using Taqman probes specific for CA-repeat motifs. We selected 3 microsatellite loci: D1S2668 (centromeric to *REN* gene), D1S504 (contained in *GAC1* gene) and D10S548 (control located on chromosome 10, known to have no genetic alterations in retinoblastoma by means of CGH).

An additional primer pair and specific probe were designed for the *MDM4* gene in the exon 10, as no microsatellite was available in this gene. As reference for *MDM4* we used *AS-SRO* gene product located on chromosome 15. The primers and probes were designed using the Primer Express software (version 2.0; ABI). Quantitative Real-Time PCRs were performed in a 25µl volume reaction containing 50 ng of DNA, 12,5 µl 1×TaqMan Universal PCR Master Mix, 300 nM of each primer and 250 nM of the TaqMan probe (ABI, Foster City, Calif.). Cycling was performed with 2 min at 50°C and 10 min at 95°C for denaturation and activation of the polymerase, and 40 cycles with a step at 95°C for 15 sec (denaturation) and a step at 60°C for 1 min (annealing).

The primer sequences used are as follow:

Table 2-4. Sequences of probes and primer pairs used in Real Time PCR.

	Sequence	**Gene**
CA-repeat probe	VIC-TGTGTGTGTGTGTGTGT-MGB	
D1S504-R	AAGGTTACATGGAGCCGTGTGT	GAC1
D1S504-F	GTTGAAGGTCAAAGTGTGGAAA	
D10S548-R	CTGCTCATAATCTTGGTTGTG	Control on
D10S548-F	TATTGAGGTATAGGGACAGGG	chromosome 10
D1S2668-R	ACTGACTGGCTGTTTCTGAG	REN
D1S2668-F	AATCACTTGAACCTGGGAG	
MDM4-R	CGACAGGAGCCGAAATGGT	
MDM4-F	TCACTGCCATACCTGAAAAGGA	
MDM4 probe	6FAM-AAGAAGGAAATGATGTCCCTGATTGTCGAAG-TAMRA	
AS-SRO-F	GCTCCATCCCAGGGTTTCTAAT	Control on
AS-SRO-R	GCACTTGTTCGAAATGCAGATT	chromosome 15
AS-SRO probe	FAM-TCAGGGTTTGGTTTGCGGCAGAA-MGB	

PCR was carried out using the ABI Prism 7000 Sequence Detection System (ABI). All reactions were performed in duplicate. Standard curves for all 10 assays were performed with 125 ng, 100 ng, 50 ng, 25 ng and 12.5 ng of DNA. As the efficiencies of all the PCR we not equal we couldn't use the Comparative C_T method, therefore we performed quantification using the standard curve method, with a control on chromosome 10 or AS-SRO as calibrators. We calculated the N value (ratio of the copy number of target gene to the copy number of reference gene, [47]) for each of the genes.

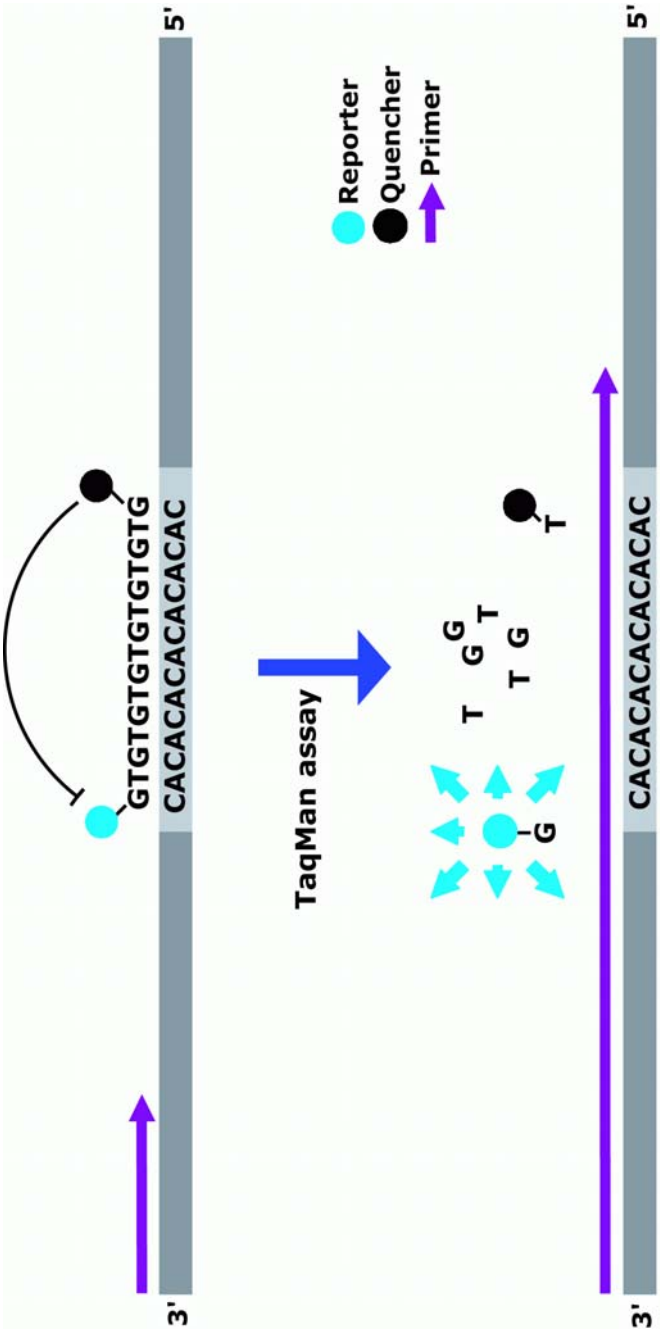

Fig 2-2. Principle of QuMA. The probe is specific to the CA-repeat sequence, which is common to all STR-loci analysed here. Probe molecules that are bound to the single stranded template (3'-5') are degraded as the Taq polymerase synthesizes the new DNA strand (5'-3'). As physical proximity of reporter and quencher is lost after degradation, the reporter becomes fluorigenic.

2.2.14 MSA for LOH study

For microsatellite analysis (MSA) 10 polymorphic microsatellite loci, all dinucleotide repeats $(CA)_n$ were chosen. To identify allele loss on the long arm of chromosome 16 the genotype of constitutional cells was compared to that obtained from DNA of tumour cells. We analyzed 2 loci on the short arm of chromosome 16, and 8 on 16q (2 in the centromeric region, 2 in the telomeric region, and 4 in the minimal region of loss 16q22, Table 2-5).

PCR was performed in two multiplex reactions each containing primer pairs for 5 products. The concentrations of the primers were adjusted to obtain balanced signals in the ABI PRISM® 3100 Genetic Analyzer. For the multiplex PCR, the QIAgen Multiplex PCR kit was used (QIAgen, Hilden, Germany) and the PCR protocol used was the same as for QMPCR (with an annealing temperature of 58°C).

Table 2-5. Loci analysed by MSA. The forward primer was labelled (FAM, PET or NED)

Location and Position (bp)	Name	Primer Sequence (Forward and Reverse)	PCR set	C° µM	Size bp
16p	D16S3093	FAM-gaaacaagggcaaaactcca gaataaagggaaggtacacctacat	2	1.75	237
16p	D16S3068	FAM-ccctgtagcaaaatttcacc ccgccacagtaaagattagg	2	1.75	104
16q 47333372	D16S409	PET-tgtgaatcttacatcccatcc agcttttagagtcagtctgtcca	1	1.8	150
16q 48240903	D16S3080	PET-ggatgcctgctctaaataccc cccaggggtcaaacttaatc	1	2.1	179
CDH11 63624548	D16S3050	NED-acagggtaatcgttcttcca gcaaactggcttgtgatttc	1	1.75	189
CDH5 65853212	D16S421	FAM-acacatgaaccgattggact ttaacatgttcctccgttcc	1	1.6	225
 66225096	D16S3085	NED-ctgggtgacagaacaagacc caggacactaagccggaaat	2	1.75	190
CDH3 67123897	D16S3025	FAM-tccattggacttataaccatgc gagacatctggggacaagaa	1	1.5	100
16q 85642280	D16S3074	PET-acatgtgctcaccaacacac ttgggtttccaaagtcagtc	2	1.75	174
16q 85862067	D16S3048	PET-tcggaggatcactggaagt gtagtgtcctgggggatttc	2	1.75	280

2.2.15 Electrophoresis and analysis

2.2.15.1 Agarose Gel electrophoresis

To verify the efficiency and specificity and to estimate the amount of DNA (BAC DNA) electrophoresis was performed in gels containing 1-3% agarose. Agarose powder was cooked in 1x TAE buffer, cooled down to 65°C. After adding 0.4 ∝g/ml Ethidium bromide the solution was poured in gel trays. From a 20 µl PCR reaction, 5 µl were loaded on the gel. The probes were previously mixed with loading buffer (end concentration 1x), and separated by applying a 3 V/cm field in 1x TAE Buffer containing 0.4 ∝g/ml Ethidium bromid. Different size standard were used: 1 kb ladder (Invitrogen), *Msp*I-splitted pUC19 DNA (MBI Fermentas, St.Leon-Roth) und *Hin*dIII-cut Lambda-DNA (Boehringer). Stained DNA was visualized with a UV-light transilluminator (302 nm) and documented on thermosensitive paper with a digital photo-system (Herolab, Wiesloch).

2.2.15.2 Automatic Capillary Electrophoresis (Genescan and Sequencing)

Automatic electrophoresis and multi-colour fluorescence-based DNA detection was performed with a 16 capillary analysis system (ABI PRISM® 3100 Genetic Analyser, Applied Biosystems). The recommended polymer (POP-6™, Applied Biosystems) was used for separation. In this analysis system the DNA fragments are separated according to their size. The fluorescence labels attached to the fragments are detected by a stationary unit consisting of a laser (for fluorescence excitation), a mirror for spectral separation, and a CCD camera that converts the luminescence signal into digital data treated by the software. Like in a conventional electrophoresis and pass at the same time a laser beam where the attached fluorochrome is excited, the fluorochrome emits a light with a wave length specific to the dye. The light is collected and detected by a spectrophotometer. When using different fluorescent dyes, several PCR products can be mixed and analysed in one capillary. A size standard is mixed with each PCR product to get a precise size value of the DNA fragments analysed (GeneScan™-500, Applied Biosystems with 6-Carboxy-X-Rhodamin, 6-ROX™, or 500 LIZ®). For size determination of the fragments and quantification we used GeneScan™ und Genotyper® (Applied Biosystems). Sequencher (Gene Codes Corporation, Ann Arbor, MI, USA) was used for sequence analysis.

2.2.15.3 DNA sequencing

The BAC DNA was sequenced with primers T7A (5'-CGGTCGAGCTTGACATTGTA) and SP6A (5'-CGATCCTCCCGAATTGACTA). These primers are not the originally T7 and SP6 primers, but are located in the same region. They have a higher Tm (60°C) to increase specificity of the sequencing reaction. For some BACs specific primers were selected to verify the results obtained with the usual T7 and SP6 primers (Table 2-6). The sequencing reaction mixture contained 2 µg DNA, 10 pmol primer, Big dye^{TM} (8 µl, according to the manufacturer's recommendation, Applied Biosystems) in a total volume of 20 µl. BAC DNA was sonicated before the sequencing reaction to improve annealing of the primer. The cycle sequencing reaction was performed with 5 min at 95°C, 50 cycles of 30 sec at 95°C, 10 sec at 60°C and 4 min at 60°C. The products of sequencing reaction obtained were precipitated. For this the reaction volume was completed with water to a final volume of 100 µl (add 80 µl). The solution was then mixed with Dextran blue (2 µl REF), NaOAc 3M (10 µl) and 100% ethanol (250 µl), vortexed, centrifuged 15 min at 13,000 rpm. The pellet was washed with 70% ethanol two times and then dried in a SpeedVac. The DNA pellet was dissolved in 20 µl formamide for electroinjection in an ABI PRISM® 3100 Genetic Analyser. The analysis of the results has been made with the software "Sequencher" from Gene Codes Corporation, Ann Arbor, MI, USA.

Table 2-6. Sequencing primers specific for BAC clones

BAC clone	Sequencing primer
RP11-184F4	TGTTCTCCTGGGTTCCAGTT
RP11-69I9	ACTATAGGGATGGCGTCTGC
RP11-348A7	ATGAGCCAGCTCCTGAATCT
RP11-203F10	GATGTCACCAGGACACTCCA
RP11-75I2	CAGGAATGCACTCCACACAC
RP11-207I9	ATGATGGTAACTGCGTGCAA
RP11-454L1	GCAACGTGGAACTATGAGGTG
RP11-108M21	TCAATCTCTTGCCCTTGTGA
RP11-164O23	GACATTCAAGAACAGAAAAGCAG

2.2.15.4 Genotyping of STR loci for identification of LOH on chromosome 16

For analysis of the PCR products obtained in QMPCR, 1 µl of the PCR products were added to 12 µl of deionised formamide containing 1 µl of ROX fluorescently labelled GeneScan-500 size standard (Applied Biosystems). Signals were evaluated using

GeneScan and Genotyper software (Applied Biosystems). QMPCR products obtained from constitutional DNAs from 5 healthy persons were included as controls for normal copy numbers.

For the analysis of the PCR products obtained in the multiplex PCR of STR loci, 0.8µl of the PCR products were diluted to 2 µl and added to 12 µl of deionised formamide and 1 µl of LYS fluorescently labelled GeneScan-500 size standard (Applied Biosystems). Analysis was performed using an ABI PRISM® 3100 Genetic Analyser and results were evaluated using GeneScan and Genotyper software (Applied Biosystems).

2.2.16 Pyrosequencing (PSQ)

This method is usually used to perform DNA sequence information for genotyping of Single Nucleotide Polymorphism (SNP), microbial typing, resequencing (for review see Ronaghi M. [48]). Here, PSQ was used for relative quantification of alleles of SNP loci that are located in genes that were also investigated by QMPCR. Relative quantification is possible for tumours from patients that are heterozygous for a SNP to be analyzed [49, 50]. The SNPs analyzed here and sequences of primers used are listed in Table 2-7. Primer sequences were chosen using "Primer3Input" and the NCBI SNP database.

We also used PSQ to investigate the loss of heterozygosity (LOH) on chromosome 16. In this case the patients that were heterozygous for a SNP in blood DNA were seen as homozygous in tumour when LOH was present. The primers used are listed in Table 2-8.

PSQ was performed using the PSQ96 Sample Prep Tool and the PSQ96 SNP reagent kit according to the manufacturer's instructions (Pyrosequencing AB, Uppsala, Sweden). Briefly, template for PSQ is prepared in a conventional 50 µl PCR reaction (reaction mix: 1 Unit *AmpliTaqGold*®-Polymerase (5 U/µl), 2.5 mM $MgCl_2$ (5 µl at 25 mM), 0.5 µM of each 5'- and 3' primer (1 µl of a primer mix at 10 µM), dNTPs (each at 1.25 mM), 1X reaction buffer (50 mM KCl, 10 mM Tris-HCl (pH 8.3), 0.001% Gelatine; 2 µl) and in general 160 to 400 ng DNA). From the PCR product 40 µl are pipetted on a PCR microtiter-plate, and mixed with binding-buffer/streptavidin coated Sepharose beads master mix (37 µl/3 µl). The PCR microtiter-plate is thoroughly mixed on a microtiter-plate shaker for 10 min. Concurrently 1.5 µl sequencing primer at 10 µM and 43.5 µl annealing-buffer are pipetted in each slot of the PSQ plate. After applying

vacuum at the workstation, the beads with immobilized PCR product are picked up by the Vacuum Prep Tool from the PCR plate and transferred to a separate trough containing 70% ethanol. After ethanol was aspirated through the filter probes, the Vacuum Prep Tool is placed in another trough containing sodium hydroxide (NaOH 0.2M). With the vacuum still on, the DNA is denatured and the single-stranded DNA released and removed. The 5'-biotinylated strands remain immobilized on the bead. Next, the tool is placed in a trough containing wash buffer and the immobilized DNA is rinsed by aspiration. The single-stranded templates are then transferred to the PSQ plate containing annealing buffer and primer. After release of the vacuum, a gentle shake of the Vacuum Prep Tool releases the beads with templates attached into the 96-well PSQ plate. After annealing the sequencing primer (80°C, 2 min) this plate is ready for analysis using a Pyrosequencing System. The program PSQ96 evaluation AQ was used to determine allele signal heights in PCR products from blood DNA and tumour DNA. The signal ratio of allele 1 to allele 2 in PCR products from blood DNA of heterozygous patients was used for normalization of the signal ratios obtained in DNA from corresponding tumours (example in Fig. 2-3).

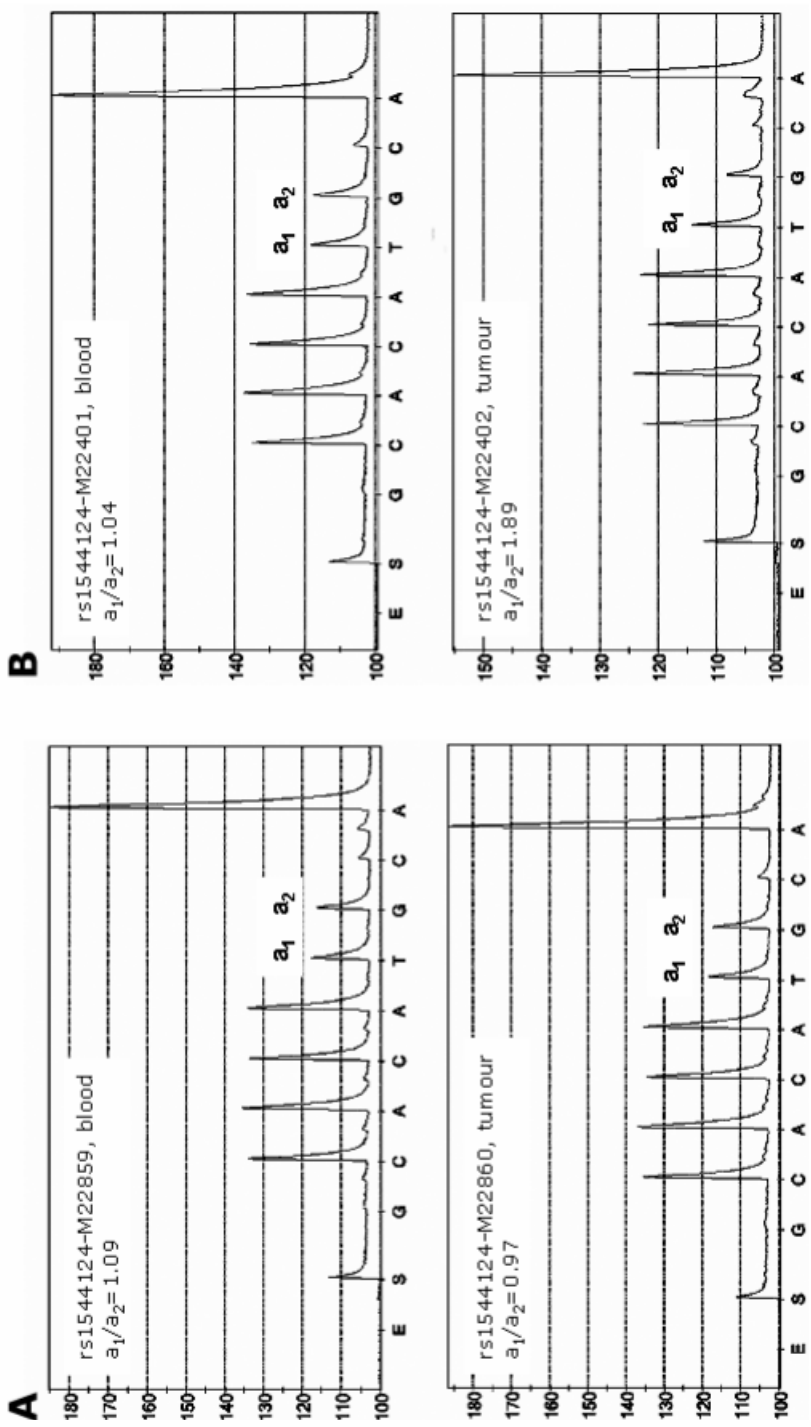

Fig 2-3. Principle of Pyrosequencing applied to relative quantification of alleles. **A** normal ratio between blood and tumour, **B** allelic imbalance for this loci in the tumour.

2.2.17 Comparative Genomic Hybridization

CGH was performed as previously described [28] at the Department of Human Genetics, Philipps University, Marburg, Germany, by Harald Rieder and Stephanie Schneider.

Table 2-7. Sequences of primers used for Pyrosequencing on chromosome 1.

SNP	*Forward Primer*	*Reverse Primer*	*Sequencing Primer*
rs1544124 (*ANGPTL1*)	TGCAGTAATTGACGACAGATG	TCGCCAATTTAAATGACACA	CTTGGCACAATTTATTTCTA
rs2280078 (*ENSA*)	CAACTATACTATCAACTTCTCCTGGAA	TCATCTTGAGCTTTAGGGATTTT	CTTTAACAGCAGAGTAGAGA
rs878471 (*MCL1*)	CGGCTTATGATCAAGAACGA	GCTTCAGTCTCGGAACATGAC	GACTAAGAATGTAATGGGGA
rs3795572 (*PEPP3*)	TGACACCAAGGACAGCACTT	CCCCATCTCTCATCACCTTG	TATCCTCGTCAGCCCCAC

Table 2-8. Sequences of primers used for Pyrosequencing on chromosome 16.

SNP	*Position (bp)*	*Forward Primer*	*Reverse Primer*	*Sequencing Primer*
rs7200919	65874101	CAGAGCAACCAGCGAATACA	CAGCCACACTTCAATCTGGA	AAAGTGAAGAGAGCTGCTAT
rs7206718	66007332	ACAGACCCTCCATGACCAAC	ACTCTTTGCCAGGCTCTGTG	AGAGGACTCCCAACAGACGT
rs8057184	66384748	ATCCAGACACTGGCCTTGAG	GCATGGTGGCGTATACCTGT	TGCTCCAGCCAGTCAAACA
rs12599580	66508114	AGGAGGAAGGCTAGCTGGAG	GGGTAGCCTGGAATCCTCTC	GAATAATTCCATCCTGTCCT
rs255049	66570972	AGAAACCACATGATGGCACA	CCTGGACAGGCTTAGAGACG	TTAGTCACCCAGAGGCTGG

2.2.18 Matrix-CGH

The matrix-CGH experiments have been conducted in collaboration with the Division of Molecular Genetics (DKFZ, Heidelberg). Two different kinds of chip were available: a chromosome 1 specific chip and a whole genome chip. The chromosome 1 specific chip contained DNA from 50 BAC clones mapping on 1q and prepared as described before in the department of Human Genetics in Essen. In addition DNA from 215 other clones covering the whole genome and prepared in Heidelberg were spotted together on this chip. The open air hybridization was made in Essen and the analysis was a share work from Essen and Heidelberg.
The whole genome chip was fully prepared and analysed in Heidelberg, with DNA from retinoblastoma coming from Essen, for description of the methods please refer to Zielinski et al. (manuscript submitted).

2.2.18.1 Chromosome 1 specific chip

The BAC DNAs prepared in Essen were spotted in Heidelberg.
Tumour DNA and reference DNA from healthy donors (300 – 500 ng) were differentially labelled with Cy3- / Cy5- conjugated dCTP by use of the BioPrime DNA Labeling Kit (Invitrogen, Karlsruhe Germany). Unincorporated nucleotides, random primers and dyes were removed by the use of MicroCon YM30 Spin Columns (Millipore, Schwalbach Germany). Incorporation of dyes into the labelled DNA was determined by UV-spectrophotometry. 10 µg each of tumour- and reference DNA were combined with 300 µg human Cot-1-DNA (Roche Diagnostics, Mannheim, Germany) and suspended in 125 µl Ultrahyb^{TM} hybridization buffer (Ambion, Bad Soden Germany). Denaturation of combined DNAs was performed at 75°C for 10 minutes followed by preannealing at 37°C for 30 minutes. The hybridization was performed on a rocking shaker (Shaker S4, Elmi, Riga, Latvia) for 48 hours at 37°C. Slides were rinsed with PN Buffer and washed with Wash A 15 min at 45°C for 2 times, and then dried by centrifugation at 500 rpm for 1 minute following by 1500 rpm for 1 minute.
The data acquisition with scanning was performed in Heidelberg, processing and analysis was a common work from both institutes.

2.2.19 Expression analysis

For microarray analysis nucleic acids to be analyzed must be labelled and hybridized to oligonucleotide arrays. These steps were performed in the microarray core facility under the supervision of Ludger Klein-Hitpass at the Institut Für Zellbiologie from the University of Duiburg-Essen.
Signal intensities and detection calls for further analysis were determined using GeneChip Microarray Suite (MAS) 5.0 Software (Affymetrix). Scaling across all probe sets of a given array to an average intensity of 1000 units compensated for variations in the amount and quality of cRNA samples and other experimental variables. Further processing of the average difference values and gene information was performed in Excel 2000 (Microsoft).

2.2.20 Statistical analysis of genetic findings and clinical manifestation

The Wilcoxon test (normal approximation) was used to test if genes are differentially expressed between tumours with or without 1q gain. “Significance Analysis of Microarrays” (SAM, Stanford University, CA, USA [51]) was used to identify genes that are consistently differentially expressed between classes of tumours – as defined by distinct patterns of DNA copy number in 1q32 – regardless of the absolute RNA expression level.

Detailed information on clinical presentation, treatment and follow up of patients were obtained. We used a data warehouse software (Cognos Series 7.1, Cognos incorporated) to link up all clinical and genetic data and to set the stage for data mining, which was performed using the tools provided by the software environment. Statistical evaluation of the findings was performed using the JMP 5.1 software (SAS Institute) and its cluster analysis platform, and InStat 3 for Macintosh.

3 RESULTS

3.1 Identification of target genes on the long arm of chromosome 1

In order to identify retinoblastomas with gains on the long arm of chromosome 1 and to narrow down the minimum region with increased copy numbers, two independent methods were employed:

- Matrix-CGH hybridization against cloned DNA from the region of interest (custom chips, 3.1.1.1) and Matrix-CGH using arrays of spotted cloned DNA representative for the whole genome (3.1.1.2).
- Quantitative multiplex PCR was used to determine relative copy numbers of genes in the candidate region on 1q that was defined by CGH previously (QMPCR, 3.1.2)

To confirm the results, we used additional approaches:

- Genomic Real-Time PCR was employed to determine DNA copy numbers of specific genes (3.1.3.1)
- Pyrosequencing of SNP loci was used to detect allelic imbalances, which often accompany an increase in copy number of genomic regions (3.1.3.2)
- Conventional comparative genomic hybridization (CGH, 3.1.3.3)

In addition, expression analysis of 21 primary retinoblastomas previously characterised at the genomic level on 1q was performed with the Affymetrix microarray chip HG-U133A (3.1.4).

The results obtained by these methods were also used to identify possible associations between different patterns of genomic gains on 1q and the clinical manifestation of the tumour (3.1.5).

3.1.1 Matrix CGH

3.1.1.1 Custom chip

Our initial strategy for identification of retinoblastomas with genomic gains in the candidate region on 1q was to use matrix CGH with an array of spotted DNA derived from BAC clones from this region. The location of the clones used is listed in Table 2-1. They cover the minimal region of gain that was previously determined by CGH [28]. After preparation, sequence verification, and spotting of BAC DNA we tested the quality of matrix CGH with these custom arrays and checked if the results could help to narrow

down the candidate region of gains on 1q. First, the quality was checked by hybridization with 2 DNA samples with known genomic gains in the region represented by the BAC array. The first sample was DNA from a glioma with high level copy number gains of material on chromosome 1q, specifically amplification of the *MDM4* gene [38, 39]. Matrix CGH with our custom chip showed a value of 5.98 for the BAC clone RP11-430C7, which contains the *MDM4* gene. This figure corresponds to a high level amplification and is concordant with reported results. Gains were also detected for three adjacent clones (Fig 3-1).

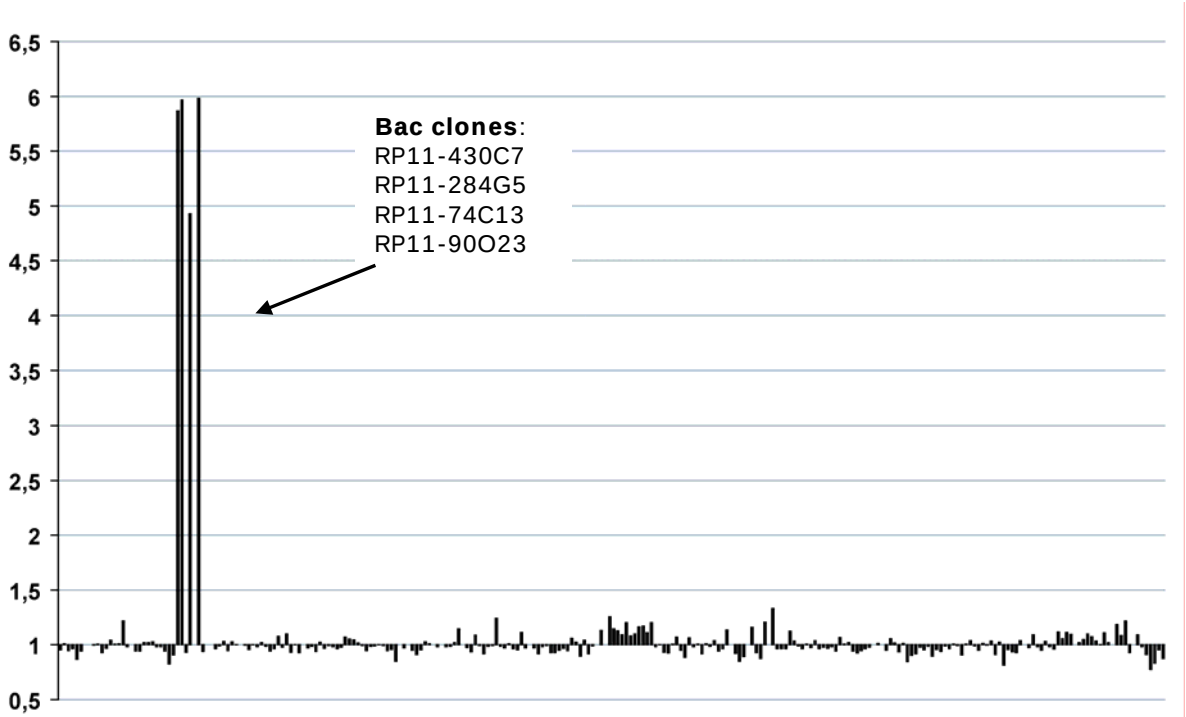

Fig 3-1. Profile of DNA from a glioma on the custom array-CGH with BACs from 1q. The clones are ordered along the abscissa according to their location on the chromosomes with clones from telomere of short arm of chromosome 1 on the left and clones from telomere of long arm to the right. The clones of the far right are from the Y-chromosome. The threshold for gains of material is 1.25. Clones with signals >4 are located on chromosome 1q.

Second, we tested if matrix CGH with the custom chip is suited to detect low level copy number gains. For this we used a control DNA from a uveal melanoma cell line (Mel202) that has a trisomy 1 and trisomy 6 as determined by cytogenetic analysis (Nareyeck G., Zeschnigk M. et al. manuscript under revision). The results of hybridization did not show any copy number change on chromosome 1 (Fig 3-2). Possibly, the failure to detect low level gains are not due to a problem related to the array but caused by the open air hybridization protocol that we used for manual assisted hybridization. This may result in

weaker specific signals and higher background noise. It is possible to improve the results to some extent by setting new thresholds. To test if useful results could be obtained with this adjustment we tested DNAs from 8 retinoblastoma samples that had shown chromosome 1q gains in conventional CGH or QMPCR. With matrix CGH gains were detected in only 6 of these tumours. The two other tumours with 1q gains were negative in matrix CGH. These tumour DNAs showed hybridization signals for 1q-clones that were close 1, which corresponds to a normal diploid gene copy number. It was not possible to improve these results by setting new thresholds. Thus we concluded that the sensitivity of matrix CGH with our custom BAC arrays does not allow to reliably identify the presence of gains in the candidate region on 1q in retinoblastomas.

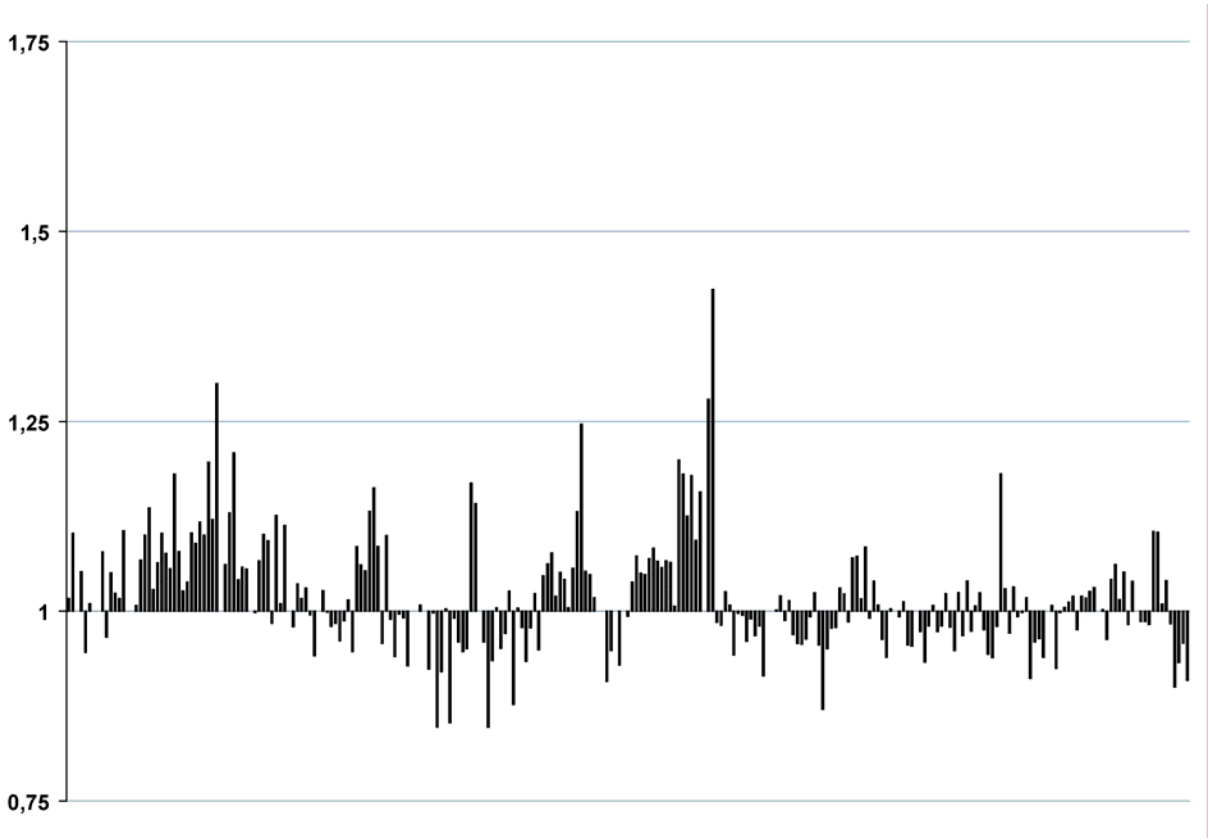

Fig 3-2. Profile of the Mel202 cell line on the custom array-CGH with BACs from 1q. The order of the clones is the same as in Fig 3-1.

3.1.1.2 Matrix CGH with DNA arrays representing the whole genome

In view of the results obtained with our custom BAC arrays and manual assisted hybridization, we decided to perform matrix CGH with a whole genome chip that was established by our cooperation partners at the DKFZ Heidelberg in the meantime.

Table 3. 1 Imbalanced chromosomal regions detected with whole genome matrix-CGH array.

Tumour	No. Aberr.	Imbalanced chromosomal regions detected by matrix-CGH
M22058	4	enh(**1q31.3q44[193.54-246.01]**, **6p25.3p11.2[0.09-58.73]**, 19p13.3q13.42[2.60-63.77]) amp(1p33p33[47.70-48.16])
M22590	5	enh(**1q21.1q44[141.79-244.84]**, **2p25.3p12[0.22-81.88]**, 11p12p12[37.68-38.64]) dim(10q24.32q26.3[104.18-135.03], **16q12.1q24.1[47.68-89.64]**)
M22808	10	enh(**1q22q22[152.06-152.49]**, **6p25.3p11.2[0.09-56.69]**, 7p22.3p21.3[1.39-8.82], 7p15.3p13 [20.66-44.82], 7q11.22q36.3[70.46-158.46],19p13.3p13.11[0.21-22.77], 20p11.23p11.22[20.23-21.54], 20q11.21q13.13[31.22-50.18]) dim(16p12.1q12.2[49.43-55.39], Xp11.22q23[53.03-113.63])
M22860	9	enh(18q11.1q23[17.22-75.94], **19q13.12q13.43[40.17-63.77]**) dim(1p36.33p36.21[1.06-12.51], 8p23.1p23.1[7.16-8.02], 12p13.33p11.21[0.64-32.93], **16q12.1q24.3[47.68-89.86]**, 17p13.3p11.2[0.38-21.41], 18p11.32p11.31[0.13-6.21], 22q11.1q13.33[15.62-49.34])
M23449	5	enh(**1q21.1q32.3[141.79-208.92]**, 14q21.3q32.2[47.80-96.93], 17q25.3q25.3[80.82-81.46]) dim(10q23.2q23.32[88.29-92.81], 21q11.2q21.2[14.63-25.64])
M23209	2	enh(**2p24.1p24.1[21.20-21.45]**) dim(8q24.12q24.12[119.69-119.91])
M20517	0	
M22233	4	enh(**6p25.3p11.2[0.09-58.73]**, **19q13.2q13.2[45.08-45.81]**), dim(13q12.3q14.3[28.81-49.73]) amp(1p34.2p34.2[39.75-40.65])
M22641	7	enh(**1q21.1q44[142.66-246.01]**, **2p25.3p12[0.22-80.04]**, **6p25.3p12.1[0.09-53.03],** 13q32.2q34[96.85-112.83], 16q21q22.3[64.14-73.26]) dim(6q22.31q22.31[118.62-119.60], **16q23.1q23.2[78.27-79.88]**)
M22731	5	enh(**1q21.1q32.2[142.66-207.74]**, 5q23.3q31.2[131.41-137.69], **6p24.3p12.3[8.60-46.97]**, 14q22.3q22.3[54.57-55.54]) dim(**16q21q22.1[63.16-65.15]**)
M22067	0	
M23215	19	enh(**1q21.1q44[141.79-246.01]**, 2q37.1q37.3[233.54-242.82], 5p15.32p15.31[5.50-7.53], 5p13.2p13.2[37.00-38.32], 5q11.2q11.2[55.53-56.29],5q13.2q13.2[72.73-72.97], 5q23.1q35.3[118.32-180.80], **6p21.33p21.1[31.64-44.29]**, 10q24.31q25.1[101.89-105.89], 10q25.2q25.2[111.49-112.17], 10q25.3q25.3[115.64-115.82], 10q26.11q26.12[119.94-121.60], 10q26.13q26.3[124.34-134.69], 13q12.13q34[24.65-113.00], 20p13p13[0.18-3.84], 22q13.2q13.2[40.42-40.72]) dim(6q22.33q27[128.38-170.74], 8p23.3p12[4.77-31.06], 17p13.2p11.2[4.07-18.37])
M23869	6	enh(**1q21.1q23.3[144.11-158.62], 1q31.3q42.2[194.68-229.94]**, **2p25.3p11.2[0.22-89.89]**, **6p25.3p11.2[0.09-58.73]**, 15q21.3q24.1[56.57-72.33]) dim(13q14.2q14.3[46.86-49.87])
M24430	2	enh(**1q21.1q25.2[141.79-174.53]**) dim(9q34.3q34.3[134.42-134.80])
M24733	7	enh(**1q21.2q44[147.66-246.01]**, **6p25.3p12.1[0.09-56.84]**, **19q13.42q13.42[59.04-59.40]**) dim(1p36.33p35.3[1.14-27.85], 8q22.3q24.3[105.89-146.86], 16p13.2p11.2[2.19-31.07], **16q12.1q24.3[47.68-89.59]**)
M24794	5	enh(**1q21.1q44[141.79-246.01]**, **2p25.3p14[0.22-64.80]**, **6p25.3p21.2[0.09-37.02]**) dim(**16q24.1q24.1[85.70-86.52]**, 17p13.2p11.2[5.60-6.66])
M24820	4	enh(**1q22.2q44[152.06-165.82]**,**1q25.3q25.3[178.43-180.01]**, **1q31.3-q44[195.63-246.01]**, **6p25.3p11.2[0.09-57.36]**)

enh: gain of chromosomal material; dim: loss of chromosomal material; amp: amplification. Megabase positions are given in square brackets. Most frequently detected aberrations are indicated in bold face.

This array is composed of BAC clones that are separated by about 1Mb and cover the whole genome. The cooperation partner performed matrix CGH with DNAs from 17 retinoblastomas using automated hybridization. These tumours were selected from specimens that had also yielded RNA suited for expression analysis (see 3.1.4). The results of whole genome matrix CGH on these tumours showed all recurrent aberrations that are frequently observed by conventional CGH: gains on 1q and 6p, and losses on 16q. In addition, a previously unreported high-level amplification was identified in a small region on the short arm of chromosome 1 (see insert from Fig 3.10). However, this novel aberration is likely to be rare because it was observed in only 1/17 retinoblastoma samples (Table 3-1).

3.1.2 Quantitative multiplex PCR (QMPCR)

3.1.2.1 Establishing and validating QMPCR

As a result of the Human Genome Project, almost complete sequence data have become available from most chromosome regions. This has opened the possibility to use QMPCR to determine the presence and extent of genomic gains in the candidate region in retinoblastoma. In addition to the 1q32 region, which was identified by CGH, we established QMPCR for the detection of copy number changes in another chromosome 1 region, 1q21. This second region was included because evaluation of RNA expression analysis with SAM (see Table 3.2) suggested that this region might show gains in some retinoblastomas. We have chosen 30 PCR targets from 1q21 and 1q32 (table 2-1). Individual PCR targets were co-amplified in 5 multiplex sets. In addition, each multiplex reaction contained primers for amplification of two control targets outside of chromosome 1. These controls were used for normalization of the intensities of product signals within individual multiplex reactions. To validate QMPCR, we performed several control experiments on samples with known copy numbers. In addition, we analyzed DNA from two tumours representing different stages of glioma. It has been reported that these two specimens have amplifications on 1q32, a finding that had been confirmed by Southern Blot hybridization [38, 39]. With QMPCR on DNA from these tumours we detected high level gains of the loci *MDM4*, *GAC1*, *PIK3C2B* and *PEPP3*. These results are in agreement with the findings reported previously [38, 39] (Fig 3-3). To determine if QMPCR can detect low level gains we also analyzed the uveal melanoma cell line Mel 202 with trisomy 1 and trisomy 6. QMPCR results showed values corresponding to 3

copies for all loci on chromosome 1 and for the control locus on chromosome 6q (median = 1.50, quartiles [1.44;1.55], Fig 3-3). This indicates that QMPCR can reliably discriminate between DNAs that have two or three copies of the regions targeted by PCR.

3.1.2.2 QMPCR of DNA from specimens of primary retinoblastoma

QMPCR was performed on DNA from samples of primary retinoblastoma from 76 patients. Most of these patients (n=73, 96%) were diagnosed with isolated unilateral retinoblastoma. The three remaining patients had isolated bilateral retinoblastoma. The results of QMPCR, which are shown as a cell plot in Fig 3-4A, showed a complex pattern of gains. Using a threshold for discrimination (definition of the threshold see section 2.2.12) we found that gains on 1q21 or 1q32 are present in 34 of 76 (45%) samples. None of the retinoblastomas showed amplification at high levels comparable to the findings in the glioma samples that were analyzed as controls (3.1.2.1). The tumour with the highest gains on 1q had a median copy number of 4 (2.03 [1.92; 2.41]). The pattern of gains did not simply point out a minimum region of gains on 1q21 or 1q32. However, a closer analysis showed recurrent patterns. Among the tumours with gains of material on 1q, four tumours had no gain at one border of the 2 regions investigated: G319 had no gain of the loci *ZNF281* and *ELF3* from 1q32, the tumour M74 had gain of material of all but the 2 telomeric loci (*COG2* and *SMYD3*), M23449 had higher copy number on 1q21 while the loci on 1q44 (*COG2* and *SMYD3*) were normal, and M10288 had no gain at the first locus on 1q21 (*GJA5*). These observations allow to define more precisely the regions of gains on 1q in retinoblastoma.

3.1.2.3 QMPCR of DNA from retinoblastoma cell lines

We also performed QMPCR on DNA from retinoblastoma cell lines WERI-Rb1, Y-79, RBL 30, RB247C3, RB383, and RB355. All 6 cell lines showed genomic gains at all 1q loci analyzed here (Fig. 3-5). On the whole, levels of gains in cell lines were higher compared to primary retinoblastoma. Gains were most pronounced in DNA from the cell line WERI-Rb1 (2.98 [2.62; 3.24]). In RB355 and RB383 the levels of gains for loci within 1q21 were distinct from those of loci in 1q32: values of 1.52 [1.48; 1.51] on 1q21 and 2.14 [2.07; 2.26] on 1q32 for RB355, and 2.45 [2.38; 2.82] on 1q21 and 1.58 [1.52; 1.70] on 1q32 for RB383.

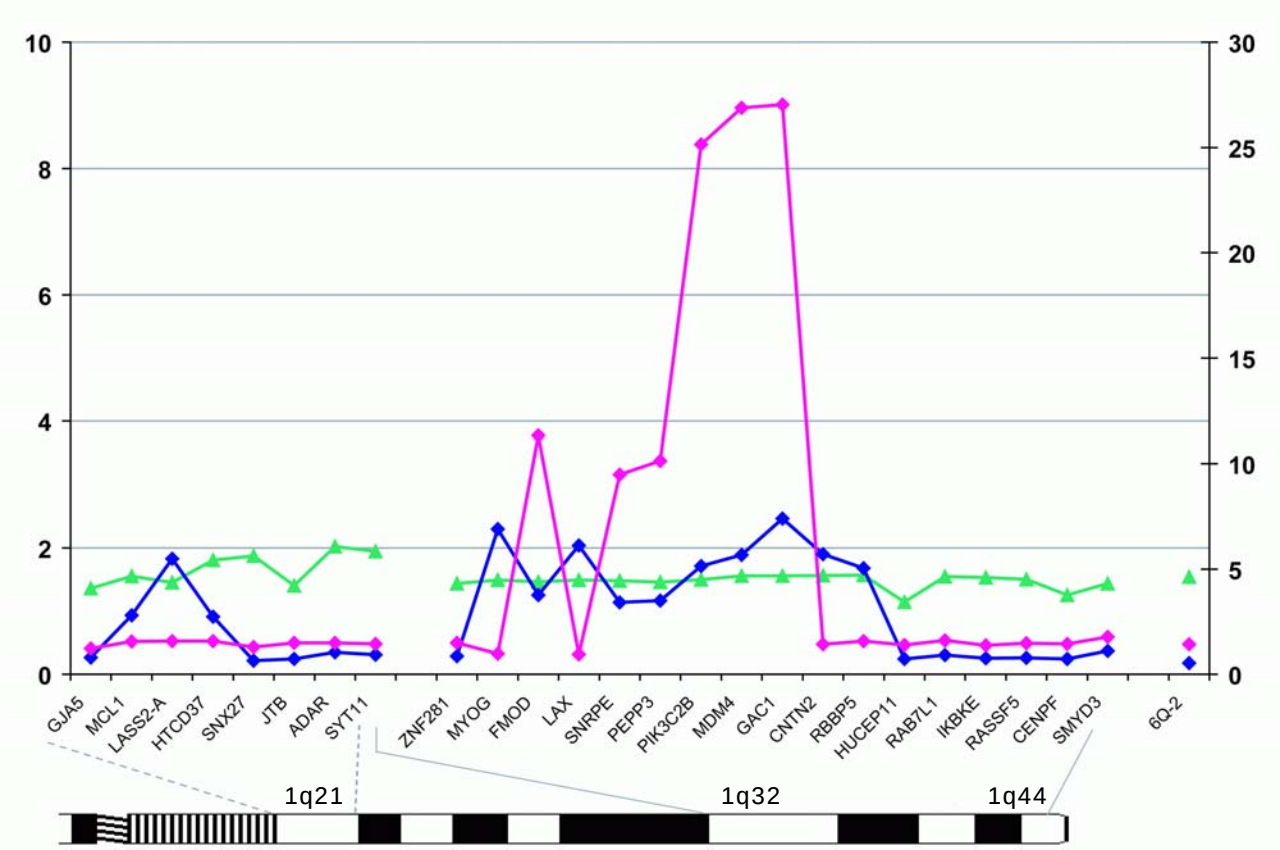

Fig 3-3 Validation of QMPCR. QMPCR was used to determine relative copy numbers of loci on chromosome 1q in DNA from the cell line Mel202 (scale on left axis, data points in green) and in DNA from two gliomas (scale on the right axis, blue and pink).

We had the opportunity to compare results of QMPCR obtained in DNA from a cell line (RBL 30) with those of the primary tumour (G319) that had been used to establish this cell line. Comparison of DNA gains on 1q showed that the genome of the cell line has obviously faithfully conserved the profile of gains that is detected in the primary tumour (Fig. 3-5 A). It is to be noted that the close correspondence of the two profiles also indicates that the error due to measurement is rather low. In fact, such a close correlation of results strongly suggests that QMPCR permits reliable relative quantification of low levels of copy number gains.

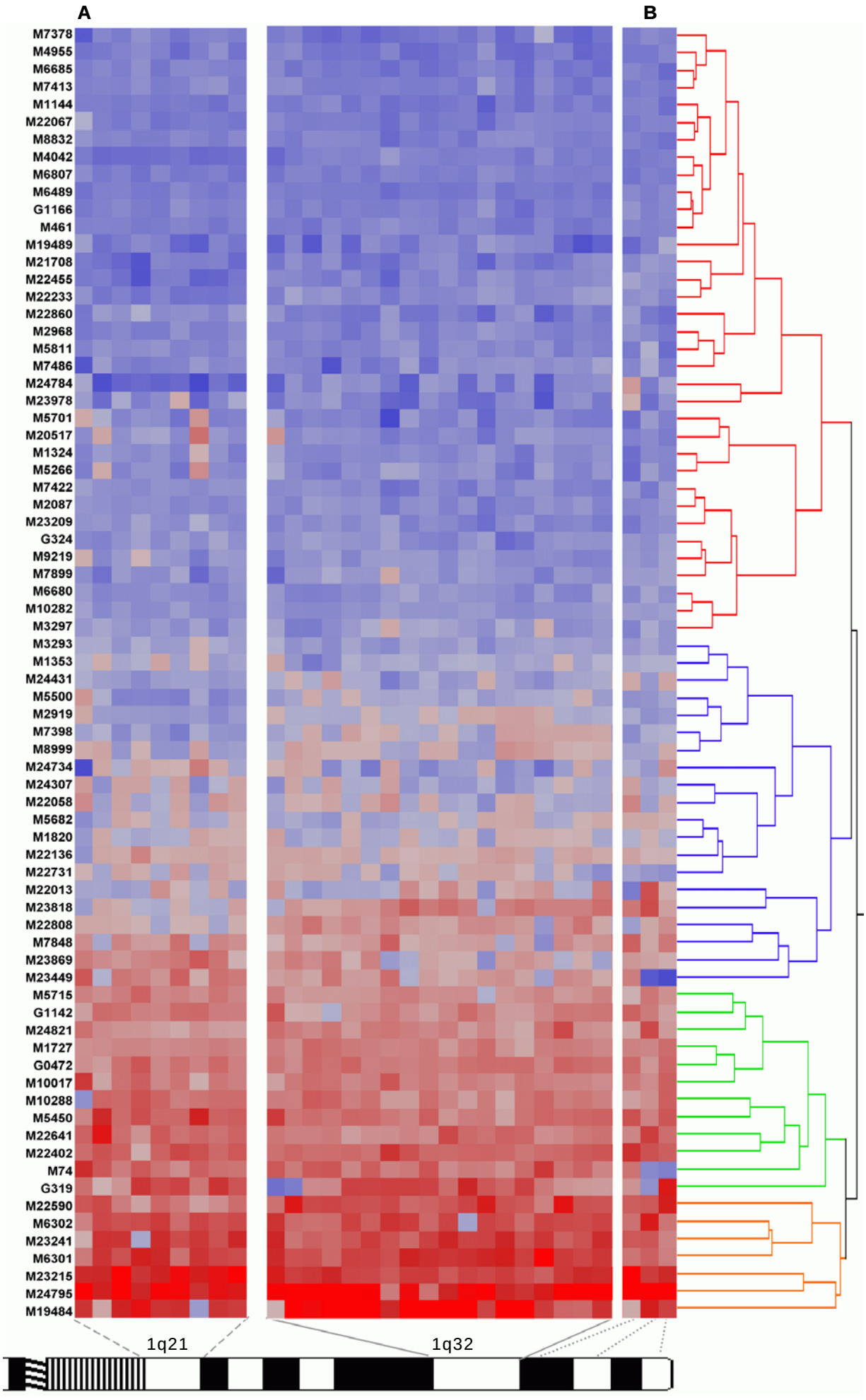
A
B
M7378
M4955
M6685
M7413
M1144
M22067
M8832
M4042
M6807
M6489
G1166
M461
M19489
M21708
M22455
M22233
M22860
M2968
M5811
M7486
M24784
M23978
M5701
M20517
M1324
M5266
M7422
M2087
M23209
G324
M9219
M7899
M6680
M10282
M3297
M3293
M1353
M24431
M5500
M2919
M7398
M8999
M24734
M24307
M22058
M5682
M1820
M22136
M22731
M22013
M23818
M22808
M7848
M23869
M23449
M5715
G1142
M24821
M1727
G0472
M10017
M10288
M5450
M22641
M22402
M74
G319
M22590
M6302
M23241
M6301
M23215
M24795
M19484
1q21
1q32

(page 44) ***Fig. 3-4.*** *A*, Cell plot of gene dosage from 74 primary tumours (2 tumours are not included because of missing data for some target genes) color scale: blue corresponds to a QMPCR result of 1 (2 copies); dark red corresponds to a result of 3 (6 copies). *B*, hierarchical cluster Ward's method, classes *ng* (dark blue), *ig* (light blue-pink), *hg* (red-pink), and *chg* (dark red).

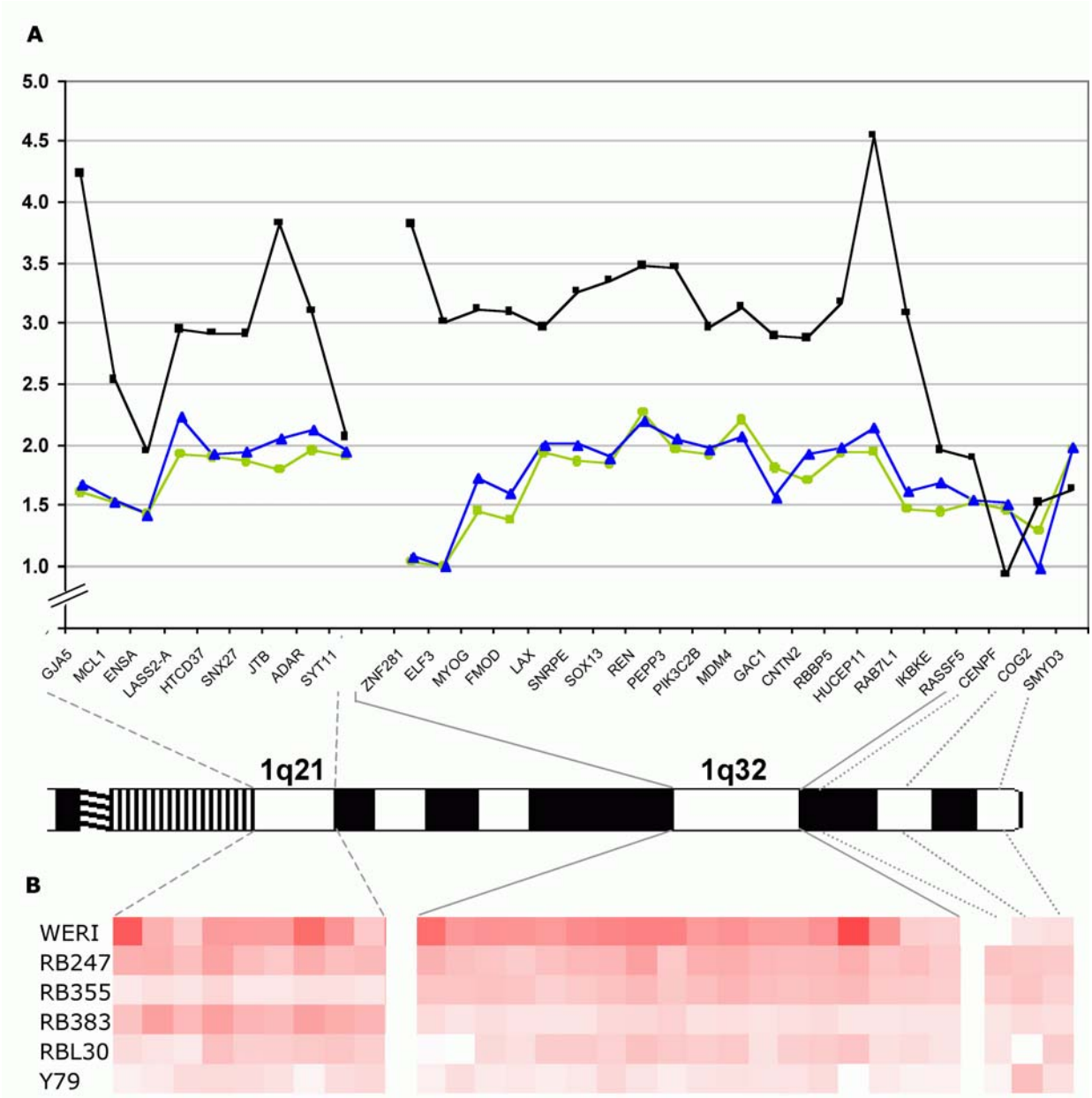

Fig 3-5. Copy number in cell lines and a primary tumour determined by QMPCR. ***A***, gene copy number of cell line RBL30 (data points in blue), primary tumour G319 (green) and cell line WERI (black). ***B*****,** Cell plot of gene dosage from several cell lines. 1 2 3 4 5

3.1.3 Confirming the results of QMPCR by independent methods

3.1.3.1 Genomic Real-Time PCR

The basic principle of Real-Time PCR is to monitor the amount of specific product that is synthesized during the progress of the reaction. We used the TaqMan detection technology, which provides high specificity and sensitivity and, in principle, allows detection of loss or gain of a single copy of a gene. We used this method to check gene copy number results obtained by QMPCR (3.1.2). We analyzed targets specific for the *GAC1*, *REN*, and *MDM4* genes in 65 retinoblastomas. To compare the results, we determined the correlation coefficients of data obtained for the same gene. The correlation coefficients (Pearson's correlation coefficient: R) of QMPCR data and results obtained by Real-Time PCR were 0.54, 0.40, and 0.51 for *GAC1*, *REN* and *MDM4*, respectively. A graphical representation of correlation data for the *GAC1* gene is shown (Fig3-6).

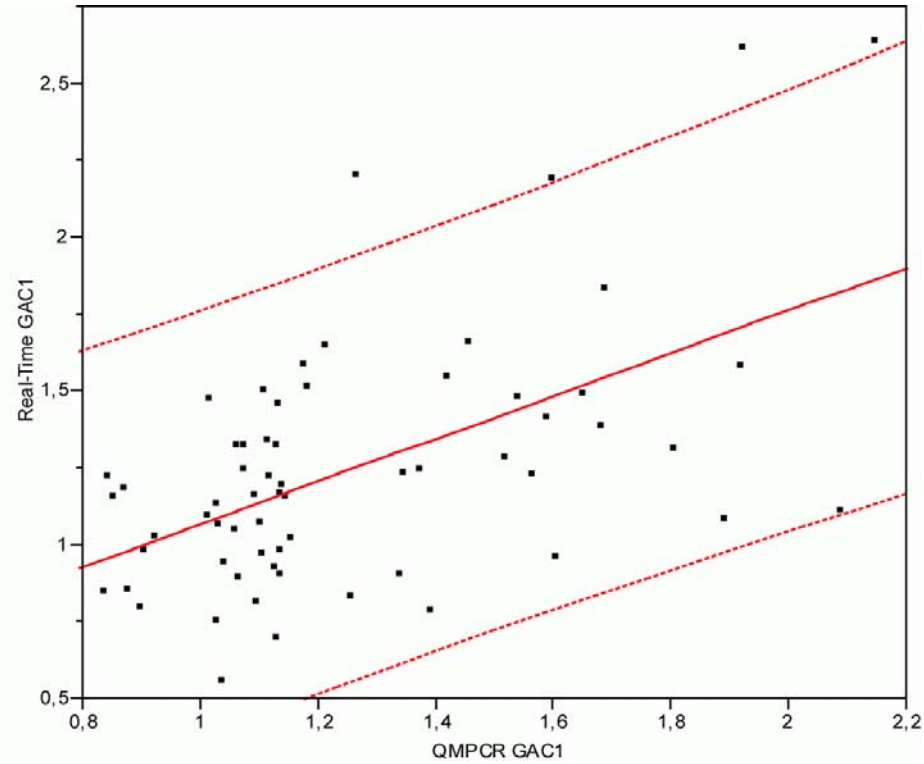

Fig 3-6. Regression analysis of Real Time PCR and QMPCR data obtained for the *GAC1* gene (dotted lines: curves of 95% confidence limits).

3.1.3.2 Pyrosequencing of SNP loci

At a heterozygous polymorphic locus, the relative copy numbers of the two alleles are expected to be equal (1:1) in normal constitutional DNA. If this locus is part of a region that has undergone copy number changes in a tumour, the allele signal ratio will depart from unity – i.e. will show allelic imbalance – if copy number changes affect only one of the two allelic regions (which is most often the case). With pyrosequencing it is possible to obtain a precise relative quantification of SNP alleles [49, 50]. In order to detect allelic imbalance in tumour DNA, it is necessary to perform two rounds of pyrosequencing analyses for each SNP and each patient. Analysis is performed on constitutional DNA (peripheral blood) first to test if a patient is heterozygous at a given SNP locus. This result is also used to normalize the signal ratio obtained in the corresponding tumour. Second, SNPs of heterozygous individuals are analyzed in tumour DNA. We found little variation of ratios in normal constitutional DNA: average ratios [(allele$_1$/allele$_2$) exp$_1$/ (allele$_1$/allele$_2$) exp$_2$] were 1.006, 1.051, 0.961 and 0.971 for SNPs in *ANGPLT1*, *ENSA*, *PEPP3* and *MCL1*genes, respectively (variation between two experiments, exp$_1$ and exp$_2$). This suggests that the stochastic measurement error is low.

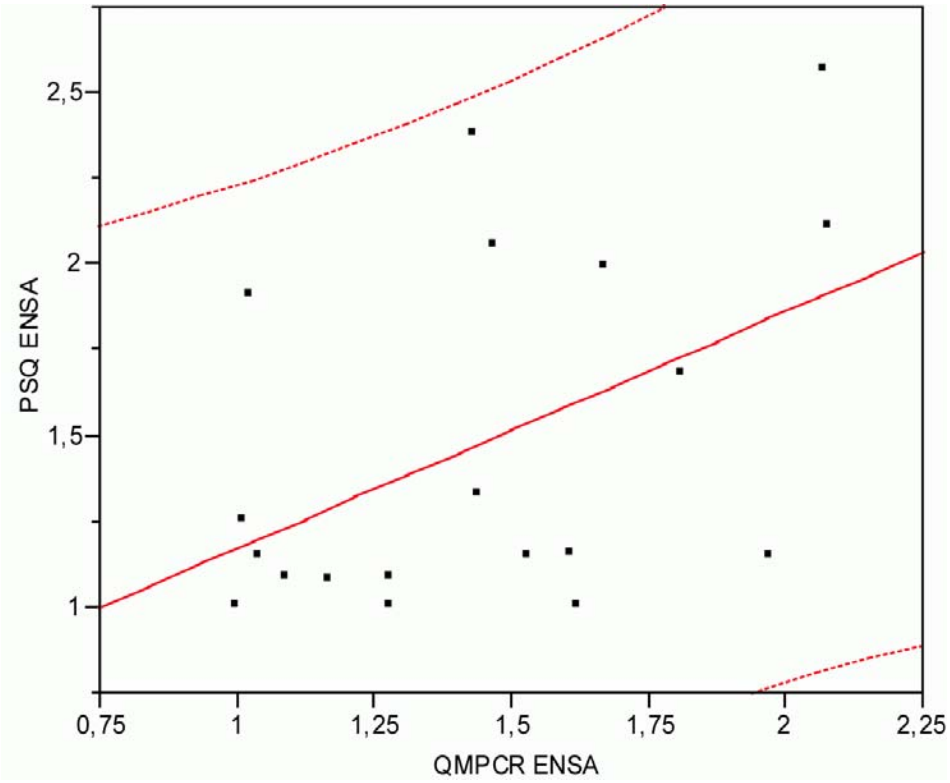

Fig 3-7. Regression analysis of pyrosequencing and QMPCR data obtained for the *ENSA* gene (dotted lines: curves of 95% confidence limits).

When comparing the results of pyrosequencing of SNP loci with those of QMPCR it must be kept in mind that pyrosequencing determines allelic imbalance, i.e. a ratio of two alleles at one locus. However, with QMPCR the copy number of a locus is determined relative to another locus. To compare the results we determined the correlation coefficients of results obtained for three loci within the 1q21 and 1q32 (*ENSA*, *PEPP3*, and *MCL1*). The correlation coefficients (Pearson's correlation coefficient: R) of QMPCR data and results obtained by pyrosequencing were 0.47, 0.24, and 0.54 for *ENSA*, *PEPP3* and *MCL1*, respectively (Fig 3-7).

We also tested a fourth locus that is mapped to the intermediary region (*ANGPTL1*). Although this precludes to correlate allelic imbalance at *ANGPTL1* gene with individual QMPCR results, the findings at this locus fit in the general pattern: of 18 tumours heterozygous for this SNP, 5 showed allelic imbalance, and these 5 tumours had also allelic imbalances on both 1q21 and 1q32.

3.1.3.3 Conventional comparative genomic hybridization (CGH)

From 68 of the 76 primary tumours investigated by QMPCR (3.1.2.2), we also had CGH results (CGH was performed at the Department of Human Genetics in Marburg). CGH data were compared with QMPCR and, in addition, to check the validity of the control used for normalisation in QMPCR and located on chromosome 10. Comparing these datasets we found that all 18 (26%) samples with 1q gains in CGH also showed gains in QMPCR. Of 50 (74%) samples without 1q gains in CGH, 37 (54%) also showed normal copy numbers of 1q loci in QMPCR. In 13 samples (19%) without CGH alterations on 1q, gains were detected by QMPCR. It has to be noted that in 7 of these tumours, copy number gains determined by QMPCR were relatively low and present at only some of the loci tested. Possibly, gains in these samples are missed by CGH because the resolution of this technique, both spatial and quantitative, is inferior to that of QMPCR [31, 52].
The pattern of 2 regions of gain on 1q obtained previously in QMPCR with the primary tumours and the cell lines was confirmed in CGH. The RBL30 cell line (derived from the G319 tumour) showed 2 distinct regions of gain. These 2 regions are also highlighted by the results from cell line WERI-Rb1 showing 2 distinct peaks of gains centred on 1q21 and 1q32 (Fig. 3-8).

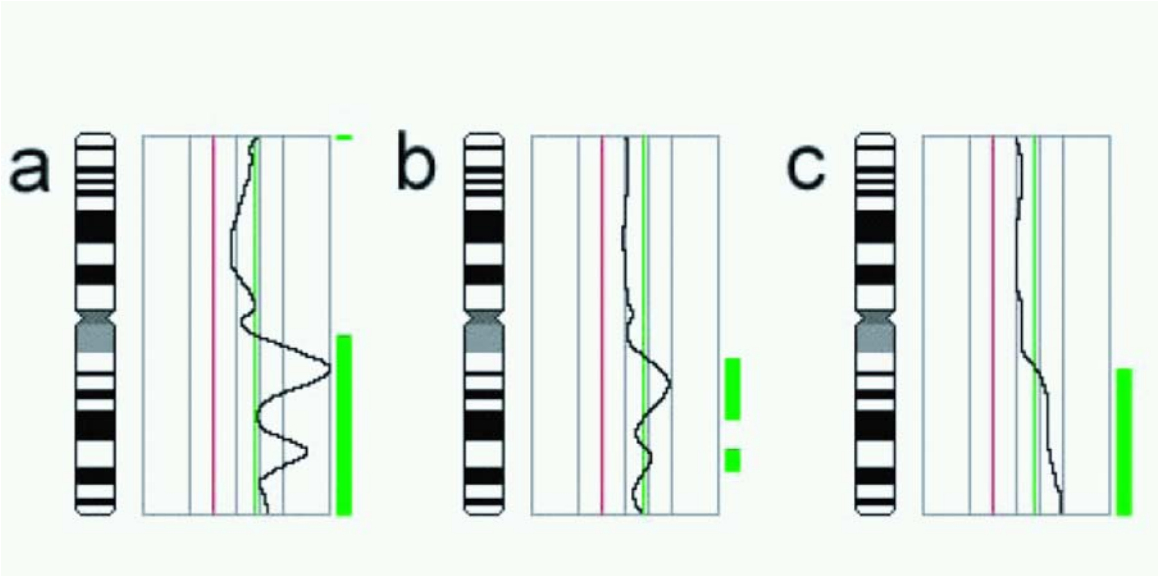

Fig 3-8. Fluorescence ratio CGH profiles of chromosome 1 showing distinct peaks of gains at 1q21q22 and 1q32 in (a) WERI-Rb1 and (b) RBL30. An increased dosage of entire 1q was found in (c) Y-79.

3.1.4 Expression data

RNA for expression analysis was available from 21 primary retinoblastomas. Of these, nine tumours had genomic gains at all loci in the 1q32 region. Ten tumours showed no gains in QMPCR. The pattern of gain on 1q32 in the remaining two tumours was intermediary with some loci showing gains while other loci had normal copy number. Significance Analysis of Microarray (SAM) was used to identify genes that, regardless of the absolute RNA expression level, are consistently differentially expressed between the 9 tumours with gains of all loci in the 1q32 region and the 10 samples without gains. A list of the first 150 genes differentially expressed is provided in Table A in annexe.

With respect to the chromosomal localization of the genes identified by SAM it is to be noted that the top 45 of these genes (Table 3-2) includes 22 genes that are located on the long arm of chromosome 1. We also noticed that 10 of these 22 genes are located in 1q21. This prompted us to establish additional QMPCR assays for the detection of DNA copy number gains of loci in the 1q21 region (Table 2-3).

Table 3-2. Genes overexpressed in tumours with gains on 1q (from SAM)

Gene Name	Affy. #	Location	Fold Change	q-value (%)	P
ZNF281	218401_s_at	Chr:1q32.1	1.51	4.90	0.0003
SYT11	209197_at	Chr:1q21.2	1.43	4.90	0.0004
ENSA	221486_at	Chr:1q21.2	1.62	4.90	0.0004
SYT11	209198_s_at	Chr:1q21.2	1.69	4.90	0.0003
ADAR	201786_s_at	Chr:1q21.1-q21.2	1.33	4.90	0.0005
SH3GLB1	210101_x_at	Chr:1p22	1.41	4.90	
MCL1	200797_s_at	Chr:1q21	1.38	4.90	0.0029
SH3GLB1	209091_s_at	Chr:1p22	1.48	4.90	
RNF19	220483_s_at	Chr:8q22	1.38	4.90	
HTCD37	209586_s_at	Chr:1q21	1.70	4.90	0.0005
KIAA0992	200897_s_at	Chr:4q32.3	1.66	4.90	
SNX27	221498_at	Chr:1q21.2	1.48	5.52	0.0022
LASS2	222212_s_at	Chr:1q21.2	1.63	5.52	0.0022
FLJ12806	220199_s_at	Chr:1q42.12	2.44	5.52	0.0017
M11S1	200723_s_at	Chr:11p13	1.38	5.52	
DUSP12	218576_s_at	Chr:1q21-q22	1.42	5.52	0.0017
POGK	218229_s_at	Chr:1q23.2	1.46	5.52	0.0003
CA12	204508_s_at	Chr:15q21.3	3.99	5.52	
CDC42BPA	214464_at	Chr:1q42.11	1.55	5.52	0.0022
SLC37A1	218928_s_at	Chr:21q22.3	2.63	5.52	
WDR26	218107_at	Chr:1q42.12	1.40	5.52	0.0017
JTB	210927_x_at	Chr:1q21	1.48	6.38	0.0013
SSA2	210438_x_at	Chr:1q31	1.48	6.59	0.0013
ARPC5	211963_s_at	Chr:1q25.1	1.53	6.59	0.0009
RPS6KB1	211578_s_at	Chr:17q23.2	1.54	8.30	
JTB	210434_x_at	Chr:1q21	1.55	8.30	0.0017
C1orf37	212165_at	Chr:1q31.3	1.63	8.30	0.0029
MAPKAPK5	212871_at	Chr:12q24.13	1.36	8.30	
NFYA	215720_s_at	Chr:6p21.3	4.11	8.30	
RBMS1	203748_x_at	Chr:2q24.2	2.74	8.30	
DKFZP434B168	222250_s_at	Chr:1p36.13-q42.3	1.45	8.30	
Ufc1	217797_at	Chr:1q23.1	1.50	8.30	0.0025
CENPF	207828_s_at	Chr:1q32-q41	2.14	8.30	0.0022
PSME4	212219_at	Chr:2p16.1	1.78	8.30	
PPP2R2A	202313_at	Chr:8p21.1	1.60	8.30	
SLC25A3	200030_s_at	Chr:12q23	1.27	8.30	
RBMS1	207266_x_at	Chr:2q24.2	3.19	8.48	
CGI-01	212405_s_at	Chr:1q24-q25.3	1.54	9.94	0.0022
KAB	212746_s_at	Chr:1q44	1.72	10.17	0.0037
GPSM2	205240_at	Chr:1p13.2	1.76	10.17	
SEMA4C	46665_at	Chr:2q11.1	1.63	10.17	
EIF5B	201027_s_at	Chr:2p11.1-q11.1	1.54	10.17	
ARID4B	221230_s_at	Chr:1q42.1-q43	1.47	10.17	0.0033
GPR161	214104_at	---	2.98	10.17	
VARS2	201796_s_at	Chr:6p21.3	2.32	10.17	

P value from Wilcoxon test, normal approximation, genes located on 1q are typed in bold face.

We also evaluated the expression of the loci that were targeted by our QMPCR assay. Of these 30 genes, *RASSF5* was not represented as on the Affymetrix U133A chip. Eight genes were not expressed at all in our retinoblastoma samples: *GJA5*, *ELF3*, *MYOG*, *SOX13*, *REN*, *PEPP3*, *IKBKE* and *CNTN2*. *PIK3C2B* and *GAC1* were present in only 11 and 6 tumours, respectively. Of these genes, only *PIK3C2B* was found to be present in normal retina.

Table 3-3. Expression of genes investigated by QMPCR

Locus	Gene Symbol	Median expression in tumours: Without gain / With gain	Expression in Normal retina
1q21	*GJA5*	A	A
	MCL1	6562.1/ 9268.3**	838.6
	ENSA	3593.35/ 6064.2**	3229.8
	LASS2	1133.1/ 1892.8**	2184.4
	HTCD37	1508.3/ 2372.3**	1928.7
	SNX27	1066.3/ 1600.6**	819.1
	JTB	7327.95/ 11227.2**	5743.1
	ADAR	3967.65/ 5178.3**	5333.7
	SYT11	2936.75/ 4511.2**	1916.8
1q32	*ZNF281*	1612.6/ 2300.3**	838.6
	ELF3	A	A
	MYOG	A	A
	FMOD	540.2/ 610.3	2667.4
	LAX	336.6/ 323.2	308.1
	SNRPE	6935.75/ 9340	5188.7
	SOX13	A	A
	REN	A	A
	PEPP3	A	A
	PIK3C2B	722.15/ 720.5	889.9
	MDM4	365.75/ 355.7	213.4
	LRRN5 (GAC1)	399/ 512.9	A
	CNTN2	A	A
	RBBP5	588.65/ 580.9	423.6
	HUCEP11	1942.65/ 2227.6	1233.5
	RAB7L1	375.95/ 286.8	951.6
	IKBKE	A	A
	RASSF5	n.r.	n.r.
1q32-41	*CENPF*	4503.7/ 7661.8**	A
1q42	*COG2*	1401.1/ 1541.2	1292.4
1q44	*SMYD3*	1112.25/ 1339.7*	673.5

Median of expression values from tumours without or with gain of material on 1q, and expression value in normal adult retina. (* P<0.05; ** P<0.0005; Wilcoxon test normal approximation; A: Absent, gene not expressed; n.r.: not represented on the array).

The 20 other genes were called present in at least 18 of the 21 tumours (Table 3-3). Of these 20 genes, 11 showed differential expression between tumours with gains and without gains thus reflecting the effect of increased gene dosage. Even though the fold changes are rather low (Table 3-2), they indicate that the two groups of tumours have a

different expression pattern. Most of the genes differentially expressed belong to the 1q21 region; only two genes, *ZNF281* and *CENPF*, belonging to 1q32 were differentially expressed.

When analyzing the expression pattern of genes in 1q21 and 1q32, we found the same genes expressed in normal adult retina and in primary retinoblastoma. It has to be noted that 5 genes were much higher expressed in the primary tumours than in the normal adult retina. Among these genes *SMYD3*, *ZNF281* and *MCL1* were present in the normal retina but at inferior levels compared to both groups of tumours (with and without gains on 1q), and *CENPF* was absent in normal adult retina. *JTB* was also expressed at higher levels in tumours than in retina, but the level of expression in retina was almost the same than the one in the tumours without gains on 1q. One gene only, *FMOD*, was expressed at lower level in the tumours compared to retina.

3.1.5 Genomic gains in 1q and clinical manifestation

In order to determine groups of tumours defined by distinct patterns of gains on 1q the multivariate DNA copy number data was analyzed by unsupervised classification algorithms. We have chosen this approach because the threshold method that was used to determine the minimum region of gains on 1q does not take into account the multivariate nature of the results. We applied different algorithms for agglomerative hierarchical clustering (single linkage, complete linkage, average linkage, centroid linkage, and Ward's method) to classify the copy number patterns on 1q. All these methods identified essentially the same 4 classes of tumours (Fig. 3-4B). One class comprises 7 tumours (9%) with increased copy number for all the 30 genes on 1q and copy numbers ranging from 3 to 6 (QMPCR values: 1.97 [1.78; 2.19]). This class is later referred to as *chg* (complete and high gain). Another class distinguished by the cluster algorithms comprises 12 tumours (16%). All tumours in this class show gains at most loci with copy numbers ranging up to 5 (QMPCR values: 1.64 [1.53; 1.77]). This class is later referred to as *hg* (high gain). The largest class contains 35 (47%) samples with no gains (abbreviated *ng*, QMPCR values: 1.11 [1.04; 1.18]). The remaining 20 (27%) samples represent a fourth class of tumours showing intermediate levels of DNA gains (abbreviated *ig*, QMPCR values: 1.35 [1.25; 1.45]).

We tested for associations between the assignment of a tumour to one of the four classes of 1q gains and various aspects of clinical manifestation. Knowing that several aspects of

clinical manifestation are different between patients with bilateral and isolated unilateral retinoblastoma, we only analyzed data from the latter group of patients. Also, in Germany, almost all patients with isolated unilateral retinoblastoma undergo enucleation as primary therapy. Therefore, our findings are likely to be representative for this group as only very few patients are not included in our study.

We observed a strong association with age at diagnosis (Fig. 3-9): most patients with tumours with no 1q gains (*ng*) were young (26/31 patients, range 0 to 18 months of age), whereas patients whose tumours showed gains (*chg* and *hg*) were older at time of diagnosis (17/17 patients, range 10 months until 5 years of age). The distribution of age at diagnosis of patients with tumours in intermediate gains class (*ig*) is in between that of *ng* and *chg/hg* tumours. The difference of the distributions of age at diagnosis in patients with *chg*/*hg* tumours and either *ng* or i*g* tumours is statistically significant as is the difference between that of patients with *ng* and *ig* tumours.

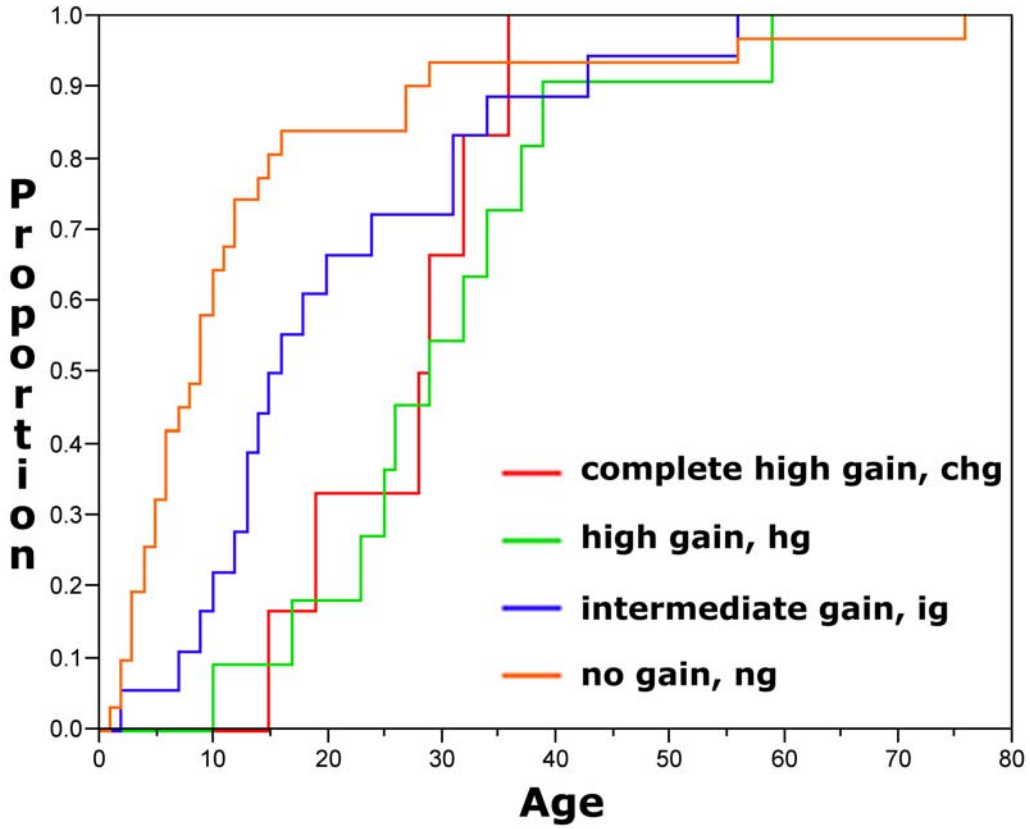

Fig 3-9. Cumulative proportion of patients diagnosed for Rb by age at diagnosis (in months) grouped by the pattern of genomic gains in chromosome 1q. Distribution of age at diagnosis is significantly different between classes *chg* and *ng* (P=0.0032) and between classes *hg* and *ng* (P=0.0003).

Although vitreous seeding was more frequent in patients with *chg* and *hg* tumours (Table 3-4), vitreous seeding was also observed in almost half of the patients with *ng* tumours. The histology of most *ng* tumours was completely differentiated whereas *chg* and *hg* tumours frequently showed only partial differentiation or were undifferentiated. The only 2 tumours with fully undifferentiated histology were genetically classified as *chg*.
We observed no significant differences between classes with 1q gains and other aspects of the tumour behaviour or genetic status of the *RB1* gene including tumour size, tumour calcification, tumour necroses, the type of mutation on the *RB1* gene or allele loss at this locus.

Table 3-4. Association of clinical characteristics and gene dosage, according to the class of the tumours (number of tumours).

		chg	*hg*	*ig*	*ng*
Tumor size	25 - 50 %	4	4	10	21
	>50%	0	3	2	1
Differentiation	Undifferentiated	1	1	2	0
	Partially differentiated	4	6	11	13
	Completely differentiated	0	2	5	18
Vitreous seeding	No seeding	0	0	5	9
	Local seeding	1	1	2	5
	Diffuse seeding	5	5	6	6
Necrosis	Necroses	6	8	14	27
	No necrosis	0	1	1	1
Calcification	Calcification	5	8	15	24
	No calcification	0	0	0	1

None of the tumour characteristics is significantly associated with gene dosage changes in 1q. *chg*, complete high gain, *hg*, high gain, *ig*, intermediate gain, *ng*, no gain.

3.2 Identification of an oncogene on chromosome 1p

3.2.1 Matrix-CGH

Matrix-CGH with a genome chip that contains BACs that represent all chromosomes was performed at the DKFZ in Heidelberg. These analyses resulted in the identification of a novel high-level amplification on 1p34.2 in one of 17 retinoblastoma specimens tested (M22234). In this tumour, 4 BACs clones showed copy number gains (name and location are shown in the insert of Fig 3-10, values ranging from 5.3 to 7.9). These BACs contain 9 known genes: *TRIT1, MYCL1, CAP1, PPT1, RLF, ZMPSTE24, COL9A2, RIMS3,* and *NFYC* (NCBI build 35.1).

3.2.2 RNA expression analysis

RNA expression data (2.2.19) were available from all 17 tumours that were analyzed by whole genome matrix CGH. All 9 genes known to be contained on the BACs with gains were represented by probe sets on the Affymetrix chip. One gene, *CAP1*, was represented by 2 probe sets. All but one (*NFYC)* of these genes had markedly higher expression levels in the tumour with the 1p34 gain compared to the tumours without genomic gains in this region (Fig 3-10). As genes located adjacent to BACs with amplification, e.g. *PPIE* and *NFYC*, showed no higher expression the region with overexpressed was restricted to the genes contained on the positive BAC clones. Although 16 tumours showed no genomic gains in 1p34 region represented by these BACs, there was some variation of expression of the genes in this region: e.g. *COL9A2* showed higher expression in tumours M22069 and M23819, *RIMS3* and *MYCL1* were overexpressed in M22069 and M22734, respectively. However, it is to be noted that expression of these genes did not reach the levels observed in tumour M22234 with DNA gains in this region.

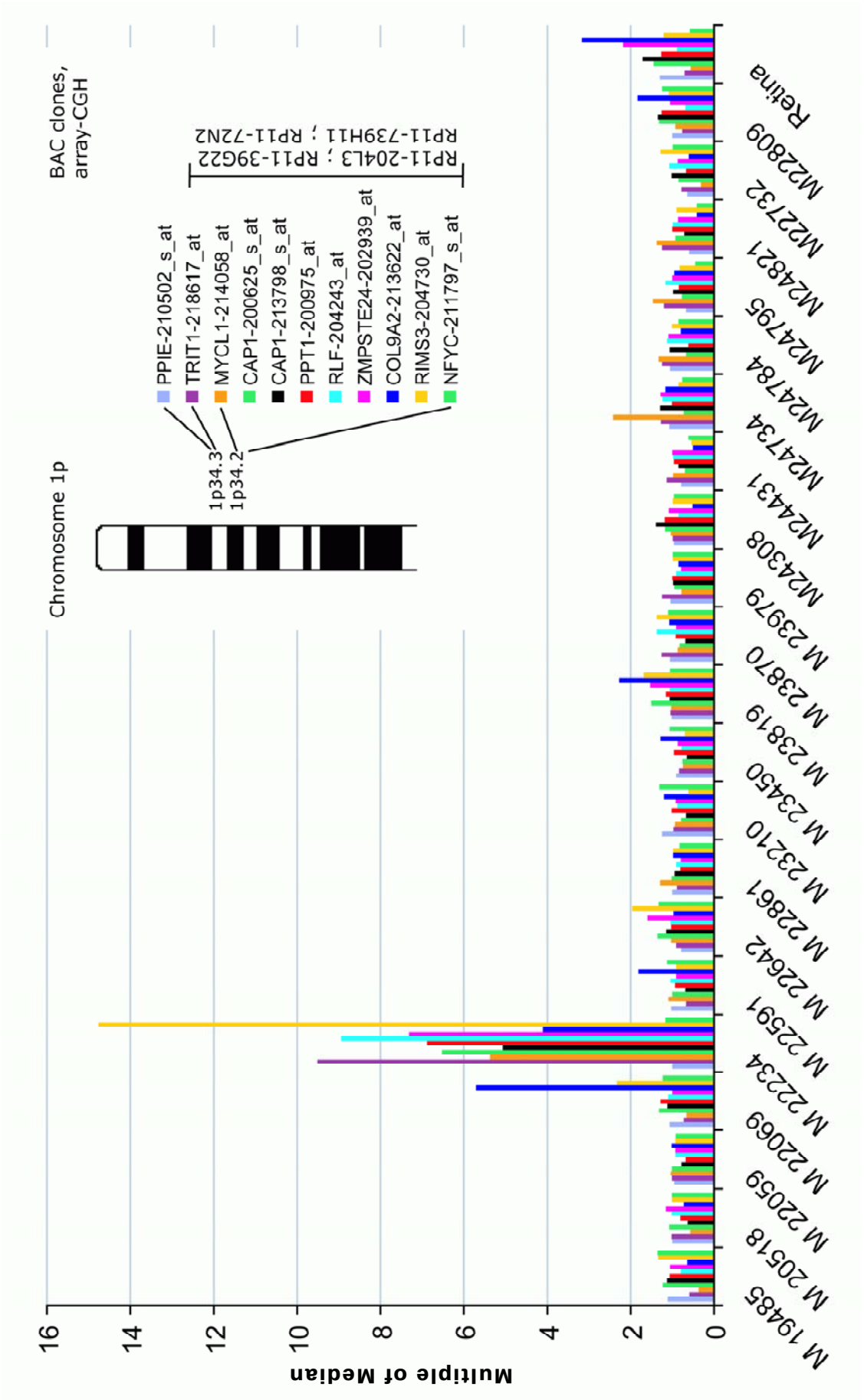

Fig 3-10. Expression of genes on 1p34.3 and 1p34.2 in tumours and retina as determined by microarray hybridization (normalized on the median).

3.3 Identification of allelic loss on chromosome 16

Regions that acquire loss of genetic material during tumorigenesis can harbour tumour suppressor genes. In retinoblastoma, markers on the long arm of chromosome 13 frequently show LOH because this region contains the *RB1* tumour suppressor gene. In addition, CGH analyses have identified loss of genetic material on the long arm of chromosome 16 (16q) in 18 to 46% of retinoblastomas. The region on 16q that is commonly lost may harbour a tumour suppressor locus with the retained allele inactivated by a local mutation or silencing by hypermethylation of the promoter. We have employed different methods to narrow down the location of this potential tumour suppressor gene:

- Microsatellite analysis (MSA) was used to determine allele loss (3.3.1). This study comprised 10 polymorphic microsatellite loci located on 16p and 16q22, a region previously highlighted by the results of Marchong et al. [40].
- Genotyping by pyrosequencing was used to confirm the results obtained with MSA (3.3.2)
- A methylation specific PCR assay was used to detect hypermethylation of the promoter of the *CDH11*, the candidate tumour suppressor gene on 16q22 proposed by Marchong et al. (3.3.3)

Furthermore, we analyzed the expression of the genes that are located in the region on 16q investigated by microsatellite analysis (3.3.4), and tested if parameters of clinical manifestation are correlated with the allele loss status of chromosome 16 (3.3.5).

3.3.1 Microsatellite analysis (MSA)

Allele loss by microsatellite analysis (MSA) was determined in those 21 tumour samples that were also analyzed on the RNA expression level. Examples of loci with LOH and retention of heterozygosity are shown in Fig 3-11. In 3 of the 21 tumours investigated, all the informative markers on 16q showed allele loss (Fig 3-12). Interestingly, one tumour (M24794) had loss of only one of the informative markers tested on 16q. It has to be noted that the two markers flanking this locus were informative and had no loss of heterozygosity. No tumour showed allele loss of a marker on the short arm of chromosome 16.

CGH data were available from 16 of the tumours tested by MSA. Results were concordant in 15 of the cases. One tumour (M23818) had a loss of material of the whole long arm of

chromosome 16 in CGH that was not detected in MSA: two of the eight loci investigated by MSA on 16q were informative and showed retention of both alleles in tumour DNA. This discrepancy between MSA and CGH result could be due to a homozygous deletion because in this case the CGH would detect a loss that MSA misses (the tumour tissue contains a little quantity of normal tissue that is the target of PCR in the MSA). However, our results are not conform with this possibility because the MSA which was performed in a multiplex PCR assay showed that the peak areas of the two heterozygous loci were comparable to those of homozygous loci. These results allow us to conclude that our MSA results are valid.

Results from matrix-CGH were available from 16 tumours tested for 16q allele loss. The status of chromosome 16 was concordant for 13 tumours. Two tumours showed losses of material in matrix-CGH that were not detected in MSA. The tumour M24794 with loss of only one marker in MSA also showed loss of a narrow region in matrix-CGH. This loss was confined to three BAC clones on 16q24. The clones were not located in the same area than the STR marker, and losses of these clones could not be detected in MSA as the region was not covered. The losses detected in this tumour with these methods were very confined, and thus we decided to use genotyping of SNPs by PSQ to delimitate the extent of allele loss in the region neighbouring the marker D16S3085.

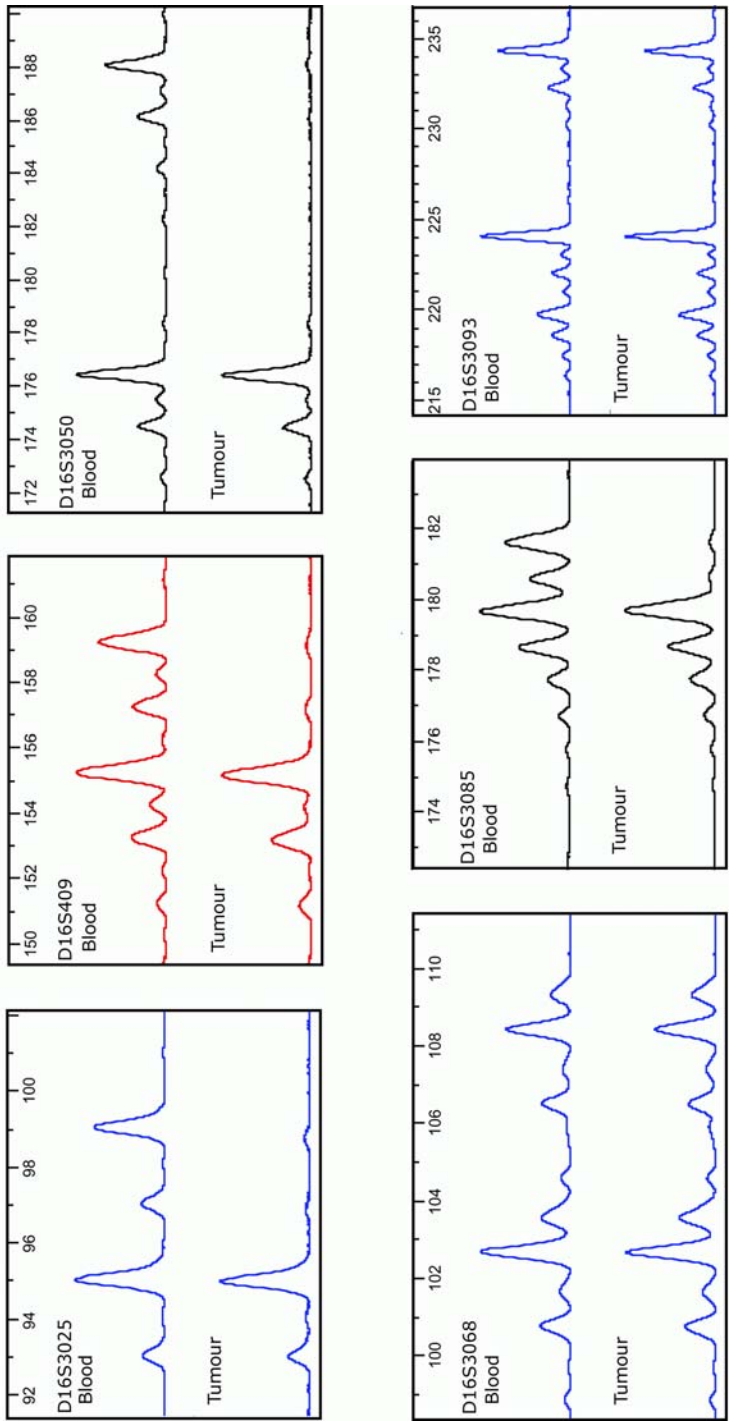

Fig 3-11 Electropherograms of some of the microsatellites used for the MSA in tumour M22590 and the corresponding sample of DNA from blood. Four of the loci (D16S3025, D16S409, D16S3050, and D16S3085) show LOH in tumour DNA.

3.3.2 PSQ

The STR D16S3085 that was the only marker with LOH in tumour M24794 is located at 66,225,096 bp on chromosome 16 (NCBI build 35.1). For further LOH analysis we have chosen five SNP loci with known allele frequencies in the regions flanking this location (Table 2-8). We have investigated 20 tumours and found that 42% of the loci were

heterozygous. Allele loss was observed only in the 3 tumours that had shown LOH in MSA (Fig 3-13). The tumour M24794 did not show LOH at any of the SNPs analysed. Unfortunately, the centromeric SNPs rs7200919 and rs7206718 were not informative (i.e. homozygous in constitutional DNA) thus precluding to further delineate the region showing with LOH. Based on these data, the minimum region of LOH in tumour M24794 has an extent of 1,270 kbp.

3.3.3 MSPCR

Aberrant methylation of gene promoter regions is a frequent genetic alteration that can be associated with tumorigenesis as it can cause transcriptional silencing and, consequently, loss of gene function. In a recent report from Marchong et *al.* it was proposed that the *CDH11* gene is the target of allele loss on chromosome 16 in retinoblastoma. This prompted us to set up an assay to detect hypermethylation of the promoter of this gene. We have investigated 54 tumours for *CDH11* methylation (Fig 3-14). In addition to tumours samples that were obtained from the Augenklinik in Essen, we also analysed samples sent to us from an outside laboratory (Zerrin Onadim, Retinoblastoma Genetic Screening Unit London NHS Trust, UK). We have also investigated the four tumours showing LOH in MSA. In three of these tumours the LOH region included *CDH11*. In tumour M24794 the region with LOH did not include the *CDH11* locus (Fig 3-15).

The result of the PCR with the primer pair specific for methylated DNA on the positive control sample (bisulfite modified fully methylated DNA) showed the expected specific product. No fragment was amplified from the positive control when using primers specific for unmethylated DNA.

PCR with primer pairs specific for unmethylated DNA amplified a product of expected length in each of the 54 and 4 tumours investigated. However, no PCR product was obtained with methylated specific primer pairs thus indicating that no promoter methylation of *CDH11* is present in any of the tumours investigated.

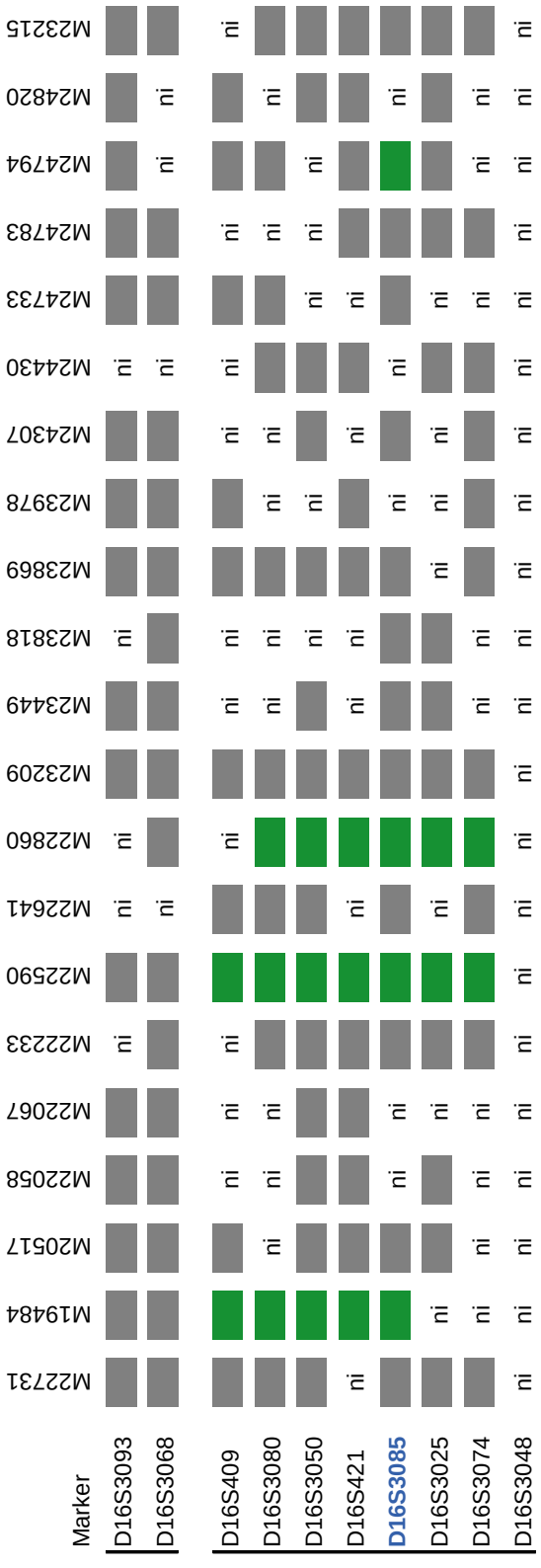

Fig 3-12. MSA analysis results of STR loci on chromosome 16. Each row represents all results for one tumour. Grey boxes indicate retention of both alleles, green boxes indicate LOH, and ni indicates non informative loci, i.e. those that show constitutional homozygosity.

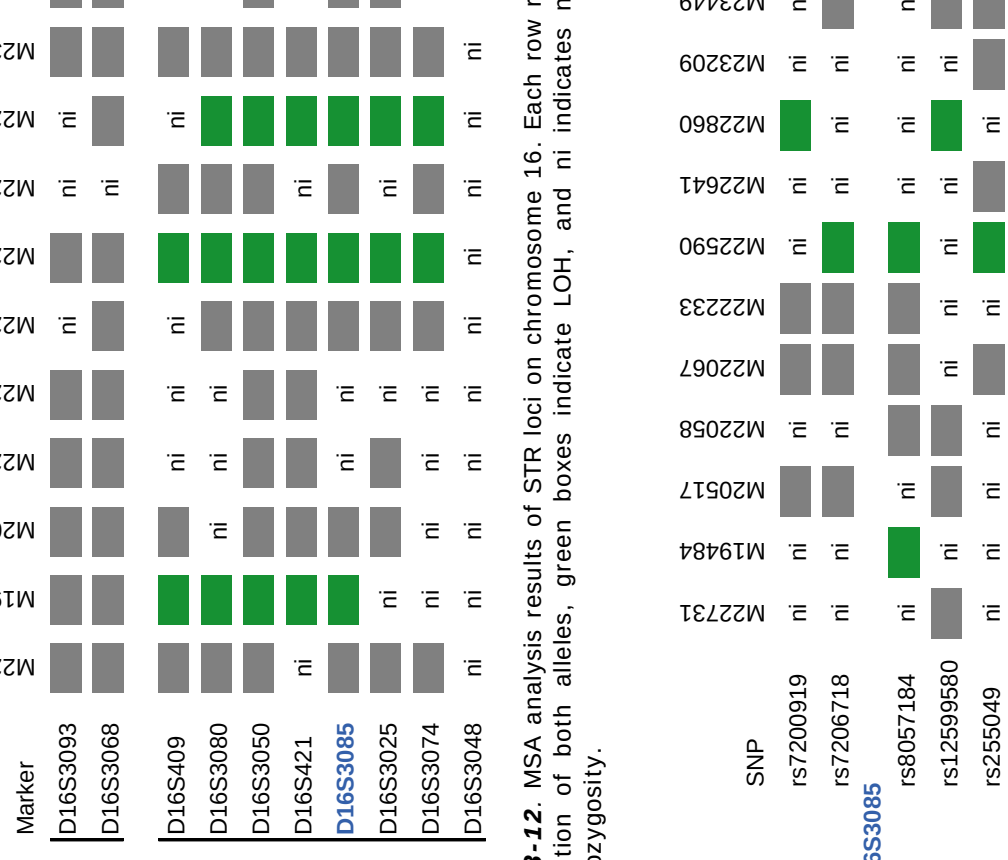

Fig 3-13. Results of Pyrosequencing analysis of SNP loci on chromosome 16. Each row represents all results for one tumour. Grey boxes indicate retention of both alleles, green boxes LOH, and ni indicates non informative loci, i.e. those that show constitutional homozygosity.

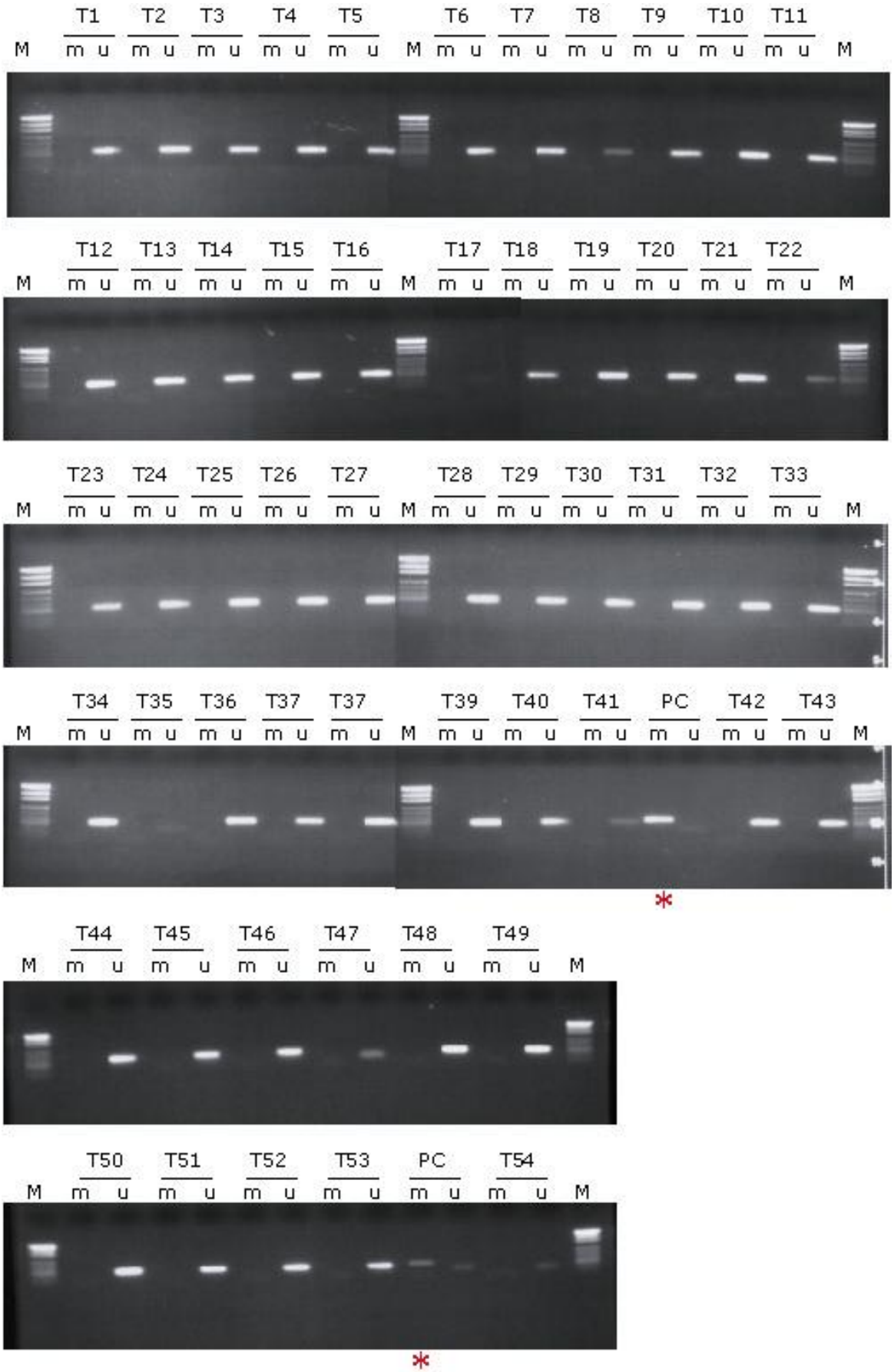
T1 T2 T3 T4 T5 T6 T7 T8 T9 T10 T11
M m u m u m u m u m u M m u m u m u m u m u m u M
T12 T13 T14 T15 T16 T17 T18 T19 T20 T21 T22
M m u m u m u m u m u M m u m u m u m u m u m u M
T23 T24 T25 T26 T27 T28 T29 T30 T31 T32 T33
M m u m u m u m u m u M m u m u m u m u m u m u M
T34 T35 T36 T37 T37 T39 T40 T41 PC T42 T43
M m u m u m u m u m u M m u m u m u m u m u m u M
*
T44 T45 T46 T47 T48 T49
M m u m u m u m u m u m u M
T50 T51 T52 T53 PC T54
M m u m u m u m u m u m u M
*

(page 62) ***Fig 3-14.*** Gel electrophoresis of products of MSPCR on 54 tumours after bisulfite treatment.
Gel electrophoresis with pUc marker (M), each tumour is represented by 2 slots: 1st slot is the PCR product obtained with methylated specific primers (m), 2nd slot is the PCR product obtained with unmethylated specific primers (u). Red stars: positive control (PC) for the methylated specific primers with artificially methylated DNA treated with bisulfite.

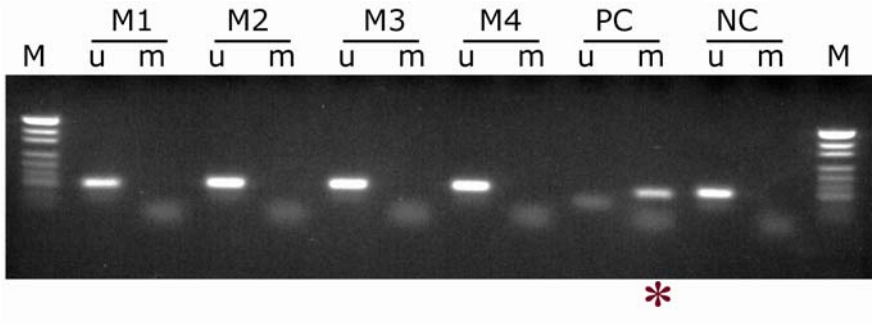

Fig 3-15. Gel electrophoresis of products of MSPCR on the 4 tumours showing LOH in MSA: M19484 (M1), M22590 (M2), M22860 (M3), M24794 (M4). Legend as in Fig 3-14, Negative Control (NC)

3.3.4 Expression data

For expression analysis of the genes on chromosome 16 data of the Affymetrix chip hybridization were used (U133A). On this array, *CDH11* is represented with 2 probe sets. One of the probe sets, 207172_s_at, was expressed in 9 of the tumours investigated with MSA and PSQ. The other probe set, 207173_x_at, was present in all the tumours (Fig 3-16). *CDH11* was also expressed in normal retina (both probe sets). Another potential target gene, *CDH1*, is also represented by two probe sets. One of them, 201130_s_at, showed absent expression in all tumours investigated. The other probe set showed expression in one tumour only. Both *CDH1* probe sets showed that this gene is expressed in normal adult retina. Another gene of the cadherin gene cluster, *CDH5*, was present in 1 tumour and in adult retina.
Analysis of genotyping and expression data did not reveal a correlation between tumours with LOH and loss or reduction of expression of genes on 16q.

3.3.5 Association with clinical parameters

We have tested the tumours for association between clinical parameters and their status on 16q. From these 21 tumours, 3 were from patient with bilateral retinoblastoma and 3 other

were from patient with unilateral retinoblastoma but with a mutation in constitutional DNA (inherited). The other patients had all unilateral not inherited Rb.
No correlation could be found between the status on 16q and the age at diagnosis, the type of retinoblastoma (uni-bilateral, inherited or sporadic).

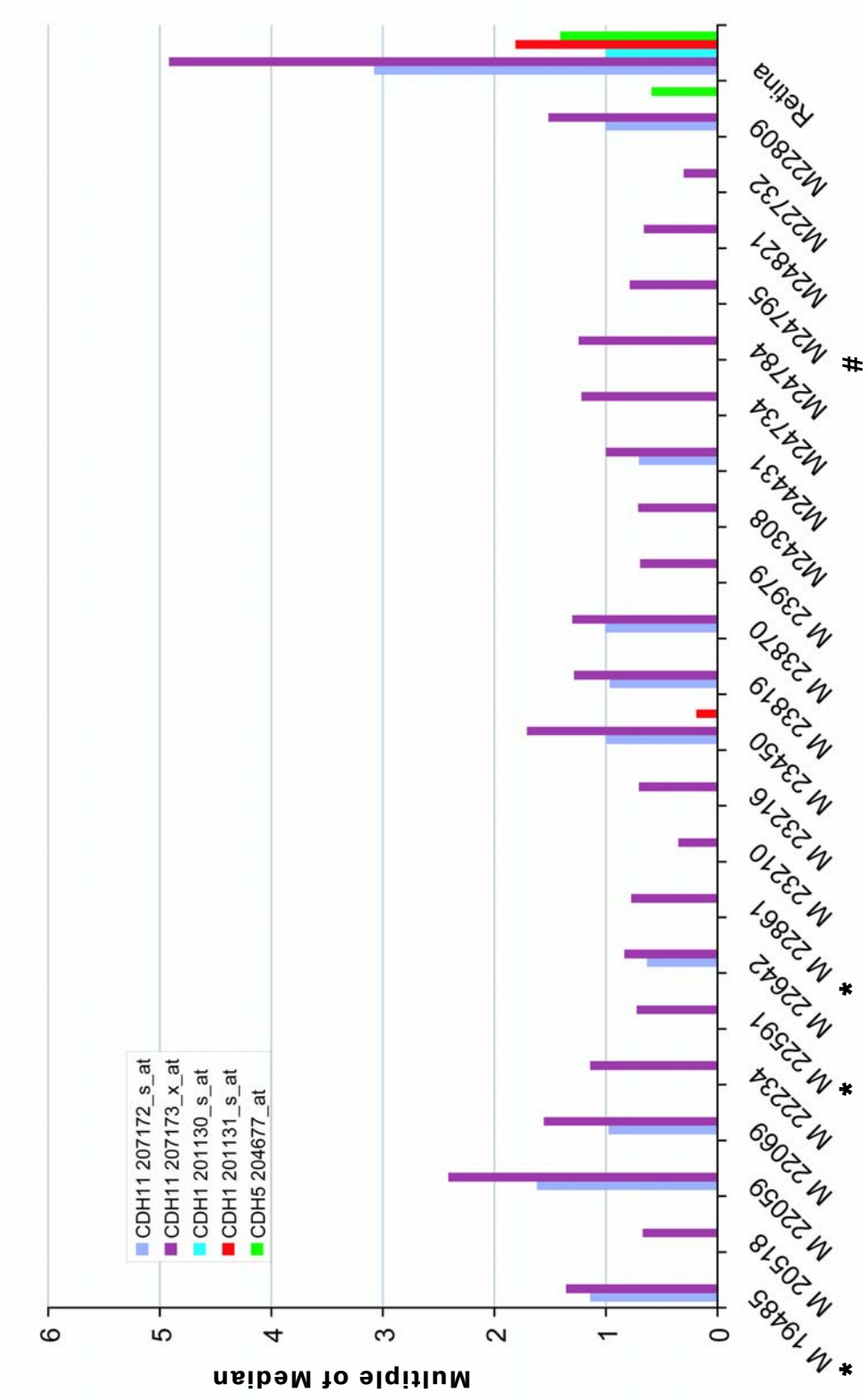

Fig 3-16. Expression of genes of the cadherin gene cluster on 16q22 in tumours and retina determined by microarray hybridization (normalized on the median). *, tumours with LOH on the whole 16q. #, LOH of one marker

4 DISCUSSION

Mutations affecting both alleles of the *RB1* gene are required to initiate retinoblastoma. Nevertheless, other genetic alterations are necessary for progression to a malignant tumour. Cytogenetic and CGH analyses, which both can identify alterations on a genomic perspective, have shown recurrent aberrations in retinoblastomas. Although these changes often affect large parts of chromosomes, the functional target of these alterations may be as small as a single gene. As the resolution needed to identify these genes is below the level of conventional cytogenetic and CGH methods we have used different techniques to determine the specific targets of mutations that occur during progression of retinoblastoma.

4.1 Gains on the long arm of chromosome 1

4.1.1 Frequency and location of DNA gains on 1q

With QMPCR 34 of 76 (45%) retinoblastomas were found to have gains involving 1q21 or 1q32. This proportion compares well to reported studies based on CGH, which have shown gains of material on chromosome 1q in 40 to 50% of retinoblastomas [25-28]. While the QMPCR assays showed relatively clear patterns of copy number changes, interpretation of the data obtained with pyrosequencing and Real Time PCR, which were used as alternative methods to confirm the presence of 1q gains, was not straightforward.

The results of pyrosequencing on DNA from peripheral blood DNA showed very little variance. This is a prerequisite when determining allelic imbalances by relative quantification of allele signals in tumour DNA. However, we found that in a few tumours the pattern of allelic imbalances detected by pyrosequencing was distinct from that of DNA gains identified by QMPCR. Specifically, two tumours with a balanced allele ratio of the *ANGPTL1*–SNP had allelic imbalances at the SNPs located on 1q21 and 1q32. However, as the same SNP showed allelic imbalance in 5 tumours with allelic imbalances of the telomeric and centromeric SNPs, this discontinuity is not likely to be a simple systematic error.

In principle, Real Time PCR permits detection of gain or loss of a single copy of a gene. Results from QMPCR and Real Time PCR were clearly correlated but the correlation coefficient was rather low. Goff et al. [56] suggested that the detection level of CGH was presumably below the one of Real Time PCR. However, with the same thresholds we

used for QMPCR (samples were considered to have gains if more than one marker showed a value equal or higher than 1.5), 76% of the tumours showed concordant results in the TaqMan and CGH assays.

With array-CGH we identified gains of material on 1q in a higher proportion of tumours (12/17, 70%). In view of the low number of tumours investigated by array-CGH this might be due to random variation. In addition, it has to be noted that these tumours had been deliberately selected because they had given enough high quality RNA suited for expression analysis. It is possible that this bias contributes to the observed higher proportion of tumours with 1q gains. The results obtained by array-CGH were concordant with those of conventional CGH and QMPCR and, therefore, we have no reason to suspect that array-CGH will identify gains that are not detected by the other techniques.

With QMPCR we detected gains in 13 of 50 tumours that had no 1q gains in CGH. This suggests that CGH fails to identify some tumours that in fact have 1q gains. Admittedly, we cannot exclude that some tumours identified as having gains by QMPCR have in fact no 1q gains. However we have controlled for stochastic and systematic errors, which both are potential sources of false positive results, by redundant measurements of some loci and by analysis of samples with known copy number of chromosome 1q, respectively. Moreover, our results confirm previous reports [31, 52] have also found that QMPCR has a higher sensitivity (i.e. lower proportion of false negatives) compared to that of CGH.

The patterns of copy number changes do not converge on a single small interval on 1q that might be regarded as a minimal region of gains. Rather, two minimally regions of gains were identified: 1q21 and 1q32.1q32.2. It is to be noted that the centromeric region, 1q21, was only identified after joint analysis of DNA copy number and expression data with the SAM method that had prompted us to perform QMPCR of loci in this region. Also with CGH we found that some cell lines showed a gain pattern with two peaks. In QMPCR, most of the 76 retinoblastomas showed increased copy numbers for loci from 1q21 and 1q32. In most tumours with gains, the level of gains corresponds to a triplication. This is in accord with previous reports of trisomy of 1q [57].

All retinoblastoma cell lines that we analyzed had gains in both regions. However, most cell lines showed higher levels of gains compared to primary tumours. The high conservation of the pattern of gains in a retinoblastoma (G319) and a cell line (RBL 30) derived from this primary tumour suggests that the quantitative differences must not reflect alterations that occurred during cell culture. It is conceivable that only those primary tumours with relatively high levels of gains in these regions on 1q can be

established as cell lines. In other words, high level gains may be a prerequisite for successful permanent growth in cell culture.

The two regions identified with QMPCR and CGH were not exactly the same as those identified with array-CGH. In array-CGH the centromeric border of gains was localized to 1q22. However, the BACs with hybridization signals indicating gains are mapped to the boundary of 1q21 and 1q22. Therefore, the genes that are represented in these clones are either located on 1q21.3 or 1q22. This does not change the essence of our finding, namely that the patterns of gains in primary retinoblastoma and in cell lines that suggest two distinct regions on 1q are the targets of genomic gains in retinoblastoma.

The mechanism underlying amplification on 1q is unknown. However, the formation of double minute chromosomes or episomes is very improbable for two reasons: i) in most of the tumours with gains, the whole long arm of chromosome 1 is triplicated, and ii) the level of gain is not high enough to be due to extra-chromosomal structures which usually induce amplifications of genes. The most probable mechanism involved in gains on 1q in retinoblastoma is duplication of one chromosome arm.

Genomic gains on chromosome 1q are observed in many tumour entities including lipomas, leiomyosarcomas and osteosarcomas [58-60]. Interestingly, these are tumours that occur with increased frequency in patients with hereditary retinoblastoma (second extraocular tumours) [61, 62]. This suggests that retinoblastoma and second extraocular tumours may have in common some of the genetic alterations that are needed for initiation and progression. Lipomas and leiomyosarcomas frequently have amplifications on 1q21-q23 [63], which overlaps with one of the regions of gains identified here. Gains of material on 1q21 are also present in osteosarcomas, although at relatively low frequency [64, 65]. The second region with gains in retinoblastoma, 1q32, has been found to be involved in gene amplifications that were detected in other tumours. Specifically, a subset of glioma has high level amplifications on 1q32 that target the *MDM4* gene [38, 39]. We analyzed the pattern of 1q gains from two glioma samples with 1q amplification by QMPCR. Our data confirmed high level gains of *MDM4* and *GAC1* and moderate gains of *PIK3C2B* and *PEPP3*, which are also located in 1q32. This shows that the pattern of gains in the two glioma samples is unlike that of retinoblastoma and indicates that distinct sets of genes are targeted by gains in these two tumour entities.

4.1.2 Candidate genes on 1q

As DNA gains in retinoblastoma do not focus on a small interval on 1q, additional data is required to narrow down the list of genes that might contribute to progression in this tumour. By joint analysis of data on DNA gains and on RNA expression, which we obtained from a subset of our samples, we could exclude a possible contribution of several genes located in regions with gains. For example, we found that *MDM4*, *PIK3C2B*, *GAC1*, and *PEPP3*, which are located in 1q32 and show gains in glioma with 1q32 amplification, were absent or not differentially expressed between retinoblastomas with or without gains in this region. This confirms that these genes are not the target of 1q gains in retinoblastoma. Gains on 1q21-q23 in liposarcomas and leiomyosarcomas have been found to consistently include the *COAS* cluster of genes [63]. We found that one of these genes, *COAS2*, is not expressed at all in retinoblastomas. The two other genes of the COAS cluster (*COAS1* and *COAS3*) are not represented on the Affymetrix chip we used. However, no data on expression of the COAS genes has been reported in liposarcomas or leiomyosarcomas and, therefore, their possible role in these tumours is also not resolved.

The oligonucleotide array that we used for RNA analysis interrogated the expression of more than 22,000 probe sets. This represents a considerable proportion of human genes known so far. When analyzing the expression data by SAM, several genes located in 1q21 and 1q32 were identified as differentially expressed between tumours with and without gains. Among them are *CENPF*, located on 1q41, and *MCL1* and *JTB*, located on 1q21 that have been associated with cancer previously.

- *CENPF* (mitosin) encodes a protein of the nuclear matrix that associates with the centromere-kinetochore complex during mitosis. Higher expression of this gene has been associated with oesophageal squamous cell carcinoma [66], progression of astrocytoma [67] and of head and neck squamous cell carcinoma [68]. Among the genes with differential expression between retinoblastoma with and without 1q gains, *CENPF* has the highest fold change (2.14, q-value: 8.3%). In normal adult retina this gene is not expressed but this might simply reflect the low mitotic activity of this terminally differentiated tissue. The “electronic northern” of this gene (http://expression.gnf.org and http://symatlas.gnf.org/SymAtlas/, Affymetrix accession # 207828_s_at) shows a median value of expression of 250 with a peak value of 5000 in bone marrow early erythroid cells. In comparison, the median obtained in retinoblastoma primary tumours is 4800, with highest values of 14600.

Such a high level of expression suggests that this gene is important for the biology of retinoblastoma.

- *MCL1* is another differentially expressed gene, which belongs to the Bcl-2 family and has been found to be overexpressed in anaplastic cell lymphoma cell lines and tumours [69, 70]. Transcripts of this gene show alternative splicing and two variants encoding distinct isoforms have been identified [71]. The product of the longer transcript enhances cell survival by inhibiting apoptosis while the alternatively spliced shorter gene product promotes apoptosis. We cannot distinguish these transcripts because the 3 different probe sets contained on the Affymetrix chip all detect both transcript variants. The electronic northern of *MCL1* (Affymetrix accession # 200797_s_at) shows a median value of expression of 100 with a peak value of 12000 in myeloid cells. In retinoblastoma primary tumours the median obtained is 7000, and the highest value 9900. These expression levels show that *MCL1* may play a role in the development of retinoblastoma.
- A third gene higher expressed in tumours with gains on 1q, *JTB* (jumping translocation breakpoint), was found to be a part of an amplicon located on 1q21 and overexpressed in hepatocellular carcinoma [72]. The function of *JTB* is not yet well characterised.

Finally, differential expression was also identified for *ZNF281*, *SYT11*, *ENSA*, *ADAR*, *LASS2*, *SNX27*, *SMYD3* and *HTCD37*. Two of these genes, *ADAR* and *HTCD37*, were not differentially expressed between normal retina and tumours with gains. *SYT11*, *ZNF281*, *SNX27*, *SMYD3* and *ENSA* have a 2 fold lower expression in normal adult retina compared to the median in retinoblastomas with gains on 1q. Increased expression of these genes in tumours has not been reported and what is known about their function, if characterized at all, yields no specific clues to a possible role in tumour progression. Nevertheless, these genes should not be disregarded as potential functional targets of 1q gains in retinoblastoma.

4.1.3 Clinical aspects

In a previous CGH based study on tumours of patients selected for early and late age at diagnosis it was observed that patients with tumours with no detectable alteration on 1q were diagnosed earlier compared to patients with tumours with gains [28]. With the copy

numbers determined by QMPCR in this study we could use clustering algorithms to classify tumours according to the pattern of 1q gains. When stratifying according to the classes obtained by this analysis, earlier diagnosis of tumours without 1q gains is evident. Interestingly, tumours with 1q intermediate gains show a significant lateral shift of the distribution towards older age at diagnosis compared to tumours without gains. Tumours with high gains and very high gains were diagnosed even later. They show almost the same distribution of age at diagnosis thus indicating that these two classes of tumours are not distinct with regard to their biologic behaviour. Different hypotheses can be put forward to explain the observed relation between 1q gains and age at diagnosis. Assuming that retinoblastoma development is initiated by mutations in both alleles of the *RB1* gene, the time course of tumour initiation should not be dependent on the presence of 1q gains. Also, tumour size at the time of diagnosis tends not to be larger in tumours with 1q gains (P=0.0640, Chi-Squared Test for trend, classes *chg* and *hg* combined) and, therefore, it is unlikely that tumours with and without 1q gains represent consecutive stages in the development of retinoblastoma. One hypothesis that may be derived from our observations is that tumours without 1q gains grow faster and thus reach the size required to be detected earlier than tumours with 1q gains. This might also account for our observation that vitreous seeding is more frequent in tumours with gains on 1q (P=0.0397 Chi-Squared Test for independence, classes *chg* and *hg* combined) because if tumours with 1q gains develop with a slow kinetic this would provide more time for seeding into the vitreous. It has been proposed by Gallie et al. (1999) that, in addition to mutational inactivation of both RB1 alleles, third mutations (M3) are required for retinoblastoma development. Assuming this model, tumours without 1q gains may have other M3 mutations in their genome that result in faster progression compared to tumours with 1q gains.

In conclusion, we identified a significant correlation between the time of clinical manifestation and the presence of 1q gains, which is evident even in retinoblastomas with low-level copy number changes.

4.2 Gains on the short arm of chromosome 1

In one of 17 retinoblastomas examined by whole genome matrix-CGH a genomic region on the short arm of chromosome 1 (1p34.2) was found to be amplified. This novel finding pointed our attention to the genes contained in the four BACs that represent this region.

Of the 9 different genes known to be located on these clones, 8 were also overexpressed in RNA from this single tumour. When combining data from the whole genome matrix-CGH and from expression analysis it is possible to delimit the size of the amplicon to an 850 kb region that is framed by the *PPIE* gene on the telomeric side and the *NFYC* on the centromeric side. The size of the amplicon suggests that it may have its origin in an extra-chromosomal structure, possibly a double minute chromosome. Such structures have been described [57] in retinoblastoma cell lines.

The amplicon contains 8 known genes (*TRIT1*, *MYCL1*, *CAP1*, *PPT1*, *RLF*, *ZMPSTE24*, *COL9A2* and *RIMS3*):

- *PPT1*, palmitoyl-protein thioesterase 1, is a small glycoprotein that removes palmitate groups from cysteine residues in lipid-modified proteins and is thought to be involved in the catabolism of lipid-modified proteins.
- *CAP1*, adenylate cyclase-associated protein 1, encodes a protein involved in the cyclic AMP pathway.
- *ZMPSTE24* encodes a zinc metalloprotease found in the endoplasmic reticulum and possibly in the Golgi compartment. It is thought to be involved in the proteolytic processing of farnesylated proteins.
- *COL9A2* encodes one of the three alpha chains of type IX collagen, a component of hyaline cartilage.

The functions of the remaining three genes, *TRIT1* (tRNA isopentenyltransferase 1), *RIMS3* (regulating synaptic membrane exocytosis 3), and *RLF* (rearranged L-myc fusion sequence), are not a well characterised.

MYCL1, an acronym which stands for v-myc myelocytomatosis viral oncogene homolog 1, has been found to be activated in different types of cancer [53-55]. *MYCL1*, is a member of the *myc* family of transcription factors. Members of this gene family are known to play important roles in the progression of cancers. Therefore, the *MYCL1* is a prime candidate for the functional target of this gene amplification. The *myc* family genes are all composed of 3 exons and 2 introns. *MYCL1*, which is less well characterised than c-*MYC*, is the third member of this family. c-*MYC* is thought to be involved in the progression of osteosarcomas, glioblastomas, melanomas [73-75] when its expression is elevated or deregulated. The *MYCL1* gene is processed into two mRNA that code for two related proteins (short and long form). The only probe set specific to *MYCL1* on the Affymetrix chip does not allow to distinguish between the two mRNAs. The long form of *MYCL1* is associated with the nucleus of the cells, whereas the short form seems to be

expressed also in the cytoplasm [76]. The half lives of both long and short peptides are relatively short. De Greve et al., Kaye et al. and Ikegaki et al. [53, 76, 77] found that *MYCL1* is amplified and overexpressed in small cell lung carcinoma cell lines. This gene was also amplified and overexpressed in other tumour types including ovarian carcinoma [55] and hormone resistant prostate cancer [54]. Another member of the myc family, *MYCN*, has been found to be amplified in retinoblastoma cell lines and, infrequently, in primary tumours. Doz et al. [78] identified gains in only 1 of 45 primary retinoblastomas while in a report by Kim et al. [79] 6 of 33 primary tumours were amplified. In the latter study, tumours with *MYCN* gains had higher proliferation levels compared to tumours without amplification. Gains and overexpression of *MYCL1* in retinoblastoma has not been reported before. The patient who carried this tumour had unilateral isolated retinoblastoma, and showed a mutation in blood DNA (inherited from the mother). In addition to MYCL1 amplification this tumour showed gains on 6p and 19q and losses on 13q.

4.3 Candidate tumour suppressor genes on the long arm of chromosome 16

We identified allele loss of at least one informative polymorphic marker on 16q in 4 of 21 (19%) retinoblastomas. This compares well with the frequency of reported chromosome 16 alterations in CGH analyses which ranges from 14 to 34% of tumours. The minimal region lost on 16q, which was delimited to 16q22 in several CGH based studies [25-28], contains a cluster of cadherin genes. Cadherins are Ca^{2+}-dependant cell-cell adhesion molecules which interact with intracellular proteins (catenins, plakoglobins, desmoplakin [80]). The proteins from the cadherin superfamily have functions in cell adhesion, cytoskeletal organisation, signal transduction, and growth control. *CDH1* (or E-cadherin) is the most studied and best characterised member of this family. Loss of function of *CDH1* contributes to progression in cancer by increasing proliferation and invasion. It is involved in many different type of tumours including brain tumour [81] and breast carcinomas [82]. In some colon and rectal cancers silencing of the *CDH1* gene by hypermethylation of its promoter has been found [83]. In a recent study, Marchong et al. pointed to *CDH11* as target of loss on chromosome 16. *CDH11* (OB-cadherin) is expressed in osteoblastic cell lines and its up-regulation during differentiation suggests a specific function in bone development and maintenance. Kawaguchi et al. [84] suggested that reduced expression of *CDH11* in osteoblasts is associated with local invasion of

osteosarcoma. Because of the association between osteosarcoma and hereditary retinoblastoma we investigated the methylation status of the CpG islands in the promoter of *CDH11* gene but identified no abnormality in any of 58 tumours. Thus our data do not support the hypothesis that *CDH11* is inactivated in retinoblastoma.

In three of the four retinoblastomas with allele loss, all informative markers on 16q showed LOH. This is compatible with loss of one whole of long arm of this chromosome (deletion) or mitotic recombination, which results in isodisomy of 16q. In one retinoblastoma (M24794), only the STR-marker D16S3085, which is located between two markers in the *CDH3* and *CDH5* genes, showed LOH. We used pyrosequencing of SNPs to delimitate more precisely the region lost in this tumour. Unfortunately, SNP genotyping in this tumour was hampered by constitutional homozygosity of SNPs next to the STR-marker D16S3085 with LOH. Therefore, we could not further narrow down the minimum region of loss in tumour M24794. Based on available data, the minimum region of LOH has 1,270 kb (NCBI database) and contains 75 genes. Specifically, this region does not include the gene *CDH11* (1.5 Mb away, NCBI database) and this in line with the negative results that we obtained by promoter methylation analysis of this gene. Among the 75 genes in this region, 28 are well characterised and some of them have been shown to have a role in tumorigenesis:

- The gene *E2F4* is a transcription factor playing a role in the control of cell cycle and binding to different tumour suppressor proteins such as pRB. The protein of this gene can induce both proliferation and apoptosis, the function is tissue specific. Its reduced expression is thought to play a role in breast carcinoma [85].
- *CTCF* (CCCTC-binding factor) is a transcription factor whose targets are, as *E2F4*, either oncogenes or tumour suppressor genes, and it has been proposed that it has a tumour suppressor role in breast, prostate, and Wilms' tumours [86].
- The *CBFB* gene (core-binding factor, beta subunit) is a transcription factor whose down-regulation has been observed in gastric cancers [87].
- Hsu et al. [88] found that overexpression of *TRADD* (tumour necrosis factor receptor 1 associated via death domain) led to 2 major TNF-induced responses, apoptosis and activation of NF-kappa-B.
- *HSD11B2* (hydroxysteroid (11-beta) dehydrogenase 2) is underexpressed in colorectal cancer [89], in pituitary adenomas [90] and in cortisol-secreting adenomas [91].

Including the data of expression analysis of the genes in the minimal LOH region defined by D16S3085 was of no help to identify potential candidate genes. For example, the tumours with LOH did not show a reduced expression of the *CDH* genes compared to tumours without loss. Among the genes located in the minimal region of loss and involved in tumour progression (described above), only *CBFB* showed differential expression between tumour with and without allele loss. The difference of the median expression in tumours with LOH was 3,200 whereas the median expression in tumours without LOH was 5,300. As is to be expected from the small sample and effect size, this difference is not statistically significant (Wilcoxon test normal approximation $P>0.5$). This is also true for another gene, *APPBP1* (amyloid beta precursor protein binding protein 1), which showed a two fold lower expression in tumours with LOH compared to tumours with both alleles.

In summary, based on the spatial pattern of allele loss and the results of methylation analysis it is unlikely that *CDH11* is the target of loss on 16q. In view of the relatively low frequency of retinoblastomas with LOH of only parts of 16q, it is likely that a larger panel of tumours must be analyzed in order to map the boundaries of the minimum region of deletion.

5 CONCLUSION

We have identified genetic alterations that occur during the development of retinoblastoma. Specifically, we have found that, in addition to gains on 1q32, gains are also frequent in 1q21. The pattern of DNA gains and the results of our expression analysis did not point to specific genes as the major targets of these alterations. However, age at clinical manifestation is correlated with the presence of 1q gains and this suggests that the deregulation of gene expression patterns caused by 1q gains is important for the clinical behaviour of this tumour, and like in other tumour entities [92] genomic gains that result in altered expression of several genes can have a tumour promoting effect. It will be difficult to identify the individual contribution of these genes to progression compared to the situation in tumours with high-level amplification of a small genomic region and, as a result of this, overexpression of a single gene [93]. However, the strong association with clinical manifestation suggests that identification of the functional targets of these changes will improve our understanding of the biology of this tumour.

Our data confirm that the minimum region of allele loss on chromosome 16 is located on 16q22. Our results also suggest that *CDH11* is not the target of loss of function mutations. Therefore, further analysis will be necessary to define precisely which gene or genes are involved in retinoblastoma progression.

We have identified a novel target of DNA gains in retinoblastoma that is located on the long arm of chromosome 1. This region contains several genes including the *MYCL1* gene, which is a potential oncogene. These genes are overexpressed when compared to tumours without amplification. Further analyses are required to determine which of these genes contribute to the progression of retinoblastoma.

6 ABSTRACT

Many retinoblastomas (RBs) show genomic alterations in addition to mutational loss of both normal *RB1* alleles. The most frequent of these changes are gains on chromosomes 1q and 6p and losses on 16q. To identify the genes targeted by gains on chromosome 1q we used quantitative-multiplex PCR and array-CGH to determine DNA copy number changes in 76 primary tumours and 6 RB cell lines. In addition, in 21 of these tumours gene expression was analyzed by cDNA microarray hybridization. We have used microsatellite analysis and pyrosequencing to further localise the region of allele loss of heterozygosity on chromosome 16. We have also set up a specific methylation assay for the *CDH11* gene located on 16p22 that was previously considered to be the target of loss on 16. The results we obtained were compared with expression of the corresponding genes. A novel region of amplification on the short arm of chromosome 1 was determined with array-CGH, and with a combination of genomic results and expression data allowed us to analyse the possibility of a novel oncogene involved in progression of retinoblastoma.

Increased copy numbers of loci on chromosome 1q were present in 34 (45%) primary tumours and in all 6 cell lines. Two regions of gain emerged, one in 1q32 and another in 1q21. Tumours with 1q gains showed higher RNA expression of several genes in these two regions. The clinical manifestation of tumours with and without gains was similar with regard to many aspects including size, necrosis and calcification. However, the distribution of age at diagnosis was remarkably distinct with earlier diagnosis in tumours without gains. This suggests that these tumours are either initiated earlier or grow faster than tumours with gains. This association with clinical manifestation indicates that gains on 1q are significant for the biology of retinoblastoma. The genes on 1q with copy number gains and overexpression here are candidates that need to be tested for their individual contribution to the progression of retinoblastoma. The targets of loss on chromosome 16 are not clearly identified, but our results suggest that the *CDH11* gene is probably not the tumour suppressor gene involved in progression of retinoblastoma that was proposed before. The results we obtained with our analyses on chromosome 1p suggest a role for *MYCL1* in retinoblastoma.

7 ANNEXES

Table A. 150 first genes overexpressed in tumours with gains on 1q (from SAM)

Affy. #	Location	Fold Change	q-value (%)
218401_s_at	Chr:1q32.1	1.51	4.90
209197_at	Chr:1q21.2	1.43	4.90
221486_at	Chr:1q21.2	1.62	4.90
209198_s_at	Chr:1q21.2	1.69	4.90
201786_s_at	Chr:1q21.1-q21.2	1.33	4.90
210101_x_at	Chr:1p22	1.41	4.90
200797_s_at	Chr:1q21	1.38	4.90
209091_s_at	Chr:1p22	1.48	4.90
220483_s_at	Chr:8q22	1.38	4.90
209586_s_at	Chr:1q21	1.70	4.90
200897_s_at	Chr:4q32.3	1.66	4.90
221498_at	Chr:1q21.2	1.48	5.52
222212_s_at	Chr:1q21.2	1.63	5.52
220199_s_at	Chr:1q42.12	2.44	5.52
200723_s_at	Chr:11p13	1.38	5.52
218576_s_at	Chr:1q21-q22	1.42	5.52
218229_s_at	Chr:1q23.2	1.46	5.52
204508_s_at	Chr:15q21.3	3.99	5.52
214464_at	Chr:1q42.11	1.55	5.52
218928_s_at	Chr:21q22.3	2.63	5.52
218107_at	Chr:1q42.12	1.40	5.52
210927_x_at	Chr:1q21	1.48	6.38
210438_x_at	Chr:1q31	1.48	6.59
211963_s_at	Chr:1q25.1	1.53	6.59
211578_s_at	Chr:17q23.2	1.54	8.30
210434_x_at	Chr:1q21	1.55	8.30
212165_at	Chr:1q31.3	1.63	8.30
212871_at	Chr:12q24.13	1.36	8.30
215720_s_at	Chr:6p21.3	4.11	8.30
203748_x_at	Chr:2q24.2	2.74	8.30
222250_s_at	Chr:1p36.13-q42.3	1.45	8.30
217797_at	Chr:1q23.1	1.50	8.30
207828_s_at	Chr:1q32-q41	2.14	8.30
212219_at	Chr:2p16.1	1.78	8.30
202313_at	Chr:8p21.1	1.60	8.30
200030_s_at	Chr:12q23	1.27	8.30
207266_x_at	Chr:2q24.2	3.19	8.48
212405_s_at	Chr:1q24-q25.3	1.54	9.94
212746_s_at	Chr:1q44	1.72	10.17
205240_at	Chr:1p13.2	1.76	10.17
46665_at	Chr:2q11.1	1.63	10.17
201027_s_at	Chr:2p11.1-q11.1	1.54	10.17
221230_s_at	Chr:1q42.1-q43	1.47	10.17
214104_at	---	2.98	10.17
201796_s_at	Chr:6p21.3	2.33	10.17
213997_at	Chr:15q12	2.63	10.17
212429_s_at	Chr:2p23.3	1.45	10.17
209647_s_at	Chr:2p21	1.40	11.44

201514_s_at	Chr:5q33.1	1.53	12.08
208490_x_at	Chr:6p21.3	1.80	12.08
201771_at	Chr:1q21	1.50	12.08
212773_s_at	Chr:1q42	1.55	12.08
218293_x_at	Chr:22q13.31	2.48	12.08
201841_s_at	Chr:7q11.23	2.02	12.08
210052_s_at	Chr:20q11.2	1.66	12.08
220042_x_at	Chr:1p34	1.88	12.08
221772_s_at	Chr:10q26.3	4.87	12.08
217864_s_at	Chr:15q	1.36	12.08
202251_at	Chr:1q21.1	1.41	12.08
214943_s_at	Chr:1q42.3	1.69	12.08
217885_at	Chr:1q31.3	1.36	12.08
215157_x_at	Chr:8q22.2-q23	1.33	12.08
218865_at	Chr:1q42.11	2.29	12.08
201112_s_at	Chr:20q13	1.38	12.08
221258_s_at	Chr:11p14.1	1.58	12.08
212591_at	Chr:1q42.3	1.58	12.08
212072_s_at	---	1.32	12.08
203155_at	Chr:1q21	1.52	12.08
202615_at	---	1.30	12.08
201387_s_at	Chr:4p14	1.60	12.08
210697_at	Chr:19q13	2.55	12.08
219536_s_at	Chr:20q13.13	2.60	12.08
212498_at	---	1.30	12.08
221487_s_at	Chr:1q21.2	1.60	12.08
220768_s_at	Chr:5q23	1.77	12.08
208778_s_at	Chr:6q25-q27	1.28	12.08
218336_at	Chr:1q23.1	1.72	12.08
204914_s_at	---	3.21	12.08
201897_s_at	Chr:1q21.2	1.98	12.08
209771_x_at	Chr:6q21	8.04	12.08
205046_at	Chr:4q24-q25	1.63	12.08
204477_at	Chr:1q32-q41	1.45	12.08
206571_s_at	Chr:2q11.2-q12	1.41	12.08
201150_s_at	Chr:22q12.3	1.99	12.08
219918_s_at	Chr:1q31	1.98	12.94
207108_s_at	Chr:5p13.2	1.42	12.94
203550_s_at	Chr:1q21	1.73	12.94
219120_at	Chr:2p24.1	1.60	12.94
203853_s_at	Chr:11q13.3	1.93	13.85
201148_s_at	Chr:22q12.3	1.51	13.85
212402_at	Chr:13q14.11	1.37	13.85
204366_s_at	Chr:2p23.3	1.62	13.85
200065_s_at	Chr:1q42	1.40	13.85
218728_s_at	Chr:1q42.12	1.63	13.85
203313_s_at	Chr:18p11.3	1.77	13.85
208796_s_at	Chr:5q32-q34	1.55	13.85
215158_s_at	Chr:1q23.1	1.30	13.85
205661_s_at	Chr:1q21.3	1.35	13.85
206928_at	Chr:1q44	1.68	14.83
201241_at	Chr:2p24	1.45	14.83
214548_x_at	Chr:20q13.2-q13.3	1.44	14.83
208744_x_at	Chr:13q12.2	1.75	15.79
204108_at	Chr:6p21.3	1.99	15.79

205070_at	Chr:7q31	1.34	15.79
203099_s_at	Chr:6p25.1	5.61	15.79
218223_s_at	Chr:1q21.2	2.97	15.79
218784_s_at	Chr:6p21.1	1.59	15.79
215509_s_at	---	1.93	15.79
202559_x_at	Chr:1q21.3	1.33	15.79
212599_at	Chr:7q11.21	1.66	15.79
200652_at	Chr:1q21-q23	1.81	15.79
201289_at	Chr:1p31-p22	2.65	15.79
204195_s_at	Chr:21q22.3	2.13	15.79
201966_at	Chr:1q23	1.30	15.79
210243_s_at	Chr:1q21-q23	1.75	15.79
215227_x_at	Chr:2p25	1.53	15.79
201938_at	Chr:12q24.31	1.27	15.79
209825_s_at	Chr:1q23	1.67	15.79
221741_s_at	Chr:20q13.33	1.32	15.79
202786_at	Chr:2q31.1	1.68	15.79
212153_at	Chr:1q21.2	1.37	15.79
218856_at	Chr:6p21.1-12.2	2.64	15.79
203755_at	Chr:15q15	1.52	15.79
208720_s_at	Chr:20q11.21	1.23	15.79
200666_s_at	Chr:19p13.2	1.47	15.79
202388_at	Chr:1q31	1.69	15.79
211609_x_at	Chr:1q21.2	1.64	16.77
207164_s_at	Chr:1q44-qter	1.48	16.77
204915_s_at	Chr:2p25	3.32	16.77
208854_s_at	Chr:13q31.2-q32.3	1.38	16.77
217919_s_at	Chr:12q22	1.57	16.77
216379_x_at	Chr:6q22	7.69	16.77
202743_at	Chr:1p33	1.57	17.57
216048_s_at	Chr:5q14.3	1.39	17.57
201023_at	Chr:5q31	1.22	17.57
218507_at	Chr:7q32.2	1.32	17.57
208655_at	Chr:4q21.21	1.50	17.57
204031_s_at	Chr:12q13.12	1.35	17.57
210387_at	Chr:6p21.3	2.52	17.57
212650_at	Chr:2p14	1.47	17.57
204373_s_at	Chr:1p36.13-q41	1.33	17.57
204471_at	Chr:3q13.1-q13.2	5.07	18.55
218177_at	Chr:18p11.21	1.38	18.55
210053_at	---	1.44	18.55
218755_at	Chr:5q31	1.56	18.55
219867_at	Chr:21q11.2	5.14	18.55
212442_s_at	Chr:2q31.1	1.75	18.55
221959_at	Chr:8q11.23	2.81	18.55
212902_at	Chr:5q31.1	1.22	19.01
203098_at	Chr:6p25.1	2.11	19.01

1. Vogelstein, B. and Kinzler, K. W. Cancer genes and the pathways they control. Nat Med, *10:* 789-799, 2004.
2. Nowell, P. C. Tumor progression: a brief historical perspective. Semin Cancer Biol, *12:* 261-266, 2002.
3. Komarova, N. L., Sengupta, A., and Nowak, M. A. Mutation-selection networks of cancer initiation: tumor suppressor genes and chromosomal instability. J Theor Biol, *223:* 433-450, 2003.
4. Hanahan, D. and Weinberg, R. A. The hallmarks of cancer. Cell, *100:* 57-70, 2000.
5. Forrester, K., Almoguera, C., Han, K., Grizzle, W. E., and Perucho, M. Detection of high incidence of K-ras oncogenes during human colon tumorigenesis. Nature, *327:* 298-303, 1987.
6. Slamon, D. J. Proto-oncogenes and human cancers. N Engl J Med, *317:* 955-957, 1987.
7. Moll, A. C., Kuik, D. J., Bouter, L. M., Den Otter, W., Bezemer, P. D., Koten, J. W., Imhof, S. M., Kuyt, B. P., and Tan, K. E. Incidence and survival of retinoblastoma in The Netherlands: a register based study 1862-1995. Br J Ophthalmol, *81:* 559-562, 1997.
8. Suckling, R. D., Fitzgerald, P. H., Stewart, J., and Wells, E. The incidence and epidemiology of retinoblastoma in New Zealand: A 30-year survey. Br J Cancer, *46:* 729-736, 1982.
9. Devesa, S. S. The incidence of retinoblastoma. Am J Ophthalmol, *80:* 263-265, 1975.
10. Knudson, A. G., Jr. Mutation and cancer: statistical study of retinoblastoma. Proc Natl Acad Sci U S A, *68:* 820-823, 1971.
11. Dryja, T. P., Friend, S., and Weinberg, R. A. Genetic sequences that predispose to retinoblastoma and osteosarcoma. Symp Fundam Cancer Res, *39:* 115-119, 1986.
12. Friend, S. H., Bernards, R., Rogelj, S., Weinberg, R. A., Rapaport, J. M., Albert, D. M., and Dryja, T. P. A human DNA segment with properties of the gene that predisposes to retinoblastoma and osteosarcoma. Nature, *323:* 643-646, 1986.
13. Graw, J. The genetic and molecular basis of congenital eye defects. Nat Rev Genet, *4:* 876-888, 2003.
14. Dyer, M. A. and Bremner, R. The search for the retinoblastoma cell of origin. Nat Rev Cancer, *5:* 91-101, 2005.
15. Dryja, T. P., Rapaport, J. M., Joyce, J. M., and Petersen, R. A. Molecular detection of deletions involving band q14 of chromosome 13 in retinoblastomas. Proc Natl Acad Sci U S A, *83:* 7391-7394, 1986.
16. Bremner, R., Cohen, B. L., Sopta, M., Hamel, P. A., Ingles, C. J., Gallie, B. L., and Phillips, R. A. Direct transcriptional repression by pRB and its reversal by specific cyclins. Mol Cell Biol, *15:* 3256-3265, 1995.
17. Bosco, G., Du, W., and Orr-Weaver, T. L. DNA replication control through interaction of E2F-RB and the origin recognition complex. Nat Cell Biol, *3:* 289-295, 2001.
18. Lipinski, M. M. and Jacks, T. The retinoblastoma gene family in differentiation and development. Oncogene, *18:* 7873-7882, 1999.
19. Hickman, E. S., Moroni, M. C., and Helin, K. The role of p53 and pRB in apoptosis and cancer. Curr Opin Genet Dev, *12:* 60-66, 2002.
20. Gallie, B. L., Campbell, C., Devlin, H., Duckett, A., and Squire, J. A. Developmental basis of retinal-specific induction of cancer by RB mutation. Cancer Res, *59:* 1731s-1735s, 1999.

21. Chen, D., Livne-bar, I., Vanderluit, J. L., Slack, R. S., Agochiya, M., and Bremner, R. Cell-specific effects of RB or RB/p107 loss on retinal development implicate an intrinsically death-resistant cell-of-origin in retinoblastoma. Cancer Cell, *5:* 539-551, 2004.
22. Kusnetsova, L. E., Prigogina, E. L., Pogosianz, H. E., and Belkina, B. M. Similar chromosomal abnormalities in several retinoblastomas. Hum Genet, *61:* 201-204, 1982.
23. Benedict, W. F., Banerjee, A., Mark, C., and Murphree, A. L. Nonrandom chromosomal changes in untreated retinoblastomas. Cancer Genet Cytogenet, *10:* 311-333, 1983.
24. Squire, J., Phillips, R. A., Boyce, S., Godbout, R., Rogers, B., and Gallie, B. L. Isochromosome 6p, a unique chromosomal abnormality in retinoblastoma: verification by standard staining techniques, new densitometric methods, and somatic cell hybridization. Hum Genet, *66:* 46-53, 1984.
25. Mairal, A., Pinglier, E., Gilbert, E., Peter, M., Validire, P., Desjardins, L., Doz, F., Aurias, A., and Couturier, J. Detection of chromosome imbalances in retinoblastoma by parallel karyotype and CGH analyses. Genes Chromosomes Cancer, *28:* 370-379, 2000.
26. Lillington, D. M., Kingston, J. E., Coen, P. G., Price, E., Hungerford, J., Domizio, P., Young, B. D., and Onadim, Z. Comparative genomic hybridization of 49 primary retinoblastoma tumors identifies chromosomal regions associated with histopathology, progression, and patient outcome. Genes Chromosomes Cancer, *36:* 121-128, 2003.
27. Chen, D., Gallie, B. L., and Squire, J. A. Minimal regions of chromosomal imbalance in retinoblastoma detected by comparative genomic hybridization. Cancer Genet Cytogenet, *129:* 57-63, 2001.
28. Herzog, S., Lohmann, D. R., Buiting, K., Schuler, A., Horsthemke, B., Rehder, H., and Rieder, H. Marked differences in unilateral isolated retinoblastomas from young and older children studied by comparative genomic hybridization. Hum Genet, *108:* 98-104, 2001.
29. Horsthemke, B., Greger, V., Becher, R., and Passarge, E. Mechanism of i(6p) formation in retinoblastoma tumor cells. Cancer Genet Cytogenet, *37:* 95-102, 1989.
30. DiCiommo, D., Gallie, B. L., and Bremner, R. Retinoblastoma: the disease, gene and protein provide critical leads to understand cancer. Semin Cancer Biol, *10:* 255-269, 2000.
31. Chen, D., Pajovic, S., Duckett, A., Brown, V. D., Squire, J. A., and Gallie, B. L. Genomic amplification in retinoblastoma narrowed to 0.6 megabase on chromosome 6p containing a kinesin-like gene, RBKIN. Cancer Res, *62:* 967-971, 2002.
32. Oliveros, O. and Yunis, E. Chromosome evolution in retinoblastoma. Cancer Genet Cytogenet, *82:* 155-160, 1995.
33. Cowell, J. K. and Hogg, A. Genetics and cytogenetics of retinoblastoma. Cancer Genet Cytogenet, *64:* 1-11, 1992.
34. Potluri, V. R., Helson, L., Ellsworth, R. M., Reid, T., and Gilbert, F. Chromosomal abnormalities in human retinoblastoma. A review. Cancer, *58:* 663-671, 1986.
35. Squire, J., Gallie, B. L., and Phillips, R. A. A detailed analysis of chromosomal changes in heritable and non-heritable retinoblastoma. Hum Genet, *70:* 291-301, 1985.

36. Lee, W. H., Murphree, A. L., and Benedict, W. F. Expression and amplification of the N-myc gene in primary retinoblastoma. Nature, *309:* 458-460, 1984.
37. Almeida, A., Zhu, X. X., Vogt, N., Tyagi, R., Muleris, M., Dutrillaux, A. M., Dutrillaux, B., Ross, D., Malfoy, B., and Hanash, S. GAC1, a new member of the leucine-rich repeat superfamily on chromosome band 1q32.1, is amplified and overexpressed in malignant gliomas. Oncogene, *16:* 2997-3002, 1998.
38. Riemenschneider, M. J., Knobbe, C. B., and Reifenberger, G. Refined mapping of 1q32 amplicons in malignant gliomas confirms MDM4 as the main amplification target. Int J Cancer, *104:* 752-757, 2003.
39. Riemenschneider, M. J., Buschges, R., Wolter, M., Reifenberger, J., Bostrom, J., Kraus, J. A., Schlegel, U., and Reifenberger, G. Amplification and overexpression of the MDM4 (MDMX) gene from 1q32 in a subset of malignant gliomas without TP53 mutation or MDM2 amplification. Cancer Res, *59:* 6091-6096, 1999.
40. Marchong, M. N., Chen, D., Corson, T. W., Lee, C., Harmandayan, M., Bowles, E., Chen, N., and Gallie, B. L. Minimal 16q genomic loss implicates cadherin-11 in retinoblastoma. Mol Cancer Res, *2:* 495-503, 2004.
41. McFall, R. C., Sery, T. W., and Makadon, M. Characterization of a new continuous cell line derived from a human retinoblastoma. Cancer Res, *37:* 1003-1010, 1977.
42. Gallie, B. L., Albert, D. M., Wong, J. J., Buyukmihci, N., and Pullafito, C. A. Heterotransplantation of retinoblastoma into the athymic "nude" mouse. Invest Ophthalmol Vis Sci, *16:* 256-259, 1977.
43. Griegel, S., Hong, C., Frotschl, R., Hulser, D. F., Greger, V., Horsthemke, B., and Rajewsky, M. F. Newly established human retinoblastoma cell lines exhibit an "immortalized" but not an invasive phenotype in vitro. Int J Cancer, *46:* 125-132, 1990.
44. Saiki, R. K., Scharf, S., Faloona, F., Mullis, K. B., Horn, G. T., Erlich, H. A., and Arnheim, N. Enzymatic amplification of beta-globin genomic sequences and restriction site analysis for diagnosis of sickle cell anemia. Science, *230:* 1350-1354, 1985.
45. Mullis, K. B. and Faloona, F. A. Specific synthesis of DNA in vitro via a polymerase-catalyzed chain reaction. Methods Enzymol, *155:* 335-350, 1987.
46. Ginzinger, D. G., Godfrey, T. E., Nigro, J., Moore, D. H., 2nd, Suzuki, S., Pallavicini, M. G., Gray, J. W., and Jensen, R. H. Measurement of DNA copy number at microsatellite loci using quantitative PCR analysis. Cancer Res, *60:* 5405-5409, 2000.
47. Bieche, I., Olivi, M., Champeme, M. H., Vidaud, D., Lidereau, R., and Vidaud, M. Novel approach to quantitative polymerase chain reaction using real-time detection: application to the detection of gene amplification in breast cancer. Int J Cancer, *78:* 661-666, 1998.
48. Ronaghi, M. Pyrosequencing sheds light on DNA sequencing. Genome Res, *11:* 3-11, 2001.
49. Hochberg, E. P., Miklos, D. B., Neuberg, D., Eichner, D. A., McLaughlin, S. F., Mattes-Ritz, A., Alyea, E. P., Antin, J. H., Soiffer, R. J., and Ritz, J. A novel rapid single nucleotide polymorphism (SNP)-based method for assessment of hematopoietic chimerism after allogeneic stem cell transplantation. Blood, *101:* 363-369, 2003.
50. Pielberg, G., Day, A. E., Plastow, G. S., and Andersson, L. A sensitive method for detecting variation in copy numbers of duplicated genes. Genome Res, *13:* 2171-2177, 2003.

51. Tusher, V. G., Tibshirani, R., and Chu, G. Significance analysis of microarrays applied to the ionizing radiation response. Proc Natl Acad Sci U S A, *98:* 5116-5121, 2001.
52. Evans, A. J., Gallie, B. L., Jewett, M. A., Pond, G. R., Vandezande, K., Underwood, J., Fradet, Y., Lim, G., Marrano, P., Zielenska, M., and Squire, J. A. Defining a 0.5-mb region of genomic gain on chromosome 6p22 in bladder cancer by quantitative-multiplex polymerase chain reaction. Am J Pathol, *164:* 285-293, 2004.
53. De Greve, J., Battey, J., Fedorko, J., Birrer, M., Evan, G., Kaye, F., Sausville, E., and Minna, J. The human L-myc gene encodes multiple nuclear phosphoproteins from alternatively processed mRNAs. Mol Cell Biol, *8:* 4381-4388, 1988.
54. Edwards, J., Krishna, N. S., Witton, C. J., and Bartlett, J. M. Gene amplifications associated with the development of hormone-resistant prostate cancer. Clin Cancer Res, *9:* 5271-5281, 2003.
55. Wu, R., Lin, L., Beer, D. G., Ellenson, L. H., Lamb, B. J., Rouillard, J. M., Kuick, R., Hanash, S., Schwartz, D. R., Fearon, E. R., and Cho, K. R. Amplification and overexpression of the L-MYC proto-oncogene in ovarian carcinomas. Am J Pathol, *162:* 1603-1610, 2003.
56. Goff, L. K., Neat, M. J., Crawley, C. R., Jones, L., Jones, E., Lister, T. A., and Gupta, R. K. The use of real-time quantitative polymerase chain reaction and comparative genomic hybridization to identify amplification of the REL gene in follicular lymphoma. Br J Haematol, *111:* 618-625, 2000.
57. Horsthemke, B. Genetics and cytogenetics of retinoblastoma. Cancer Genet Cytogenet, *63:* 1-7, 1992.
58. Abramson, D. H., Ellsworth, R. M., and Zimmerman, L. E. Nonocular cancer in retinoblastoma survivors. Trans Sect Ophthalmol Am Acad Ophtalmol Otolaryngol, *81:* 454-457, 1976.
59. Francois, J. Retinoblastoma and osteogenic sarcoma. Ophthalmologica, *175:* 185-191, 1977.
60. Matsunaga, E. Hereditary retinoblastoma: host resistance and second primary tumors. J Natl Cancer Inst, *65:* 47-51, 1980.
61. Li, F. P., Abramson, D. H., Tarone, R. E., Kleinerman, R. A., Fraumeni, J. F., Jr., and Boice, J. D., Jr. Hereditary retinoblastoma, lipoma, and second primary cancers. J Natl Cancer Inst, *89:* 83-84, 1997.
62. Eng, C., Li, F. P., Abramson, D. H., Ellsworth, R. M., Wong, F. L., Goldman, M. B., Seddon, J., Tarbell, N., and Boice, J. D., Jr. Mortality from second tumors among long-term survivors of retinoblastoma. J Natl Cancer Inst, *85:* 1121-1128, 1993.
63. Nilsson, M., Meza-Zepeda, L. A., Mertens, F., Forus, A., Myklebost, O., and Mandahl, N. Amplification of chromosome 1 sequences in lipomatous tumors and other sarcomas. Int J Cancer, *109:* 363-369, 2004.
64. Knuutila, S., Bjorkqvist, A. M., Autio, K., Tarkkanen, M., Wolf, M., Monni, O., Szymanska, J., Larramendy, M. L., Tapper, J., Pere, H., El-Rifai, W., Hemmer, S., Wasenius, V. M., Vidgren, V., and Zhu, Y. DNA copy number amplifications in human neoplasms: review of comparative genomic hybridization studies. Am J Pathol, *152:* 1107-1123, 1998.
65. Lau, C. C., Harris, C. P., Lu, X. Y., Perlaky, L., Gogineni, S., Chintagumpala, M., Hicks, J., Johnson, M. E., Davino, N. A., Huvos, A. G., Meyers, P. A., Healy, J. H., Gorlick, R., and Rao, P. H. Frequent amplification and rearrangement of chromosomal bands 6p12-p21 and 17p11.2 in osteosarcoma. Genes Chromosomes Cancer, *39:* 11-21, 2004.

66. Pimkhaokham, A., Shimada, Y., Fukuda, Y., Kurihara, N., Imoto, I., Yang, Z. Q., Imamura, M., Nakamura, Y., Amagasa, T., and Inazawa, J. Nonrandom chromosomal imbalances in esophageal squamous cell carcinoma cell lines: possible involvement of the ATF3 and CENPF genes in the 1q32 amplicon. Jpn J Cancer Res, *91:* 1126-1133, 2000.
67. van den Boom, J., Wolter, M., Kuick, R., Misek, D. E., Youkilis, A. S., Wechsler, D. S., Sommer, C., Reifenberger, G., and Hanash, S. M. Characterization of gene expression profiles associated with glioma progression using oligonucleotide-based microarray analysis and real-time reverse transcription-polymerase chain reaction. Am J Pathol, *163:* 1033-1043, 2003.
68. de la Guardia, C., Casiano, C. A., Trinidad-Pinedo, J., and Baez, A. CENP-F gene amplification and overexpression in head and neck squamous cell carcinomas. Head Neck, *23:* 104-112, 2001.
69. Rassidakis, G. Z., Lai, R., McDonnell, T. J., Cabanillas, F., Sarris, A. H., and Medeiros, L. J. Overexpression of Mcl-1 in anaplastic large cell lymphoma cell lines and tumors. Am J Pathol, *160:* 2309-2310, 2002.
70. Cho-Vega, J. H., Rassidakis, G. Z., Admirand, J. H., Oyarzo, M., Ramalingam, P., Paraguya, A., McDonnell, T. J., Amin, H. M., and Medeiros, L. J. MCL-1 expression in B-cell non-Hodgkin's lymphomas. Hum Pathol, *35:* 1095-1100, 2004.
71. Bae, J., Leo, C. P., Hsu, S. Y., and Hsueh, A. J. MCL-1S, a splicing variant of the antiapoptotic BCL-2 family member MCL-1, encodes a proapoptotic protein possessing only the BH3 domain. J Biol Chem, *275:* 25255-25261, 2000.
72. Wong, N., Chan, A., Lee, S. W., Lam, E., To, K. F., Lai, P. B., Li, X. N., Liew, C. T., and Johnson, P. J. Positional mapping for amplified DNA sequences on 1q21-q22 in hepatocellular carcinoma indicates candidate genes over-expression. J Hepatol, *38:* 298-306, 2003.
73. Dang, C. V. c-Myc target genes involved in cell growth, apoptosis, and metabolism. Mol Cell Biol, *19:* 1-11, 1999.
74. Nesbit, C. E., Tersak, J. M., and Prochownik, E. V. MYC oncogenes and human neoplastic disease. Oncogene, *18:* 3004-3016, 1999.
75. Schlagbauer-Wadl, H., Griffioen, M., van Elsas, A., Schrier, P. I., Pustelnik, T., Eichler, H. G., Wolff, K., Pehamberger, H., and Jansen, B. Influence of increased c-Myc expression on the growth characteristics of human melanoma. J Invest Dermatol, *112:* 332-336, 1999.
76. Kaye, F., Battey, J., Nau, M., Brooks, B., Seifter, E., De Greve, J., Birrer, M., Sausville, E., and Minna, J. Structure and expression of the human L-myc gene reveal a complex pattern of alternative mRNA processing. Mol Cell Biol, *8:* 186-195, 1988.
77. Ikegaki, N., Minna, J., and Kennett, R. H. The human L-myc gene is expressed as two forms of protein in small cell lung carcinoma cell lines: detection by monoclonal antibodies specific to two myc homology box sequences. Embo J, *8:* 1793-1799, 1989.
78. Doz, F., Peter, M., Schleiermacher, G., Vielh, P., Validire, P., Putterman, M., Blanquet, V., Desjardins, L., Dufier, J. L., Zucker, J. M., Mosseri, V., Thomas, G., Magdelenat, H., and Delattre, O. N-MYC amplification, loss of heterozygosity on the short arm of chromosome 1 and DNA ploidy in retinoblastoma. Eur J Cancer, *32A:* 645-649, 1996.
79. Kim, C. J., Chi, J. G., Choi, H. S., Shin, H. Y., Ahn, H. S., Yoo, Y. S., and Chang, K. Y. Proliferation not apoptosis as a prognostic indicator in retinoblastoma. Virchows Arch, *434:* 301-305, 1999.

80. Angst, B. D., Marcozzi, C., and Magee, A. I. The cadherin superfamily: diversity in form and function. J Cell Sci, *114:* 629-641, 2001.
81. Howng, S. L., Wu, C. H., Cheng, T. S., Sy, W. D., Lin, P. C., Wang, C., and Hong, Y. R. Differential expression of Wnt genes, beta-catenin and E-cadherin in human brain tumors. Cancer Lett, *183:* 95-101, 2002.
82. Sarrio, D., Moreno-Bueno, G., Hardisson, D., Sanchez-Estevez, C., Guo, M., Herman, J. G., Gamallo, C., Esteller, M., and Palacios, J. Epigenetic and genetic alterations of APC and CDH1 genes in lobular breast cancer: relationships with abnormal E-cadherin and catenin expression and microsatellite instability. Int J Cancer, *106:* 208-215, 2003.
83. Kanazawa, T., Watanabe, T., Kazama, S., Tada, T., Koketsu, S., and Nagawa, H. Poorly differentiated adenocarcinoma and mucinous carcinoma of the colon and rectum show higher rates of loss of heterozygosity and loss of E-cadherin expression due to methylation of promoter region. Int J Cancer, *102:* 225-229, 2002.
84. Kawaguchi, J., Takeshita, S., Kashima, T., Imai, T., Machinami, R., and Kudo, A. Expression and function of the splice variant of the human cadherin-11 gene in subordination to intact cadherin-11. J Bone Miner Res, *14:* 764-775, 1999.
85. Ho, G. H., Calvano, J. E., Bisogna, M., Abouezzi, Z., Borgen, P. I., Cordon-Cardo, C., and van Zee, K. J. Genetic alterations of the p14ARF -hdm2-p53 regulatory pathway in breast carcinoma. Breast Cancer Res Treat, *65:* 225-232, 2001.
86. Filippova, G. N., Qi, C. F., Ulmer, J. E., Moore, J. M., Ward, M. D., Hu, Y. J., Loukinov, D. I., Pugacheva, E. M., Klenova, E. M., Grundy, P. E., Feinberg, A. P., Cleton-Jansen, A. M., Moerland, E. W., Cornelisse, C. J., Suzuki, H., Komiya, A., Lindblom, A., Dorion-Bonnet, F., Neiman, P. E., Morse, H. C., 3rd, Collins, S. J., and Lobanenkov, V. V. Tumor-associated zinc finger mutations in the CTCF transcription factor selectively alter tts DNA-binding specificity. Cancer Res, *62:* 48-52, 2002.
87. Sakakura, C., Hagiwara, A., Miyagawa, K., Nakashima, S., Yoshikawa, T., Kin, S., Nakase, Y., Ito, K., Yamagishi, H., Yazumi, S., Chiba, T., and Ito, Y. Frequent downregulation of the runt domain transcription factors RUNX1, RUNX3 and their cofactor CBFB in gastric cancer. Int J Cancer, *113:* 221-228, 2005.
88. Hsu, H., Xiong, J., and Goeddel, D. V. The TNF receptor 1-associated protein TRADD signals cell death and NF-kappa B activation. Cell, *81:* 495-504, 1995.
89. Zbankova, S., Bryndova, J., Kment, M., and Pacha, J. Expression of 11beta-hydroxysteroid dehydrogenase types 1 and 2 in colorectal cancer. Cancer Lett, *210:* 95-100, 2004.
90. Rabbitt, E. H., Ayuk, J., Boelaert, K., Sheppard, M. C., Hewison, M., Stewart, P. M., and Gittoes, N. J. Abnormal expression of 11 beta-hydroxysteroid dehydrogenase type 2 in human pituitary adenomas: a prereceptor determinant of pituitary cell proliferation. Oncogene, *22:* 1663-1667, 2003.
91. Mazzocchi, G., Malendowicz, L. K., Aragona, F., Tortorella, C., Gottardo, L., and Nussdorfer, G. G. 11beta-Hydroxysteroid dehydrogenase types 1 and 2 are up- and downregulated in cortisol-secreting adrenal adenomas. J Investig Med, *50:* 288-292, 2002.
92. Hyman, E., Kauraniemi, P., Hautaniemi, S., Wolf, M., Mousses, S., Rozenblum, E., Ringner, M., Sauter, G., Monni, O., Elkahloun, A., Kallioniemi, O. P., and Kallioniemi, A. Impact of DNA amplification on gene expression patterns in breast cancer. Cancer Res, *62:* 6240-6245, 2002.

93. Reifenberger, G., Reifenberger, J., Ichimura, K., Meltzer, P. S., and Collins, V. P. Amplification of multiple genes from chromosomal region 12q13-14 in human malignant gliomas: preliminary mapping of the amplicons shows preferential involvement of CDK4, SAS, and MDM2. Cancer Res, *54:* 4299-4303, 1994.

Nareyeck G., Zeschnigk M., Prescher G., Hüsing J., Lohmann DR., Anastassiou G.. Establishment and characterization of two uveal melanoma cell lines derived from tumors with loss of one chromosome 3. Submitted and under revision by IOVS.

REMERCIEMENTS

Herzlichen Dank an Herrn Prof. Dr. Dietmar Lohmann für die Überlasssung dieses interessanten Themas und für seine wissenschaftliche Betreuung meiner Arbeit. Vielen Dank auch für seine geduldigen Erklärungen, Ratschläge, Ideen, Hilfsbereitschaft und Optimismus in kritischen Momenten.

Ich bedanke mich bei Herrn Prof. Dr. Bernhard Horsthemke, der mich in seinem Labor und innerhalb seiner Gruppe freundlich empfangen hat, für seine wissenschaftliche Betreuung.

Mein Dank gilt auch Herrn Dr. Michael Zeschnigk für sein Interesse an meiner Arbeit sowie für Ideen und Ratschläge.

Insgesamt haben alle Mitarbeiter des Instituts dazu beigetragen, mir den Anfang so leicht wie möglich zu machen. Dafür sowie für ihre Hilfsbereitschaft, die gute Arbeitsatmosphäre und die freundschaftlichen Momente außerhalb des Labors möchte ich mich ganz herzlich bedanken.

A Paola Brega senza la quale tutto sarebbe stato più difficile. Grazie per il tuo sostegno morale, le nostre chiacchierate, la pasta squisita, Roma, l'atmosfera calda... E' stata una grande fortuna incontrarsi.

Ein großes Dankeschön an Jasmin Hefendehl für Übersetzungen, Erklärungen, Ratschläge...

J’adresse toute mon affection et ma reconnaissance à mes parents pour m’avoir permis d’en arriver là. Merci à eux et à ma soeur pour leurs encouragements et leur soutien, et pour les visites fréquentes en pays parfois hostile.
Vielen Dank an Martin für die moralische Unterstützung und deine Geduld.

Curriculum vitae

Name:	Sandrine GRATIAS
Nationality:	French
Date of birth:	20th May 1977
Place of birth:	Figeac, France
Address:	Sophienstr. 11, 45130 Essen

Education

06.1995	General Certificate of Education in Sciences (Baccalauréat S)
1995-1998	Two-year University Degree in Sciences (DEUG Sciences), Université Paul Sabatier, Toulouse
1998-1999	Bachelor's Degree in Cell Biology and Physiology (Licence), UPS, Toulouse
1999-2000	Master's Degree in Cell Biology and Physiology (Maitrise), UPS, Toulouse
2000-2001	Postgraduate Degree (DESS), UPS, Toulouse Training at Institut de Recherche Pierre Fabre
Since 17.10.2001	PhD student in the Department of Human Genetics at the University Duisburg-Essen, with Prof. Dr. Bernhard Horsthemke

Essen, April 2005

Erklärung:

Hiermit erkläre ich, gem. 6 Abs. 2, Nr. 7 der Promotionsordnung der Fachbereiche 6 bis 9 zur Erlangung des Dr. rer. nat., dass ich das Arbeitsgebiet, dem das Thema "Identification of genes involved in progression of retinoblastoma" zuzuordnen ist, in Forschung und Lehre vertrete und den Antrag von Frau Sandrine Gratias befürworte.

Essen, den 04.04.2005

(Prof. Dr. Bernhard Horsthemke)

Erklärung:

Hiermit erkläre ich, gem. 6 Abs. 2, Nr. 6 der Promotionsordnung der Fachbereiche 6 bis 9 zur Erlangung des Dr. rer. nat., dass ich die vorliegende Dissertation selbständig verfasst und mich keiner anderen als der angegebenen Hilfsmittel bedient habe.

Essen, den 04.04.2005

(Sandrine Gratias)

Erklärung:

Hiermit erkläre ich, gem. 6 Abs. 2, Nr. 8 der Promotionsordnung der Fachbereiche 6 bis 9 zur Erlangung des Dr. rer. nat., dass ich keine anderen Promotionen bzw. Promotionsversuche in der Vergangenheit durchgeführt habe und dass diese Arbeit von keiner anderen Fakultät abgelehnt worden ist.

Essen, den 04.04.2005

(Sandrine Gratias)